NEOTECTONICS AND PALEOEARTHQUAKES ALONG MAE HONG SON FAULT, NORTHERN THAILAND

Miss Chanista Chansom

จุฬาลงกรณ์มหาวิทยาลัย
Chulalongkorn University

A Thesis Submitted in Partial Fulfillment of the Requirements
for the Degree of Master of Science in Geology
Department of Geology
Faculty of Science
Chulalongkorn University
Academic Year 2019

Copyright of Chulalongkorn University

ธรณีแปรสัณฐานยุคใหม่และแผ่นดินไหวบรรพกาลตามแนวรอยเลื่อนแม่ฮ่องสอน ภาคเหนือของประเทศไทย

น.ส.จณิสตา จันสม

จุฬาลงกรณ์มหาวิทยาลัย
CHULALONGKORN UNIVERSITY

วิทยานิพนธ์นี้เป็นส่วนหนึ่งของการศึกษาตามหลักสูตรปริญญาวิทยาศาสตรมหาบัณฑิต
สาขาวิชาธรณีวิทยา ภาควิชาธรณีวิทยา
คณะวิทยาศาสตร์ จุฬาลงกรณ์มหาวิทยาลัย
ปีการศึกษา 2562
ลิขสิทธิ์ของจุฬาลงกรณ์มหาวิทยาลัย

Thesis Title	NEOTECTONICS AND PALEOEARTHQUAKES ALONG MAE HONG SON FAULT, NORTHERN THAILAND
By	Miss Chanista Chansom
Field of Study	Geology
Thesis Advisor	SUKONMETH JITMAHANTAKUL, Ph.D.
Thesis Co Advisor	Professor Punya Charusiri, Ph.D.

Accepted by the Faculty of Science, Chulalongkorn University in Partial Fulfillment of the Requirement for the Master of Science

..... Dean of the Faculty of Science
(Professor POLKIT SANGVANICH, Ph.D.)

THESIS COMMITTEE

..... Chairman
(Assistant Professor VICHAI CHUTAKOSITKANON, Ph.D.)

..... Thesis Advisor
(SUKONMETH JITMAHANTAKUL, Ph.D.)

..... Thesis Co-Advisor
(Professor Punya Charusiri, Ph.D.)

..... Examiner
(Associate Professor SANTI PAILOPLEE, Ph.D.)

..... External Examiner
(Weerachat Wiwegwin, Ph.D.)

จุฬาลงกรณ์มหาวิทยาลัย
Chulalongkorn University

จณิสตา จันสม : ธรณีแปรสัณฐานยุคใหม่และแผ่นดินไหวบรรพกาลตามแนวรอยเลื่อนแม่ฮ่องสอน ภาคเหนือของประเทศไทย.
(NEOTECTONICS AND PALEOEARTHQUAKES ALONG MAE HONG SON FAULT, NORTHERN THAILAND) อ.ที่ปรึกษาหลัก : ดร.สุคนธ์เมธ จิตรมหันตกุล, อ.ที่ปรึกษาร่วม : ศ. ดร. ปัญญา จารุศิริ

การศึกษาแผ่นดินไหวบรรพกาลของรอยเลื่อนมีพลังได้นำมาใช้ในการศึกษาบริเวณพื้นที่แม่ฮ่องสอน ภาคเหนือประเทศไทย จากเหตุการณ์แผ่นดินไหวทางตอนใต้ของจังหวัดแม่ฮ่องสอนเมื่อเดือนกุมภาพันธ์ พ.ศ. 2518 ขนาด 5.6 บริเวณบ้านท่าสองยาง จังหวัดตาก แสดงให้เห็นว่าพื้นที่บริเวณนี้ยังคงมีพลังจนถึงปัจจุบัน การศึกษานี้มีวัตถุประสงค์เพื่ออธิบายธรณีวิทยาแปรสัณฐานของรอยเลื่อน พฤติกรรมการเลื่อนตัว ตลอดจนบ่งชี้อายุการเลื่อนตัวครั้งล่าสุดของรอยเลื่อน ระบุคาบอุบัติซ้ำของการเกิดแผ่นดินไหวบรรพกาลและอัตราการเลื่อนตัวของรอยเลื่อน จากข้อมูลโทรสัมผัสและการขุดร่องสำรวจแผ่นดินไหวบรรพกาล ผลการศึกษาพบว่ารอยเลื่อนแม่ฮ่องสอนเป็นรอยเลื่อนที่วางตัวในแนวเหนือ-ใต้ พาดผ่านพื้นที่จังหวัดแม่ฮ่องสอนและจังหวัดตากบางส่วน แสดงลักษณะการเลื่อนตัวของรอยเลื่อนแบบขวาเข้าประกอบกับรอยเลื่อนปกติ พบลักษณะธรณีสัณฐานที่สัมพันธ์กับรอยเลื่อน ได้แก่ธารเหลื่อม หุบเขาเส้นตรง สันเขาเหลื่อม และผารอยเลื่อน จากการแปลความหมายทางธรณีแปรสัญฐานและการวิเคราะห์ทางแอ่งสะสมตะกอน พบว่าพื้นที่แม่ฮ่องสอนประกอบด้วยสองแอ่งสะสมตะกอน ได้แก่ แอ่งแม่ฮ่องสอนทางตอนเหนือและแอ่งแม่สะเรียงทางตอนใต้ โดยพื้นที่ระหว่างสองแอ่งสะสมตะกอนนี้คือโซนรอยต่อขุนยวม เป็นพื้นที่สูงที่เกิดจากการเคลื่อนตัวของรอยเลื่อนตามแนวระดับ จากค่าความยาวรอยแตกปรากฏบนพื้นผิว สามารถเกิดแผ่นดินไหวขนาดสูงสุดระหว่าง 5.8 และ 6.3 ผลการหาอายุโดยวิธีเรืองแสงด้วยความร้อนของชั้นตะกอนในร่องสำรวจที่สัมพันธ์กับรอยเลื่อน บ่งชี้ว่าเคยเกิดแผ่นดินไหวมาแล้ว 9 ครั้ง เมื่อประมาณ 78,000, 68,000, 58,000, 48,000, 35,000, 30,000, 25,000, 8,000 และ 3,000 ปี มีคาบอุบัติซ้ำประมาณ 5,000 ปี และอัตราการเลื่อนตัวประมาณ 0.04-0.15 มิลลิเมตรต่อปี

CHULALONGKORN UNIVERSITY

สาขาวิชา ธรณีวิทยา ลายมือชื่อนิสิต .....
ปีการศึกษา 2562 ลายมือชื่อ อ.ที่ปรึกษาหลัก .....
ลายมือชื่อ อ.ที่ปรึกษาร่วม .....

6072029823 : MAJOR GEOLOGY

KEYWORD: Paleoearthquake, Mae Hong Son Fault, Active fault, Basin

Chanista Chansom :

NEOTECTONICS AND PALEOEARTHQUAKES ALONG MAE HONG SON FAULT, NOR THERN THAILAND. Advisor: SUKONMETH JITMAHANTAKUL, Ph.D. Co-advisor: Prof. Punya Charusiri, Ph.D.

Mae Hong Son Fault (MHSF) is a north-south-trending active fault in Northern Thailand. Last earthquake occurred on February, 1975 with a magnitude of 5.6 at Ban Tha Song Young in Tak Province. This study aims to describe morphological characteristics of MHSF using high (12.5m) resolution Digital Elevation Model (DEM) and to evaluate paleoearthquake magnitudes, recurrence intervals, and slip rates of MHSF by excavating paleoearthquake trenches. According to morphotectonic analysis, offset streams, linear valleys, triangular facets and scarplets were formed as a result of dextral movement within the active fault zone. There are two separate basins associated with the MHSF, which include the Mae Hong Son Basin to the north and the Mae Sariang Basin the south. Between these basins, fault displacements decrease towards Khun Yuam area suggesting a linkage zone in the Mae Hong Son strike-slip fault systems. Surface rupture length investigation from fault segments in both basins indicates maximum credible earthquake between M5.8 - M6.3. Nine paleoearthquake events were identified in Mae Hong Son Province based on trenching and road-cut outcrop studies, and optically stimulated luminescence (OSL) dating. The OSL ages of the events are 78,000, 68,000, 58,000, 48,000, 35,000, 30,000, 25,000, 8,000 and 3,000 years ago. The recurrence interval of earthquake events on the MHSF appears to be ca. 5,000 years, and the slip rate was estimated as ca. 0.04–0.15 mm/yr.

จุฬาลงกรณ์มหาวิทยาลัย
CHULALONGKORN UNIVERSITY

Field of Study: Geology

Academic Year: 2019

Student's Signature .....

Advisor's Signature .....

Co-advisor's Signature .....

ACKNOWLEDGEMENTS

I would like to this opportunity to express my graduate to all persons who contribute and involve in this thesis. First of all, I would like to thank the Science Achievement Scholarship of Thailand (SAST) for the opportunity and scholarship for studying the Degree of Master of Science Program in Geology at Chulalongkorn University.

I would like to express my special appreciation to Dr. Sukonmeth Jitmahantakul and Prof. Punya Charusiri for supervising, his impact guidance, support and encouragement to me during this research. Without their guidance and support, this work would not have reached a final stage. I would like to thank all of lecturers for their expertise and knowledge through the Science Program in Geology. I am appreciated to Mr. Suwith Kosuwan and Dr. Weerachart Wiwegwin for their support and discussion through this research and Dr. Peerasit Surakiatchai for their helping manage all sample analyses.

Special thanks extend to Professor Lewis A. Owen and Dr. Paula Marques Figueiredo from Department of Geology, University of Cincinnati, USA for their effort and support to accelerate the processing of my samples at the Quaternary Geochronology Laboratories.

I would like to have a special thanks to all friends in this program for their support, discussion and friendship through this program. Special thanks to my family and Ms. Ratapong Jamroenkahjohnsuk for supporting and encouragement through this program. Without all of you this work could not be completed.

Chanista Chansom

จุฬาลงกรณ์มหาวิทยาลัย
Chulalongkorn University

TABLE OF CONTENTS

Page

..... iii

ABSTRACT (THAI) iii

..... iv

ABSTRACT (ENGLISH) iv

ACKNOWLEDGEMENTS v

TABLE OF CONTENTS vi

List of tables ix

List of figures x

CHAPTER I INTRODUCTION 1

Background 1

Objectives of the study 4

Location of study area 5

Methodology 5

Thesis Outline 7

CHAPTER II LITERATURE REVIEW 8

Tectonic setting 8

Geological setting 10

The Lower Paleozoic 10

The upper Paleozoic 14

Cenozoic 14

Igneous rock 14

จุฬาลงกรณ์มหาวิทยาลัย
Chulalongkorn University

Structural setting 15
Neotectonics and active fault in the Mae Hong Son are 15
CHAPTER III REMOTE SENSING INTERPRETATION 23
Satellite images and interpretation 23
1. Landsat 7 ETM+ 25
2. ALOS PALSAR Digital Elevation Model (ALOS DEM) 26
Morphotectonic landforms interpretation 30
Lineament and fault segments 39
Basins associated with the MHSF 39
Determination of Maximum Credible Earthquakes 45
CHAPTER IV
PALEOEARTHQUAKE INVESTIGATIONS 48
Field evidence of morphotectonic landforms 48
Paleoearthquake trenches 53
1. Doi Wiang Luang road-cut outcrop 53
2. Mae Tha Lu trench 56
3. Khun Yuam trench 59
4. Ban Yod trench 63
Optical Stimulated Luminescence (OSL) dating 68
Water content analysis 68
Annual Dose Evaluation 70
Paleodose or Equivalent Dose Evaluation 70
Dating results 73
CHAPTER IV Discussion 78

จุฬาลงกรณ์มหาวิทยาลัย
Chulalongkorn University

Influence of pre-existing fabrics on fault kinematics and basin geometry 78

Paleoearthquake events and recurrence interval of MHSF 83

Determination on slip rates 85

Evolution of the basins along the MHSF 87

CHAPTER V CONCLUSION 89

REFERENCES 90

APPENDIX 93

VITA 112

จุฬาลงกรณ์มหาวิทยาลัย
Chulalongkorn University

List of tables

Page

Table 1 Spectral bands and wavelength interval of Landsat 7 ETM+ 25

Table 2 Image information from Landsat 7 ETM+ applied in this study 26

Table 3 Image information from ALOS DEM applied in this study..... 27

Table 4 Fifty-five fault segments of the MHSF with essential information of earthquake source parameters identified in this study. 46

Table 5 Summary of OSL dating results of extracted sediments from study area, Mae Hon Son Province, northern Thailand, containing radioisotope concentrations, moisture contents total dose rate, equivalent dose estimates and absolute ages..... 73

จุฬาลงกรณ์มหาวิทยาลัย
Chulalongkorn University

List of figures

Page

Figure 1 Map of Thailand and adjacent areas showing major active faults (compiled from DMR (2018), Wang et al. (2014) and Morley, Charusiri, and Watkinson (2011)) and epicentral distribution from 1912 to 2018 (TMD, 2016 and USGS, 2016). The rectangle shows the location of the study area. 2

Figure 2 Map of the MHSF shows fault segments with north-south direction (modified from DMR, 2019). 3

Figure 3 Simplified flow chart illustrating the methodology applied in this study. 6

Figure 4 Major tectonic elements in Southeast Asia and Southern China. Arrows show relative directions of motion of crustal blocks during the Late Cenozoic. MPFZ - Mae Ping Fault Zone; NTFZ – Northern Thailand Fault Zone; TPFZ - Three Pagodas Fault Zone and UFZ - Uttaradit Fault Zone (from Fenton et al. (2003)). 9

Figure 5 Geologic map on scale 1:250,000 of Mae Hong Son province showing the distribution of rock units. The explanation of these rock units shown in Figure 6 (from DMR (2007)). 11

Figure 6 The explanation of geologic map of the Mae Hong Son province in Figure 5 (from DMR, 2007) 12

Figure 7 Seismic source zones in the Indochina region (from Nutalaya et al. (1985)) Note that study area (Mae Hong Son region) is in zone G. 16

Figure 8 Map of major fault zones in Thailand which is the first active fault map in Thailand (from Chuaviroj (1991)). 17

Figure 9 Map shows active faults in Thailand consist of 15 fault zones (from DMR (2018)). Red box shows the study area. 19

Figure 10 Map shows seismic hazard zones in Thailand related with 15 active fault zones (from DMR (2016) and DMR (2018)). Red box shows the study area. 20

จุฬาลงกรณ์มหาวิทยาลัย
Chulalongkorn University

Figure 11 PSHA map of Thailand showing the probabilities (%) that the greatest potential to generate earthquakes is the western of Thailand and related with 15 active fault zones (from Pailoplee and Charusiri (2016) and DMR (2018)). Red box shows the study area. 22

Figure 12 Morphotectonic landforms associated with active strike-slip movement (from Keller and Pinter (1996)). 24

Figure 13 Features associated with strike-slip restraining and releasing bends (from Cunningham and Mann (2007)) 24

Figure 14 Enhancement Landsat 7 by the false-colored composite image data of bands 4 (red), 5 (green), and 7 (blue) showing physiographic features of the study area. 28

Figure 15 (A) Shaded relief (sunlight angle = 30°, sunlight direction = 313 and z factor = 2) and (B) Enhanced ALOS DEM map (sunlight elevation = 30°, sunlight direction azimuth = 313 and z factor = 1) show physiographic features of Mae Hong Son Province. 29

Figure 16 (A) Enhanced ALOS DEM data showing clearly the fault segments which oriented in north-south direction and cover Mae Hong Son province. (B) Boxes with number indicate selected areas for morphotectonic landforms using enhanced ALOS DEM and Google Earth images interpretation. 32

Figure 17 Detail interpreted map from ALOS DEM at Ban Pha Bong show offset stream of Sa Mad river is about 7.9 km. from right lateral strike-slip fault movement. Location shows in Figure 16B. 33

Figure 18 Detail interpreted map from ALOS DEM at Ban Mae Surin show offset stream of Sa Surin river is about 9.5 km. from right lateral strike-slip fault movement. Location shows in Figure 16B. 34

Figure 19 Detail interpreted map from ALOS DEM at Mae Sariang show offset stream of Huai Mae Han is about 4.6 km (north) and Huai Mae Salab is about 4.3 km (south) from right lateral strike-slip fault movement. Location shows Figure 16B. 35

จุฬาลงกรณ์มหาวิทยาลัย
Chulalongkorn University

Figure 20 Detail interpreted map from ALOS DEM at Sob Moei show shuttle ridge which is the ridge moved out from the originally mountain from right lateral strike-slip fault movement. Location shows in Figure 16B. 36

Figure 21 Detail interpreted map from Google Earth with geologic map at Ban Huai Pong show triangular facets from normal fault movement. Location shows in Figure 16B. 37

Figure 22 Detailed interpretion map from Google Earth with geologic map at Tham Pla – Pha Suea National Park show anticline folds with N-S fold axes and small basins that are occurred by subsidence parallel with the MHSF. Location shows in Figure 16B. 38

Figure 23 Topographic profile across the MHSF (Northern part). Profile locations shown in inset map. Brown lines show lower (dashed) and upper (dotted) of paleotopography and red line (dashed) show fault. 42

Figure 24 Topographic profile across the MHSF (southern part). Profile locations shown in inset map. Brown lines show lower (dashed) and upper (dotted) of paleotopography and red line (dashed) show fault. 43

Figure 25 Graph showing total offsets down to west and east plotted along the length of the fault. Location shown in Figure 23 and Figure 24. 44

Figure 26 (A) Enhanced ALOS DEM Map showing the location of trenches and road-cut exposure which were examined for a paleoearthquake study. (B) Index map for detailed survey..... 49

Figure 27 (A) Hill shade ALOS DEM and (B) Google Earth image show the location of the Ban Yod trench site, MHSB. C) Photograph of the north trending mountain range, showing the fault scarp and triangular facet covered mostly by tree. Note that red line is the fault line, and yellow triangular is triangular facet. Location shows in Figure 26B. 50

Figure 28 (A) Hill shade ALOS DEM and (B) Google Earth image show the location of the Khun Yuam trench site. C) Photograph of the north trending mountain range,

จุฬาลงกรณ์มหาวิทยาลัย
Chulalongkorn University

showing the fault scarp covered mostly by tree. Note that red line is the fault line, and yellow triangular is fault scarp. Location shows in Figure 26B. 51

Figure 29 (A) Hill shade ALOS DEM and (B) Google Earth image show the location of the Mae Tha Lu trench site, MSB. C) Photograph of the north trending mountain range, showing the triangular facet covered mostly by tree. Note that red line is the fault line, and yellow triangular is triangular facet. Location shows in Figure 26B..... 52

Figure 30 (A) Photograph of Doi Wiang Luang area. (B) and (C) Closed-up photographs show the fault traces were found on the wall. (Red lines). 54

Figure 31 Road cut outcrop section and wall log section on the north wall at Doi Wiang Luang showing sediment stratigraphy, fault orientation and sample location for dating. Location shows in Figure 26A. 55

Figure 32 Paleoearthquake trench section and wall log section on the north wall at Ban Mae Tha Lu showing sediment stratigraphy, fault orientation and sample location for dating. Location shows in Figure 26A. 57

Figure 33 Paleoearthquake trench section and wall log section on the south wall at Ban Mae Tha Lu showing sediment stratigraphy and fault orientation. Location shows in Figure 26A. 58

Figure 34 (A) Photograph of Khun Yuam area. (B) Closed-up photograph shows discontinuity of sediment layer that it is possibly a soft sediment deformation and (C) Closed-up photographs show the fault traces were found on the wall. (Red lines)... 60

Figure 35 Paleoearthquake trench section and wall log section on the north wall at Ban Khun Yuam showing sediment stratigraphy, fault orientation and sample location for dating. Location shows in Figure 26A. 61

Figure 36 Paleoearthquake trench section and wall log section on the south wall at Ban Khun Yuam showing sediment stratigraphy and fault orientation. Location shows in Figure 26A. 62

จุฬาลงกรณ์มหาวิทยาลัย
Chulalongkorn University

Figure 37 (A) Photograph of Ban Yod area. (B) and (C) Closed-up photographs show the fault traces were found on the wall (Red lines). (D) Closed-up photograph shows discontinuity of sediment layer that it is possibly a soft sediment deformation. 65

Figure 38 Paleoearthquake trench section and wall log section on the north wall at Ban Yod showing sediment stratigraphy, fault orientation and sample location for dating. Location shows in Figure 26A. 66

Figure 39 Paleoearthquake trench section and wall log section on the south wall at Ban Yod showing sediment stratigraphy and fault orientation. Location shows in Figure 26A. 67

Figure 40 Chart of annual dose and equivalent dose for OSL dating, (modified after Frankel et al. (2015)) 69

Figure 41 The Riso TLD dosimeter installed at Department of Geology Faculty of Science, University of Cincinnati, USA. 72

Figure 42 Trench-log stratigraphy and photograph show fault orientation and OSL ages of sediment layers on road-cut wall of Doi Wiang Luang site. Location shows Figure 26A. 75

Figure 43 Trench-log stratigraphy and photograph show fault orientation and OSL ages of sediment layers on north wall of Mae Tha Lu site. Location shows Figure 26A. 75

Figure 44 Trench-log stratigraphy and photograph show fault orientation and OSL ages of sediment layers on north wall of Khun Yuam site. Location shows Figure 26A. 76

Figure 45 Trench-log stratigraphy and photograph show fault orientation and OSL ages of sediment layers on north wall of Ban Yod site. Location shows Figure 26A. . 76

Figure 46 Length versus width plot for natural pull-apart basins (data from Aydin and Nur (1982)) and pull-apart basins in Mae Hong Son area from this study. 81

จุฬาลงกรณ์มหาวิทยาลัย
Chulalongkorn University

Figure 47 Simplified model explaining the neotectonics of the MHSF, high elevation area between the MHSB and the MSB is defined as the Khun Yuam Linkage Zone (KYLZ). 82

Figure 49 Diagram showing the depositional ages of sediments in the road-cut wall and trenches from the OSL ages and paleoearthquake events. 86

Figure 50 Comparative chart of the regional tectonic events (modified from Kaewpradit., 2018 and Morley et al., 2011) and the evolution of the MSB from this study. 88

จุฬาลงกรณ์มหาวิทยาลัย
CHULALONGKORN UNIVERSITY

CHAPTER I
INTRODUCTION

Background

Thailand has experienced many moderate earthquakes (magnitude 3–6) and several large earthquakes (magnitude ≥ 6) since at least 624 BC from both historic records (Nutalaya, Sodsri, and Arnold, 1985) and instrumental records (TMD, 2018 and USGS, 2018) (Figure 1). The earthquakes have been detected along major fault traces in northern Thailand. In 2014, the largest instrumentally recorded earthquake and caused the largest amount of damage in Thai history occurred with a *Mw* 6.2 by the Mae Lao Fault, Chiang Rai Province, northern Thailand (see Figure 1). More than 50,000 people felt this earthquake (also felt in Bangkok) and more than 15,000 buildings were damaged, resulting in one death and 107 injuries (Department of Disaster Prevention and Mitigation at Chiang Rai, 2014).

Based on earthquake data recorded in northern Thailand and morphotectonic landforms, the Mae Hong Son Fault (MHSF) can be delineated and classified as one of the active faults in Thailand (Charusiri et al., 2007 and DMR, 2019). In detail, the MHSF clearly indicated by geological and remote sensing investigations. The fault is a sharp lineament and consists of several fault segments as shown Figure 2. The fault has a length of at less 200 kilometers that extends in north-south direction from Muang Mae Hong Son, Khun Yuam, Mae La Noi and Mae Sariang Districts of Mae Hong Son Province to the northern part of the Tha Song Yang District, Tak Province. In 1975, a moderate earthquake of m_b 5.6 (body wave magnitude determined by the Thailand Meteorological Department: TMD) in the southern part of the MHSF, people in northern and central parts of Thailand felt this earthquake (also felt in Myanmar) and this event caused minor damage in the Mae Hong Son Province and surrounding area. This event indicates that there are possibly related to the MHSF. Present-day morphotectonic landforms also suggest on-going activity along the fault.

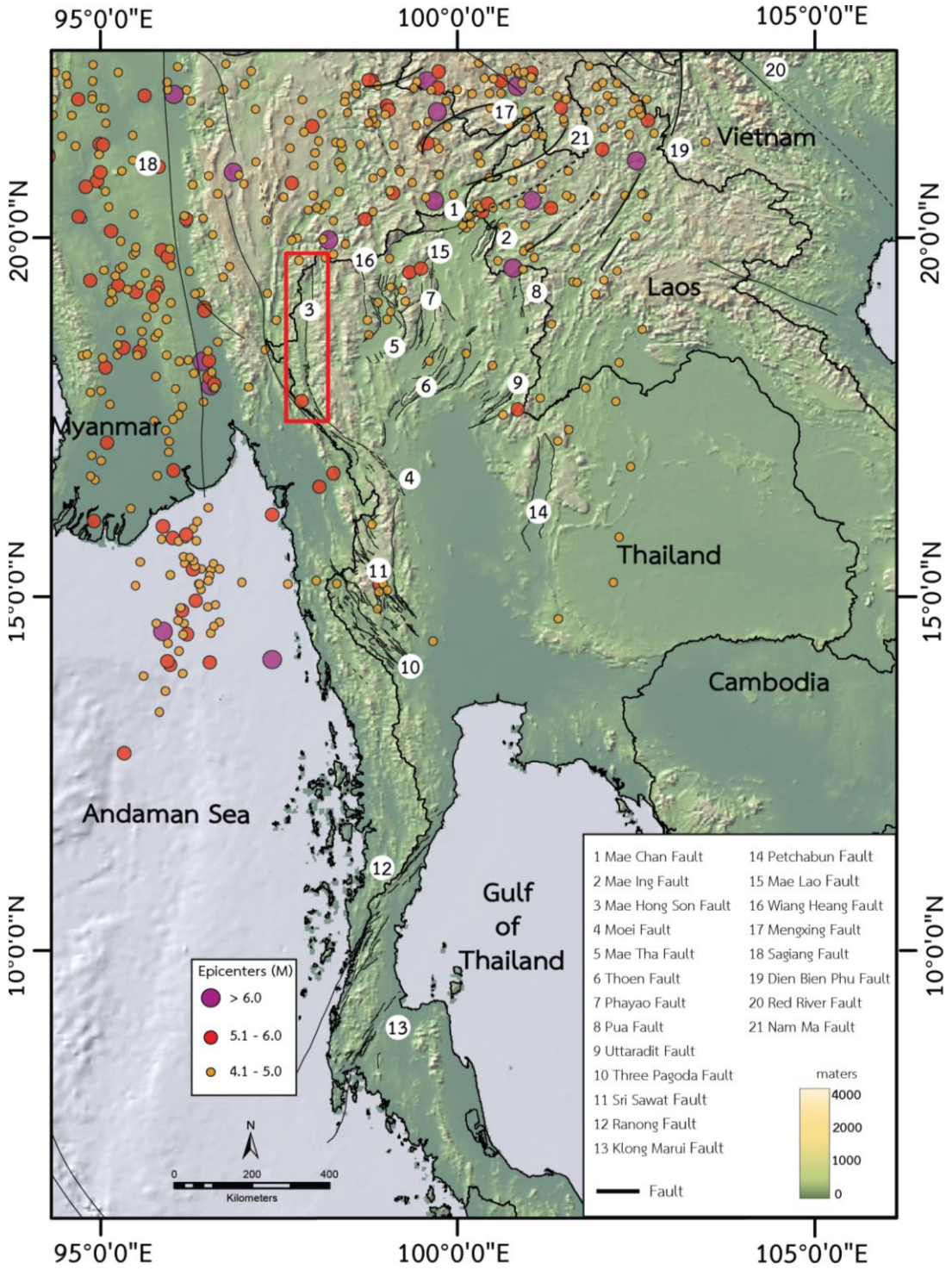

Figure 1 Map of Thailand and adjacent areas showing major active faults (compiled from DMR (2018), Wang et al. (2014) and Morley, Charusiri, and Watkinson (2011)) and epicentral distribution from 1912 to 2018 (TMD, 2016 and USGS, 2016). The rectangle shows the location of the study area.

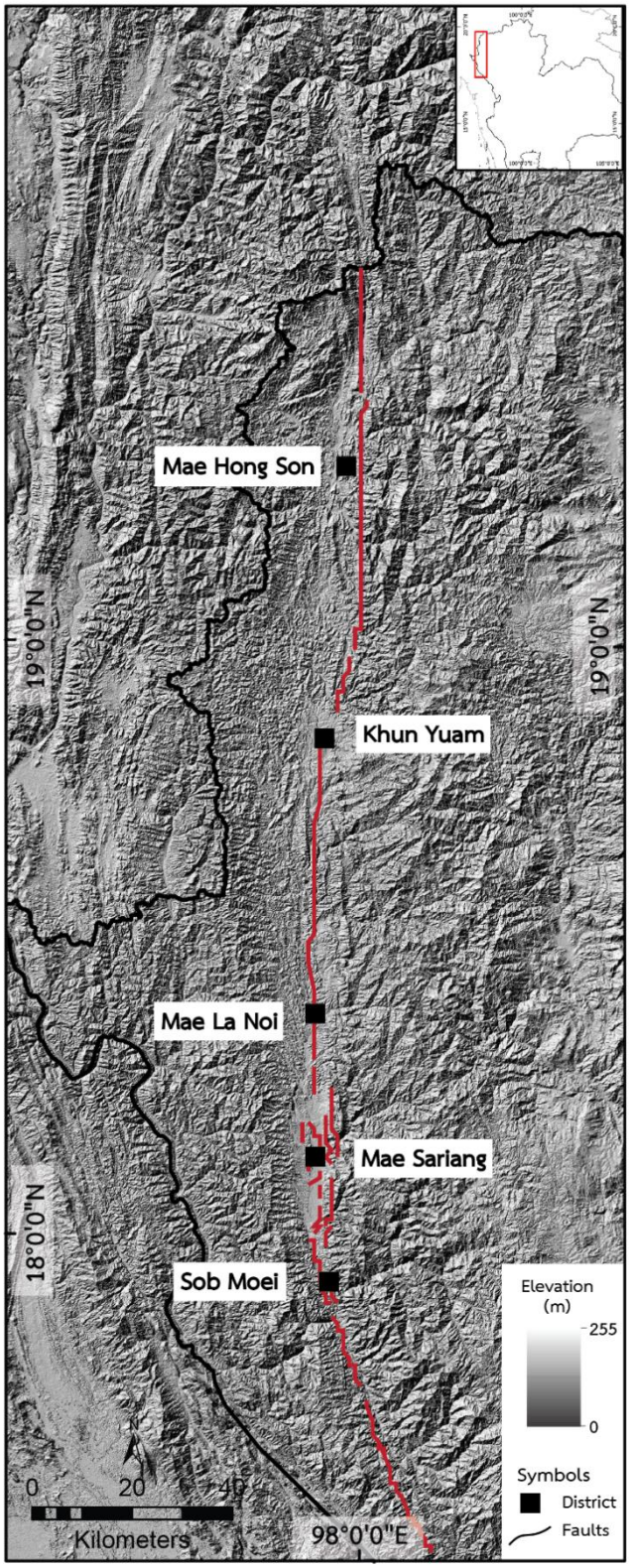

Figure 2 Map of the MHSF shows fault segments with north-south direction (modified from DMR, 2019).

The MHSF is important because it is the fault with a trend parallel and closes to the Sagaing Fault in Myanmar as showing in Figure 1. The detailed studies of neotectonics and paleoearthquakes were conducted by DMR (2007) and Wiwegwin et al (2014). However, recent study on neotectonics and paleoearthquakes by Wiwegwin et al. (2014) reported that the MHSF is an active fault and there were at least eight earthquake events occurred within the Mae Hong Son area in the last 78,000 years with a recurrence interval of 10,000 years. They also suggested that there is a low possibility of a large earthquake on the MHSF. In addition, an analysis of the seismic hazard by probabilistic seismic hazard analysis (PSHA) by Pailoplee and Charusiri (2016) found that 22% of the Mae Hong Son region has the potential to generate earthquakes annual magnitude of 7.0 within 50 years.

Thus, to better understand and to clarify the nature of seismicity in the Mae Hong Son area, the paleoearthquake of faults along the MHSF was examined. It is essential to use new data (updated remote-sensing data), new techniques, more systematic and more detailed surveys for investigation paleoearthquake of the Mae Hong Son area. This study is studying about the morphotectonic landforms resulting from the fault movements using Digital Elevation Model (DEM) with high resolution 12.5 m together with the satellite images to describe the characteristics of the MHSF. Moreover, the paleoearthquake investigation is being investigated the history of displacement along the fault.

Objectives of the study

The purposes of this study are to identify and characterize morphotectonic landforms resulting from fault movements along the MHSF base on DEM with resolution 12.5 m, Landsat 7 with resolution 30 m from National Aeronautics and Space Administration (NASA) and satellite images from Google Earth Pro. In addition, this study investigates the behavioral characteristic of the fault (slip rate and recurrence intervals) and determine the numbers of paleoearthquake events along the MHSF.

Location of study area

This study focuses on the MHSF in the northern part of Thailand. The study area for remote sensing interpretation (Chapter III) bounded by latitude 17°38'N to 19°48'N and longitude 97°20'E to 98°39'E covered Mae Hong Son province, the total study area is approximately 25,587 km^2. The study area for paleoearthquake investigation (Chapter IV) located at Ban Yod fault segment, Doi Wiang Luang fault segment, Khun Yuam fault segment and Mae Tha Lu fault segment along the MHSF.

Methodology

The overview methodology of this study can be described in six steps (Figure 3) as following;

Firstly, reviewing background information of the MHSF including previous studies, geological maps, satellite images and DEM and reviews basic understanding about the neotectonics in study area. This step presented in Chapter I and Chapter II.

Secondly, regional geomorphology is interpreted using remote-sensing techniques. The DEM with high resolution of 12.5 m and satellite images have been analyzed for constructing of lineaments and basin analysis. Morphotectonic landforms associated with the faults are also assessed and interpreted. Results are presented in Chapter III.

จุฬาลงกรณ์มหาวิทยาลัย
Chulalongkorn University

Thirdly, the results of remote sensing interpretation and morphotectonic landforms were applied for evaluating the locations of the active faults and selecting locations for trenching sites. Trenches were excavated across fault traces. The stratigraphic units and the faults exposed were recorded and mapped. Soil samples were collected Optical Stimulated Luminescence (OSL) dating. Results are presented in Chapter IV.

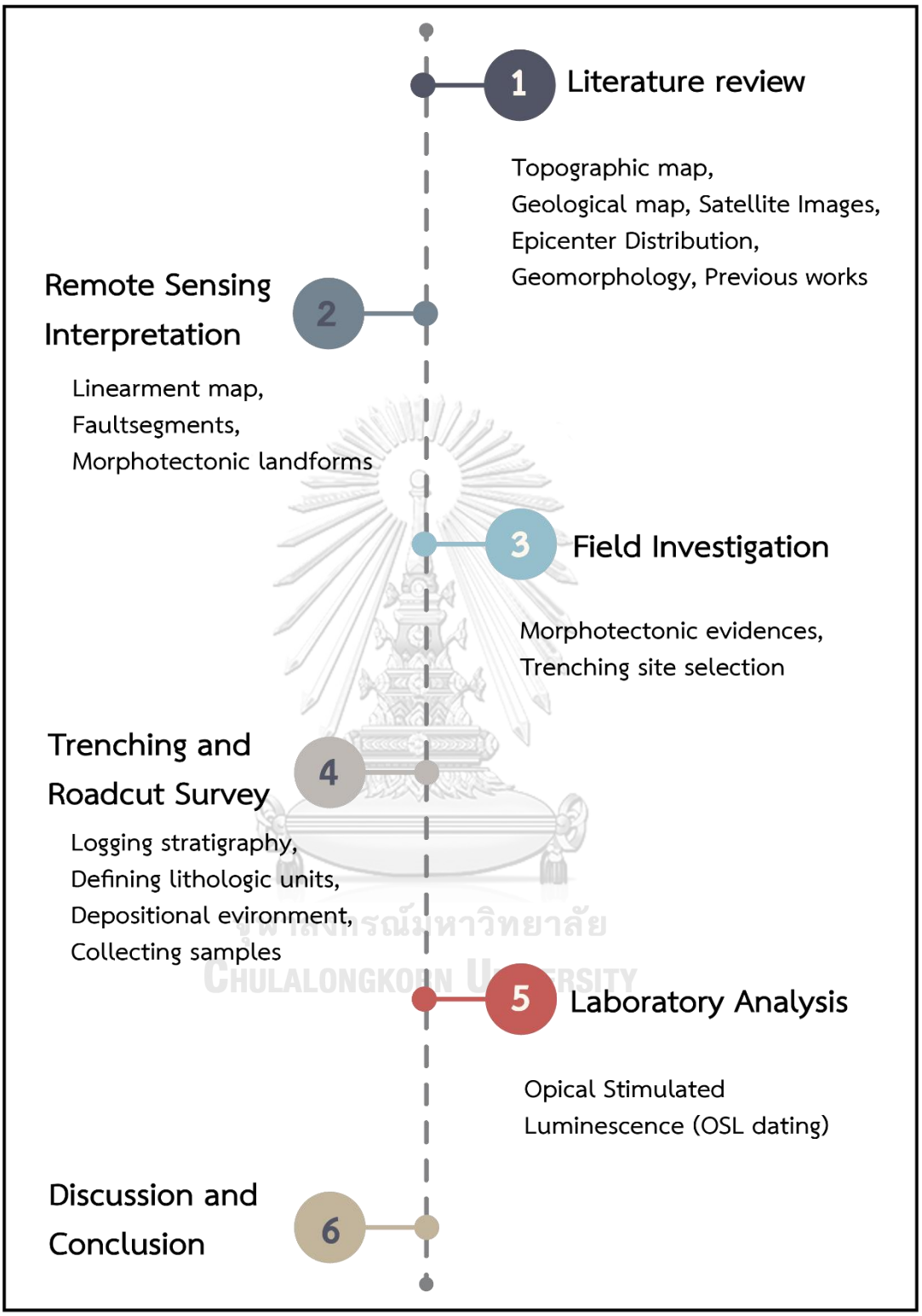

Figure 3 Simplified flow chart illustrating the methodology applied in this study.

Finally, all the data and results from this study and previous works are applied to determine the number of paleoearthquake events, estimated slip rates and recurrence intervals for the faulting.

Thesis Outline

This thesis provides an emphasis on neotectonics geomorphology and geochronology of the MHSF in succession of chapters as following:

Chapter I	an introduction, objective, study area, methodology and previous study.
Chapter II	literature reviews of study area
Chapter III	remote sensing interpretation
Chapter IV	paleoearthquake investigation
Chapter V	discussion
Chapter VI	conclusion

จุฬาลงกรณ์มหาวิทยาลัย
Chulalongkorn University

CHAPTER II
LITERATURE REVIEW

Tectonic setting

The interaction of three major lithospheric plates consists of the Eurasian, the Indian, and the Philippine plates have dominated the modern tectonic model of Southeast Asia (Fenton, Charusiri, and Wood, 2003) (Figure 4). Thailand has an intraplate setting within the Eurasian plate which is enclosed by colliding boundaries, with the Sunda arc to the south and the Andaman thrust to the west along the Sumatra-Java trench. The experiments with plasticine of Tapponnier et al. (1982) indicated many similarities between the results of their experiments and those of the geology of the Southeast Asia.

The collision of Eurasian with Indian plates around 50 Ma (Middle Eocene) cause the Cenozoic tectonics of Southeast Asia, it resulted shortening across the Himalayan Orogen (Peltzer & Tapponnier, 1988). During the first 20-30 million years of the collision as Indian plate pushed into the southern margin of the Eurasian plate, Indochina rotated about 25° clockwise and extruded to the southeast by approximately 800 km along the Red River and Wang Chao-Three Pagodas fault zones (Peltzer & Tapponnier, 1988). As the collision progressed, extrusions migrated north towards the Altyn Tagh Fault. As the rotation continued the left-lateral sense of motion of the Red River, Mae Ping and Three Pagoda faults were reversed to a right-lateral (Allen et al., 1984; Peltzer and Tapponnier,1988).

The opening of the tertiary basins by transtensional stress was caused by a differential slip between the main strike-slip faults in the Red River, Mae Ping, Three Pagodas, and Sumatra fault zones (Ducrocq et al., 1992). In Thailand, the tertiary basins are grabens or half grabens, typically bounded by north to northwest striking normal faults (Lorenzetti, Brennan, & Hook, 1994; Polachan et al., 1991) with

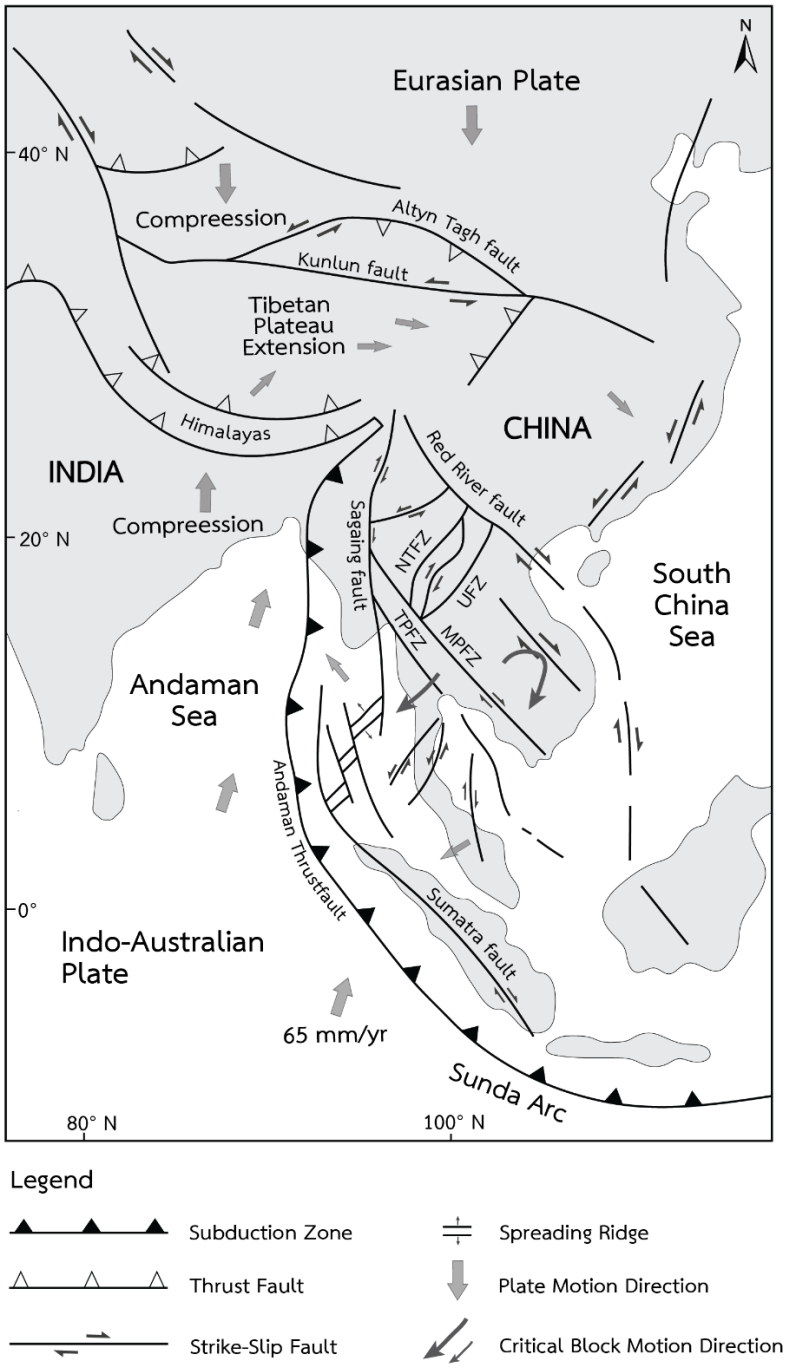

Figure 4 Major tectonic elements in Southeast Asia and Southern China. Arrows show relative directions of motion of crustal blocks during the Late Cenozoic. MPFZ - Mae Ping Fault Zone; NTFZ – Northern Thailand Fault Zone; TPFZ - Three Pagodas Fault Zone and UFZ - Uttaradit Fault Zone (from Fenton et al. (2003)).

geometry and location controlled by the north-south-trending structural grain in preTriassic rocks and pre-existing northwest-southeast trending, strike-slip faults (O'Leary & Hill, 1989). Throughout Thailand basin evolution follows similar chain of events. The main phase of strike-slip tectonism with extensive fluvial sedimentation resulted in rapid extension (Oligocene-Early Miocene) followed by lacustrine sedimentation as basins became increasingly isolated (Early-Middle Miocene). A flood of rough terrigenous clastics took place as Lacustrine sedimentation ceased, which suggests a period of rapid, localized uplift (Middle-Late Miocene).

Geological setting

Geological data of the study area is modified based on geologic map with scale 1:250,000 (DMR., 2007) of Mae Hong Son Province and it consists mainly of several rock units of sedimentary and meta-sediments rocks and intrusive rocks. The rocks units ranging from Paleozoic to Quaternary in the Mae Hong Son area; these rock units were cut by the MHSF. In this thesis, the rock units are explained only along and within the MHSF (Figure 5 and Figure 6). Details of each rock unit are as follow;

The Lower Paleozoic

The Lower Paleozoic are common cropped out in the eastern area of the Mae Hong Son province. These have been strongly deformed and largely metamorphosed; there are mainly low-grade quartzite, schistose rocks and calc-silicate (Bunopas, 1981).

Cambrian rocks or The Pha Bong quartzite (Bunopas, 1981) is the oldest section of Mae Hong Son are with its type section at Pha Bong Dam. This formation is distributed in the north to east of Muang Mae Hong Son, Khun Yuam and Mae La Noi districts, northwest of Mae Sariang district, and northwest of Pai district. The generally low grade metamorphosed Pha Bong quartzite varies in color between pinkish brown and pale brown.

จุฬาลงกรณ์มหาวิทยาลัย
Chulalongkorn University

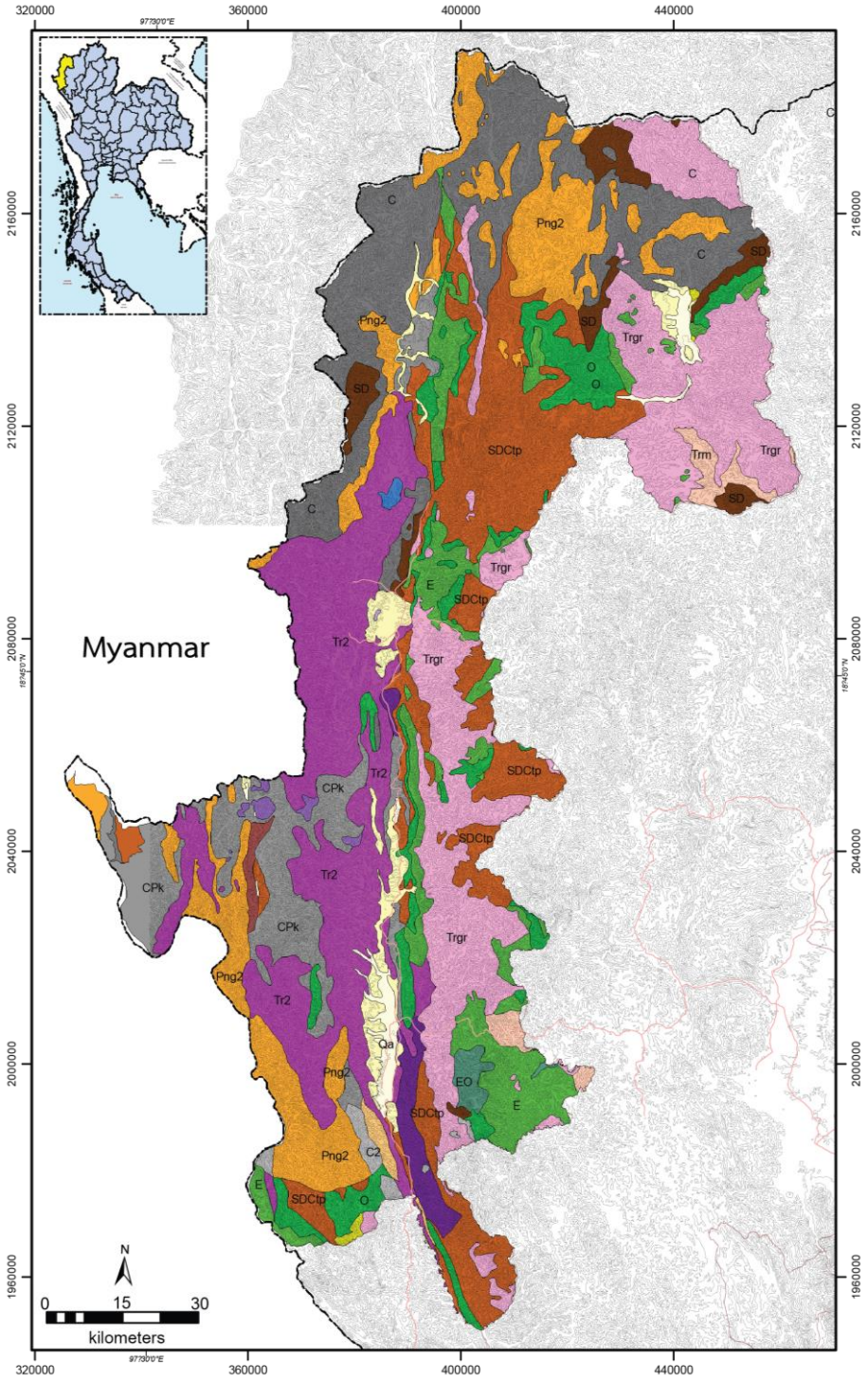

Figure 5 Geologic map on scale 1:250,000 of Mae Hong Son province showing the distribution of rock units. The explanation of these rock units shown in Figure 6 (from DMR (2007)).

EXPLANATION

SEDIMENT, SEDIMENTARY AND METAMORPHIC ROCKS		FORMATION/ GROUP	PERIOD	AGE (my)
Qa	Alluvial deposits: sandy clay, clayey sand, lateritic soil and clay		QUATERNARY	0.01
Qt	Terrace deposits: gravel, sand and laterite			
Tmm	Claystone, siltstone, sandstone, mudstone, diatomite and lignite	Mae Moh Formation	TERTIARY	66.4
J	Red conglomerate, reddish brown sandstine, intercalated with shale and mundstone		JURASSIC	210
TrJ	Greenish gray sandstone, reddish brown siltstone, limestone and conglomerate			
Tr_2	Shale, chert and thin-bedded limestone with bivalve fossils		TRIASSIC	245
Tr_1	Red conglomerate, red to reddish brown sandstone and shale			
PTr	Shale, siltstone and dark gray to greenish gray sandstone, intercalated with thin-bedded chert			
Png_2	Gray thick-bedded limestone, distinct karst topography and shale	Ngao Group	PERMIAN	286
Png_1	Sandstone, chert and gray shale			
C_2	Shale, siltstone and gray sandstone, siltstone interbedded with chert	Mae Tha Group	CARBONIFEROUS	360
CPk	Gray sandstone, gray shale, green to gray chert and limestone interbedded with shale			
C	Sandstone interbedded with gray shale, shale, conglomerate, chert, limestone and mudstone			
D	Shale interbedded with limestone and sandstone		DEVONIAN	408
SDCtp	Gray shale interbedded with limestone, with fossils of nautiloid, gastropod and conodont	Thong Pha Phum Group	SILURIAN	438
SD	Sandstone interbedded with siltstone and shale, limestone, phyllitic shale, with tentaculite fossils	Donchai Group		
O	Gray argillacous limestone interbedded with mudstone and shale, with fossils of conodont and nautiloid	Hod limestone, Thung Song Group	ORDOVICIAN	505
EO	White banded marble and quartz-mica schist			
E	Quartzite, sandstone interbedded with shale and slaty shale	Pha Bong Group	CAMBRIAN	570
IGNEOUS ROCKS				AGE (my)
TRgr	Igneous rock: biotite granite, hornblend biotite granite, muscovite granite, equigranular to porphyritic texture and fine-grained leucogranite			210-245
Trm	Migmatite, unclassified granite, gneiss, schist, quartzite and sandstone			

จุฬาลงกรณ์มหาวิทยาลัย
Chulalongkorn University

Figure 6 The explanation of geologic map of the Mae Hong Son province in Figure 5 (from DMR, 2007)

Cambrian – Ordovician rocks, found in the north and south of Mae La Noi district, eastern of Mae Sariang and Sob Moi districts. The rocks are mainly white banded marble and quartz-mica schist.

Ordovician rocks or known as Hot limestone (Bunopas, 1981), the type section is situated on the limestone terrain and oriented in north – south along west of Hot district, Chiang Mai province. This formation found in Mae Sariang, Pai, Mae La Noi, Khun Yuam and Muang Mae Hong Son districts. The rocks consist of gray argillaceous limestone interbedded with mudstone and shale and also found conodont and nautiloid in this rock unit.

Silurian – Ordovician rocks or Donchai Group (Piyasin, 1972), the type section is situated on the west of Hot district, Chiang Mai province. This rock unit is distributed at Ban Nam Piang Din (Pha Bong sub-district and Muang Mae Hong Son districts), Ban Mae Surin (Khun Yuam sub-district, Khun Yuam district), Ban Huai Heang and Ban Seang Kham Luen Khun (Tham Lod sub-district). The rocks consist of sandstone interbedded with siltstone and shale, limestone, phillitic shale and also found tentaculate fossils.

Silurian – Devonian – Carboniferous rocks or Mae Hong Son formation (Bunopas, 1981). Its type section represents shale, chert, limestone and sandstone at a quarry, south of Mae Hong Son province. This formation is distributed along the southwestern part of Muang Mae Hong Son district to eastern part of Khun Yuam, Mae La Noi, Mae Sariang and Sob Moi. The formation is characterized by brown to black chert intercalated with sandstone and brown shale. And found nautiloid, gastropod and conodont in this rock unit.

จุฬาลงกรณ์มหาวิทยาลัย
CHULALONGKORN UNIVERSITY

Devonian rocks found in the northwest of Mae Sariang and Sob Moi districts. The rocks consist of shale interbedded with limestone and sandstone.

The upper Paleozoic

Carboniferous rocks are distributed to the north of Mueang Mae Hong Son, Pai district, Mae La Noi and Mae Sariang districts of Mae Hong Son province. This group is subdivided into three formations from bottom upward, namely the Carboniferous formation (C), the lower Carboniferous formation (CPk) and the upper Carboniferous formation (C2), respectively.

Permian rocks or Ngao Group (Piyasin 1972), the type section is situated on the northwestern of Khun Yuam, Mae La Noi and Mae Sariang districts. This group is subdivided into two formations; the Kui Lom and Pha Huat Formations.

Cenozoic

The Cenozoic sedimentary are mainly young and semi-consolidated deposits. Shoreline sediment (Q) is composed of unconsolidated near-shore sediment, such as sand and fine sand with shell leavings and corals. Alluvial sediment (Qa) is deposited from active rivers covering some coast and tidal flat plain. Terrace deposits consist of pebble, sand, clay, and mud. Colluvial sediment (Qt) includes of gravel, sand, laterite and alluvial terrace this sediment often appears to follow the foothills and short hill.

จุฬาลงกรณ์มหาวิทยาลัย
Chulalongkorn University

Igneous rock

Igneous rock Triassic are mainly of intrusive igneous rocks which is granite. Granite in Mae Hong Son province is the central belt of Thailand. This belt formed a large north-south trending mountain range covers two areas; the eastern part of Khun Yuam and Pai districts.

Structural setting

Fault zone or MHSF zone trends in a N-S direction traverse the Mae Hong Son Basin (MHSB) and Mae Sariang Basin (MSB) from Myanmar to terminate at the Mae Ping fault zone with a total length of about 200 km via Mueang Mae Hong Son, Khun Yuam and Mae Sariang districts of Mae Hong Son province. This fault zone is separate the Mesozoic rocks from the Paleozoic rocks, and also the basins in this area are formed by this fault ((Baum et al., 1970)

Folds in the Mae Hong Son province are mainly asymmetrical folds, tight folds and overturned folds with N-S fold axes. Some fold axes are oriented NW-SE with some parallel with Mae Ping fault and MHSF. Large anticlines are found in many areas with inferred Precambrian rocks as the core of the anticline such as at Muang Mae Hong Son district where the inferred Precambrian rocks form a central body orientated in N-S direction and overlain by Ordovician limestone on both fold limbs. The fold axes of these anticlines are consistent with Triassic granite intrusions.

Neotectonics and active fault in the Mae Hong Son are

The MHSF in the northern part of Thailand has been studied for paleoearthquake and neotectonics since 1985. However, there are hardly any published papers on geology of the MHSF. Based on seismological and geological evidence, Nutalaya et al. (1985) were the first to introduce the concept of seismic source zones in mainland Southeast Asia into 12 zones (Figure 7), covers Thailand and neighboring countries. The MHSF is in zone G, covers the Northern Highlands of Thailand. This area consists of Mae Tha, Thoen, and Phrea faults. However, the MHSF is probably active in this area but more evidences on both seismicity and geology are needed before definite conclusions can be made. Chuaviroj (1991) studied major faults in Thailand and identified 13 faults including the MHSF. He said that MHSF was strike-slip faults and mainly trend in the north-south direction (Figure 8). Hinthong (1997) conducted a project titled “Study of Active Faults in Thailand”, and used geological, historical, and seismological data to identify 22 active faults and seismogenic regimes in Thailand and reported on the earthquakes that had occurred

จุฬาลงกรณ์มหาวิทยาลัย
Chulalongkorn University

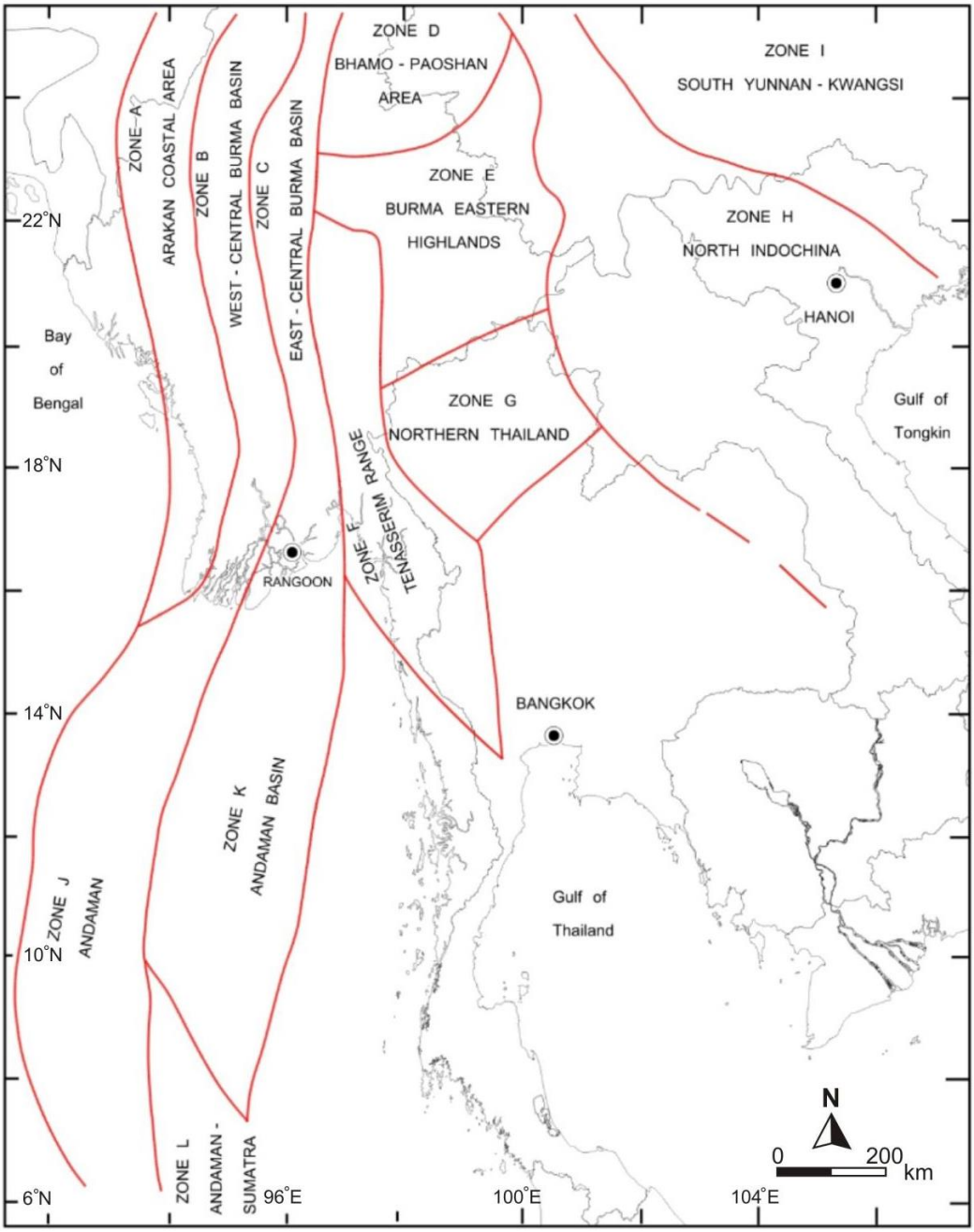

Figure 7 Seismic source zones in the Indochina region (from Nutalaya et al. (1985)) Note that study area (Mae Hong Son region) is in zone G.

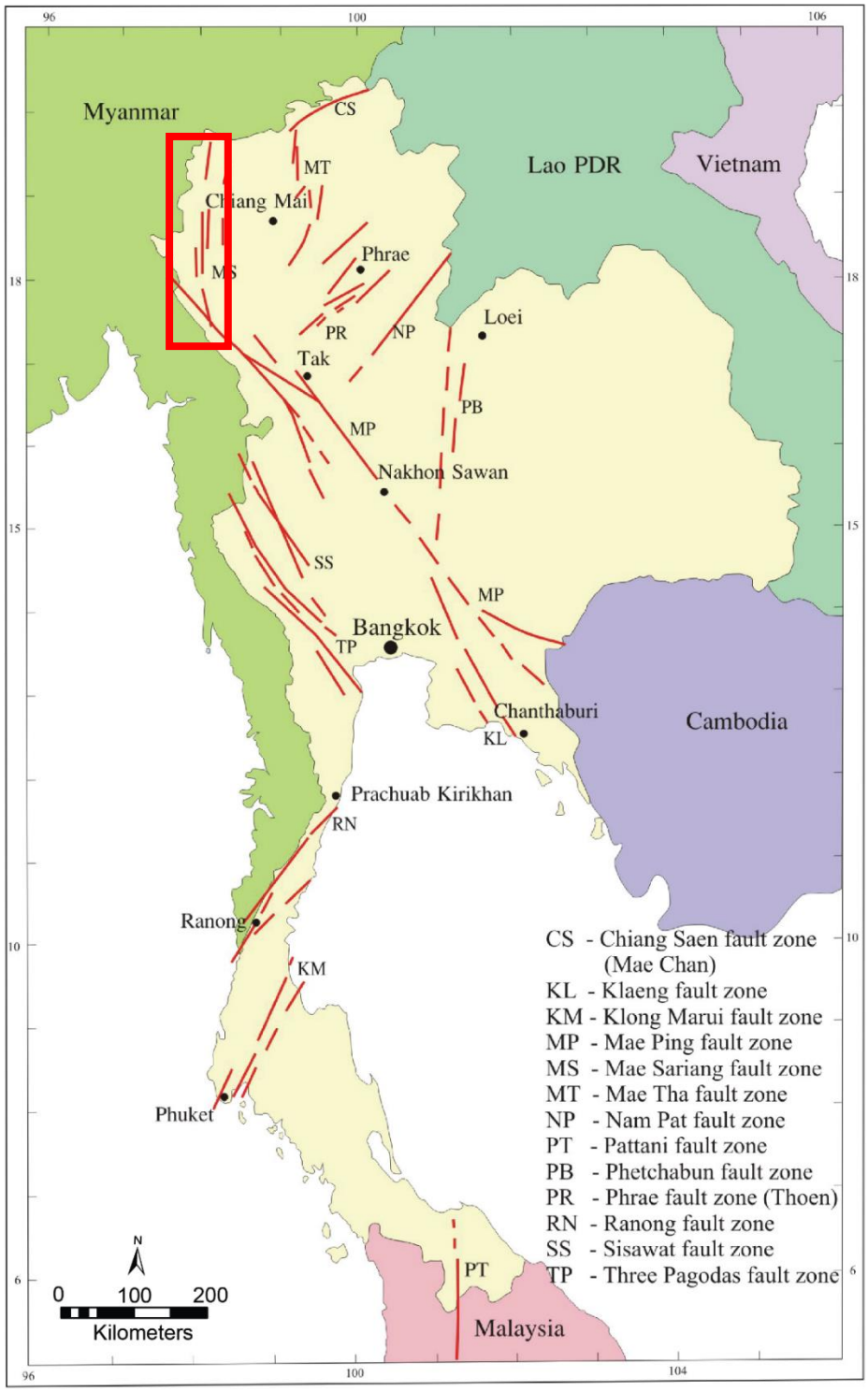

Figure 8 Map of major fault zones in Thailand which is the first active fault map in Thailand (from Chuaviroj (1991)).

in Thailand throughout the past 1,500 years. Many of these earthquakes were closely related to the Three Pagoda Fault, the Mae Ping Fault, and the MHSF.

Charusiri, Daorerk, and Supajanya (1996) applied several remote sensing techniques to a study of earthquakes in Thailand and neighboring countries and reclassed the active faults in Thailand into three classes, namely active, potentially active, and tentatively active based on results of morphotectonic and TL dating results. The MHSF has been classed as potentially active fault (Charusiri et al., 1998). Later, the active faults map was updated until the Department of Mineral Resource (DMR) has sent survey teams to investigated effects of the earthquake found that the fault with large quantity of energy of 15 active faults crosses upon 21 provinces (Figure 9). These faults may cause impact related to earthquake. In addition, DMR have been studying geological earthquake, active fault, geological condition and epicenter, Seismic hazard map of Thailand has been published (DMR, 2016) (Figure 10).

Based on field and geochronological evidences, Charusiri et al. (1996) suggested that the MHSF may have been active during the period of 27.3–1.6 Ma. A fault in the MSB has been interpreted as a splay fault of the active Mae Ping Fault to the south (Morley et al., 2007). Age dating by TL has revealed that the MHSF was active from 0.89 to 0.32 Ma (Hinthong, 1997). Wiwegwin et al. (2014) also reported the most recent movement upon Mae La Noi segment no. 1 of the MHSF occurred several thousand years ago. The MHSF has been classified as active by Hinthong (1997), Charusiri et al. (2007), and Wiwegwin et al. (2014).

จุฬาลงกรณ์มหาวิทยาลัย
Chulalongkorn University

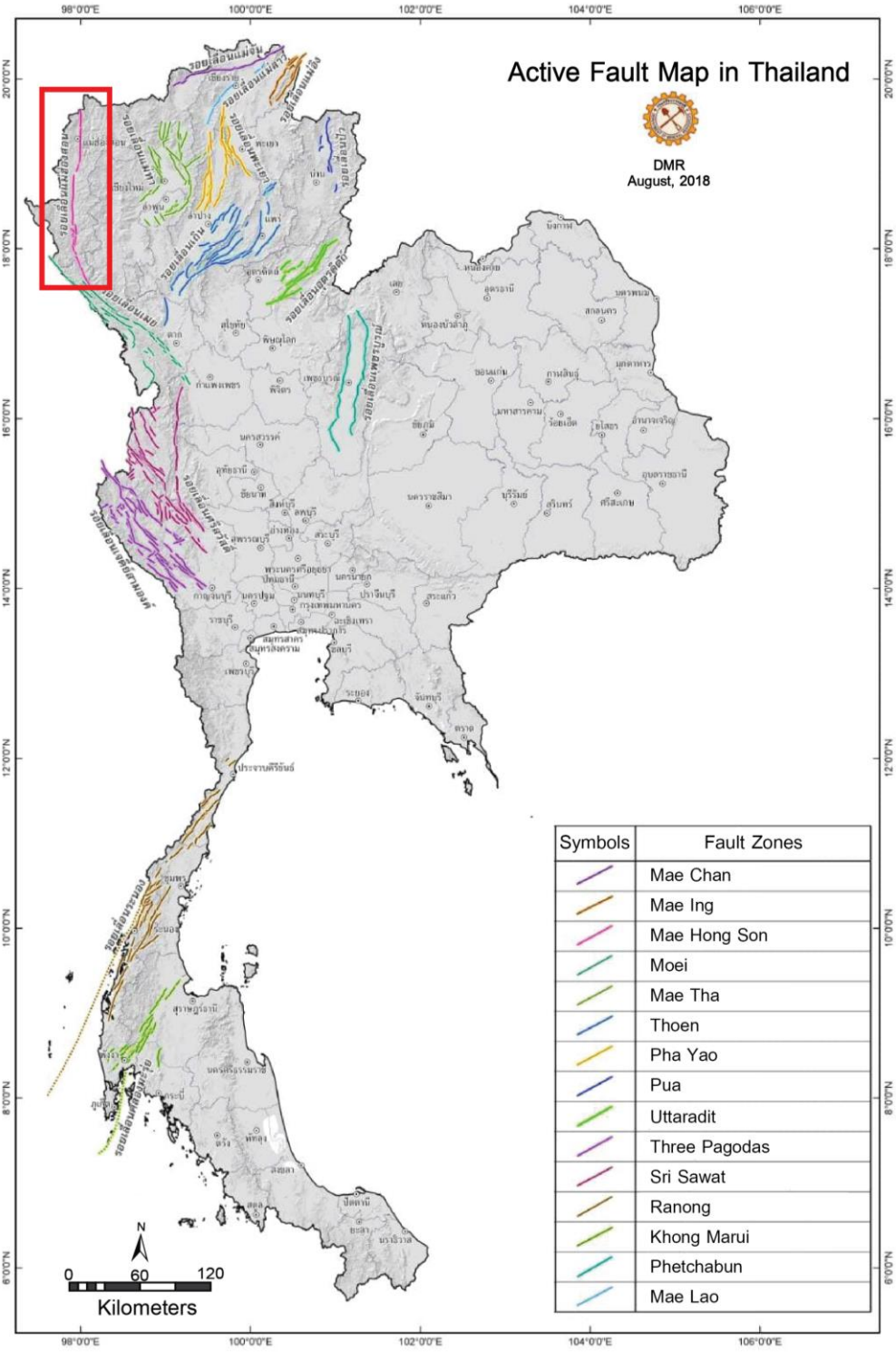

Figure 9 Map shows active faults in Thailand consist of 15 fault zones (from DMR (2018)). Red box shows the study area.

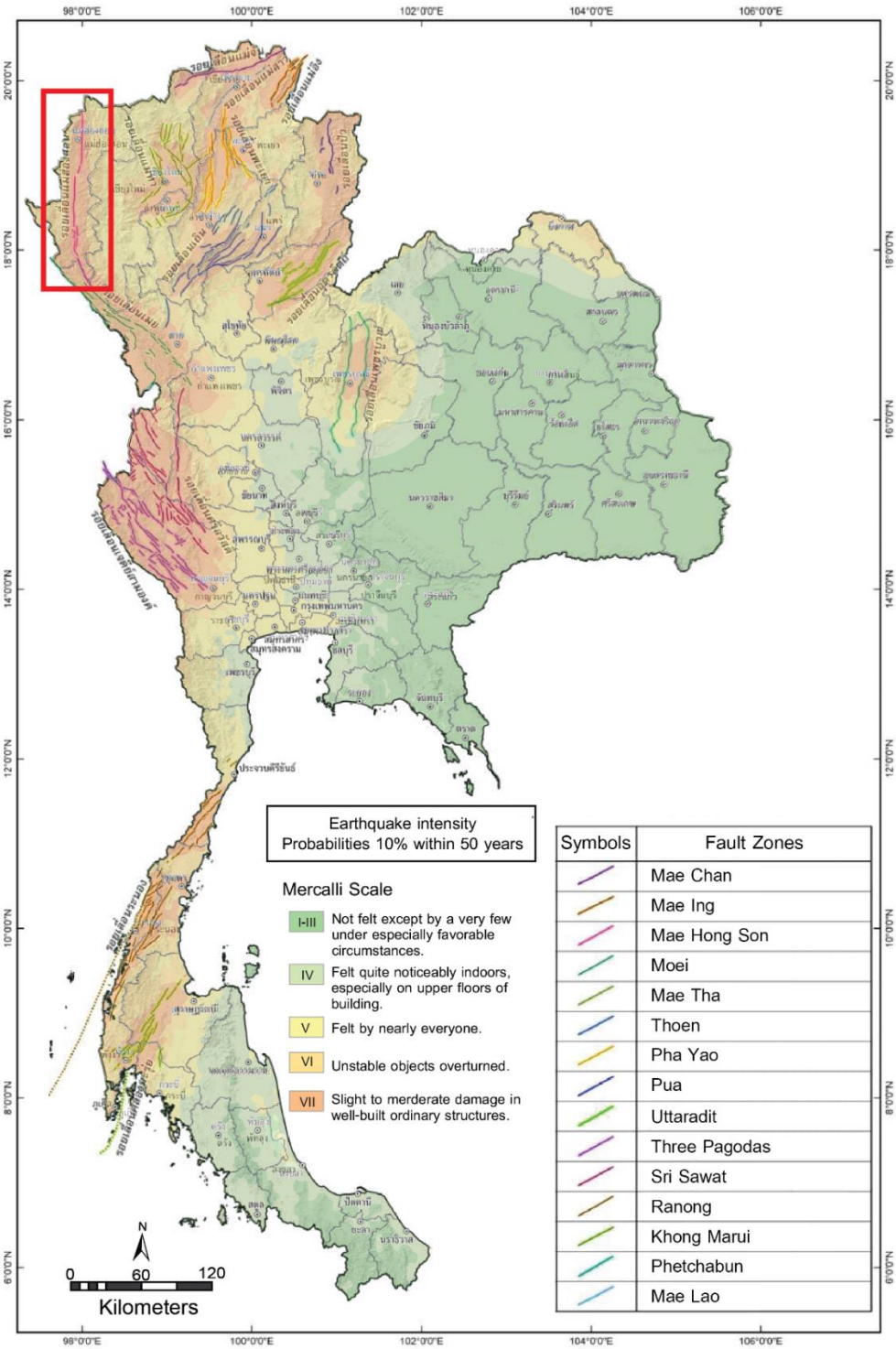

Figure 10 Map shows seismic hazard zones in Thailand related with 15 active fault zones (from DMR (2016) and DMR (2018)). Red box shows the study area.

Wiwegwin et al. (2014) interpreted remote sensing and aerial photographic of the MHSF, located in the Mae Hong Son region, northern Thailand, shows several fault lines in the region, trending mainly NE–SW, NW–SE, and N–S. The main morphotectonic landforms associated with the MHSF are fault scarps, offset streams, linear valleys, triangular facets, offset ridge crests, hot springs, and linear mountain fronts. A trench, a quarry, and a road cut in Cenozoic strata were applied to analyze fault geometries in the area. The author identified eight paleoearthquake events from trenching, quarry, and road-cut data, and from optically stimulated luminescence (OSL) and thermoluminescence (TL) dating. The slip rate was estimated as 0.03–0.13mm/yr. There is a low possibility of a large earthquake on the MHSF in the near future. The probabilistic seismic hazard analysis was studied by Pailoplee and Charusiri (2016). They identified active fault zones using remote-sensing data and a statistical investigation of recorded earthquakes to locate potential sources of future earthquakes and estimate the maximum possible magnitudes and recurrence intervals using the probabilistic seismic hazard analysis method (PSHA). The results suggest that the greatest potential to generate earthquakes is the western of Thailand (Figure 8). The first is Kanchanaburi province, a potential to generate earthquakes annual magnitude of 7.0 within 50 years estimate at 37%. On the behalf on Mae Hong Son province is the second, a potential to generate earthquakes annual magnitude of 7.0 within 50 years estimate at 22% (Figure 11).

จุฬาลงกรณ์มหาวิทยาลัย
Chulalongkorn University

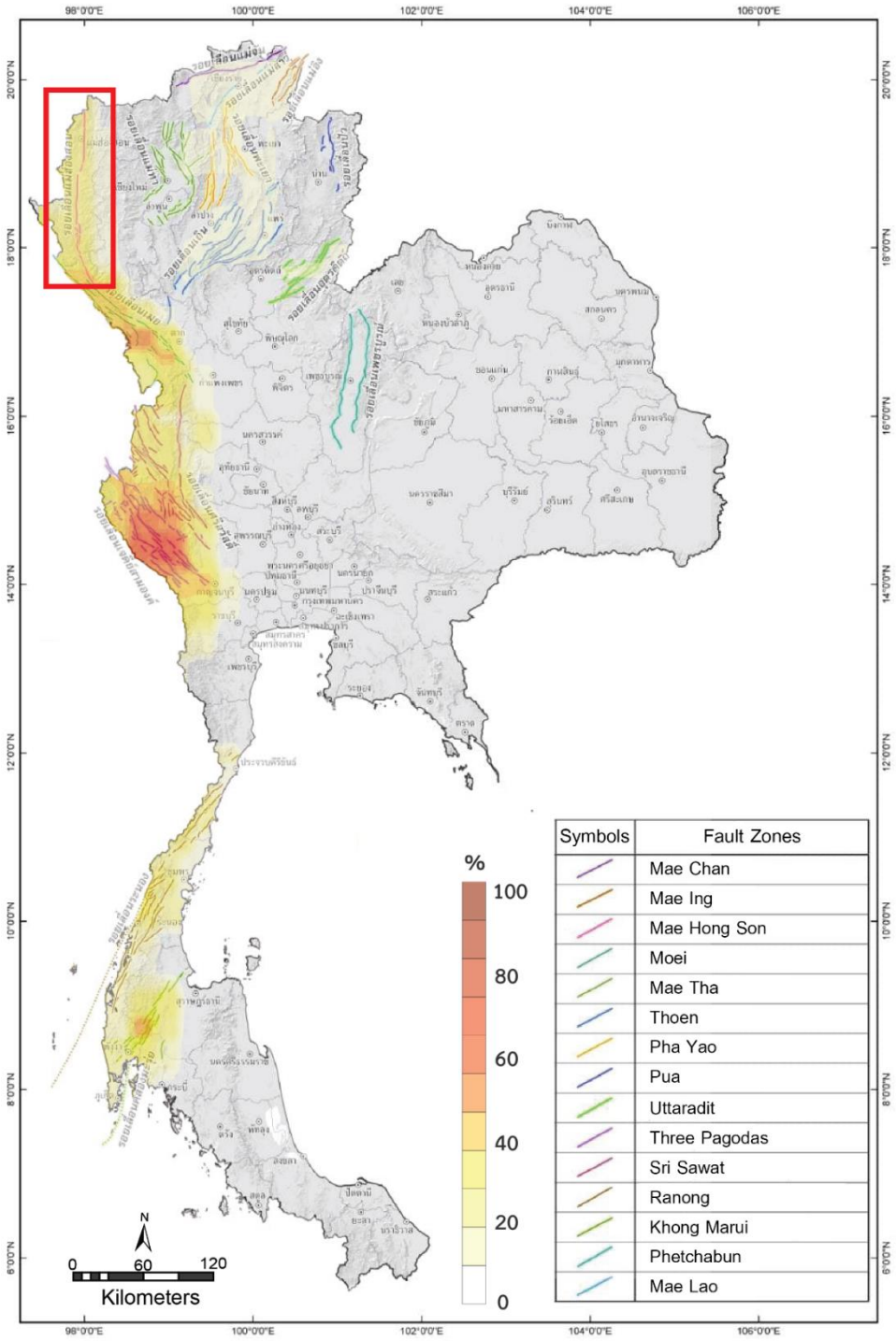

Figure 11 PSHA map of Thailand showing the probabilities (%) that the greatest potential to generate earthquakes is the western of Thailand and related with 15 active fault zones (from Pailoplee and Charusiri (2016) and DMR (2018)). Red box shows the study area.

CHAPTER III
REMOTE SENSING INTERPRETATION

The remote-sensing is the most important tools and very useful in the planning process of the environment and it is also valuable for detecting and mapping many types of natural hazards. In this chapter, the remote-sensing data are compiled and analyzed in this study to infer the active faults in study area. The purpose of remote-sensing interpretation is to identify and to characterize morphotectonic landforms on the earth surface, resulting from strike slip fault movement along the MHSF such as fault scarps, triangular facets, shutter ridges, offset streams and pull-apart basin etc. (Figure 12 and Figure 13)

The remote-sensing interpretation in this chapter composes of three sections, the first section is focused on investigate geological lineaments, fault segment and Cenozoic basins interpretation in a regional scale using Landsat 7 Enhanced Thematic Mapper (Landsat 7 ETM+) and Space Shuttle Radar and Topography Mission Digital Elevation Model (STRM DEM) imageries. The second section describes fault segmentation of the MHSF, and criteria used. The last section is focused on the detailed study of morphotectonic landforms and results on morphotectonic interpretation of individual selected segments. In addition, morphotectonic landforms, which include fault segments and morphotectonic evidences of fault movements are also shown in this chapter.

จุฬาลงกรณ์มหาวิทยาลัย
Chulalongkorn University

Satellite images and interpretation

Satellite images are imageries data from a multitude of cameras, which instruments, and sensors are installed in satellites orbiting the earth. Satellites record the electromagnetic radiation emitted or reflected by the surface or objects. Satellites record the electromagnetic radiation emitted or reflected by the surface. The data are converted to images or rasters, where each element represents a

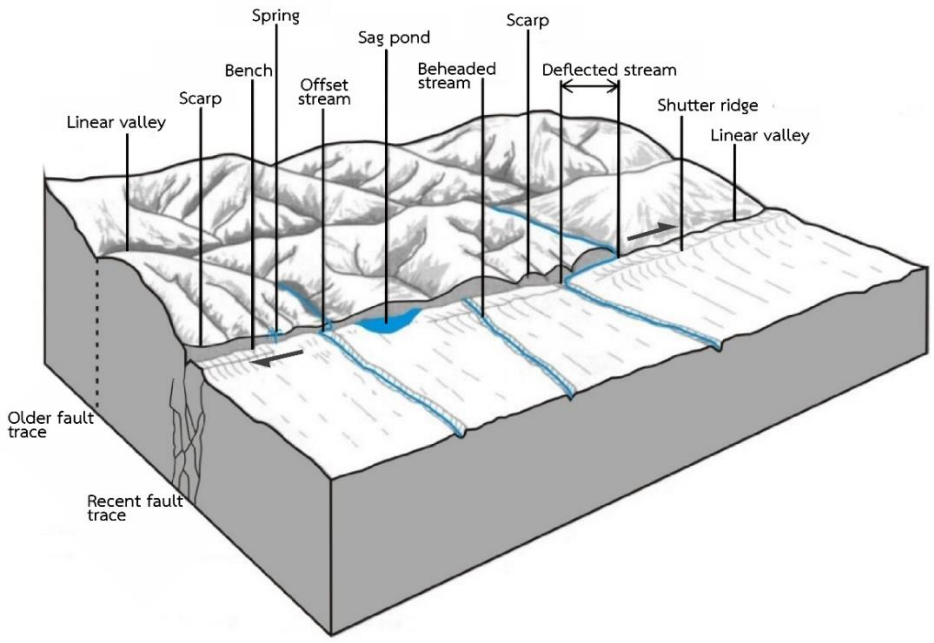

Figure 12 Morphotectonic landforms associated with active strike-slip movement (from Keller and Pinter (1996)).

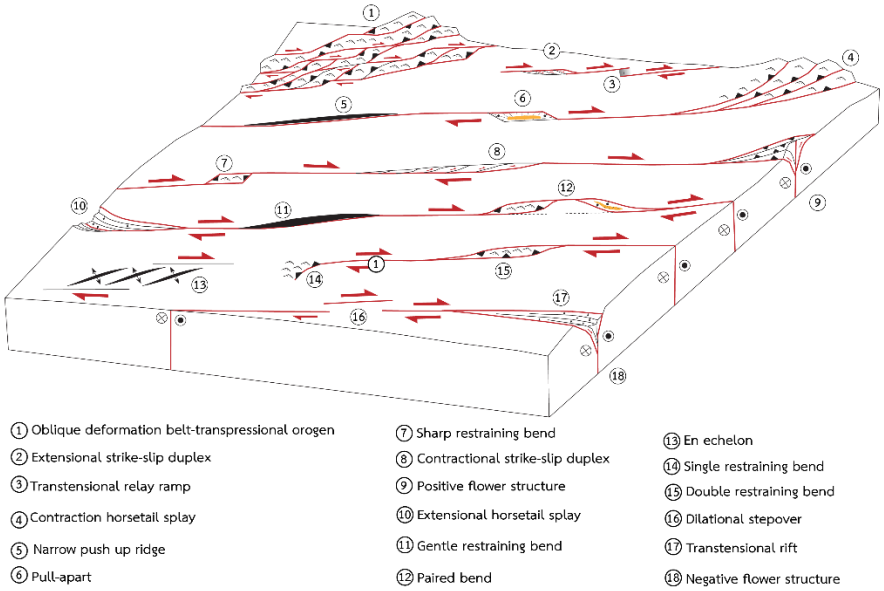

Figure 13 Features associated with strike-slip restraining and releasing bends (from Cunningham and Mann (2007))

measurement in that point. Data points can be visible wavelengths (e.g. color), but also heights, surface material or temperature. The remote sensing data provided from these are very useful for various applications, such as climate monitoring, mapping and monitoring of disasters. In this study Landsat 7 ETM+ and STRM DEM were applied to investigate morphotectonic landforms as describe below;

1. Landsat 7 ETM+

The Landsat 7 satellite was successfully launched from Vandenburg Air Force based on April 15, 1999. A single scene image from the satellite covers a land area of about 185 x 180 kilometers. Landsat 7 was designed to collect eight spectral bands of reflected electromagnetic radiation: The first set of bands 1, 2 and 3, there are the visible wavelengths, followed by bands 4, 5 and 7 for infrared. The two remaining bands are band 6 for thermal infrared wavelength and band 8 for panchromatic as listed in Table 1.

Table 1 Spectral bands and wavelength interval of Landsat 7 ETM+

Landsat 7 ETM+			
Band	**Band name**	**Wavelength (μm)**	**Resolution (m)**
1	Blue	0.45-0.52	30
2	Green	0.52-0.60	30
3	Red	0.63-0.69	30
4	NIR	0.77-0.90	30
5	SWIR 1	1.55-1.75	30
6	Thermal	10.40-12.50	60*(30)
7	SWIR 2	2.09-2.35	30
8	Pan	0.52-0.90	15
9	-	-	-
10	-	-	-
11	-	-	-

จุฬาลงกรณ์มหาวิทยาลัย
Chulalongkorn University

In this study, there are 6 images data from the satellite Landsat 7 ETM+ with spatial resolution of 30×30m retrieved from NASA Landsat Program (2000) were applied to identify and automatically extract lineament in the study area. The informative image detail is shown in Table 2

Table 2 Image information from Landsat 7 ETM+ applied in this study

No.	Path/Row	Date of acquisition	Spectral bands	Spatial resolution (m)
1	131/46	19-02-2018	7	30 x 30
2	131/47	19-02-2018	7	30 x 30
3	131/48	19-02-2018	7	30 x 30
4	132/46	14-03-2018	7	30 x 30
5	132/47	14-03-2018	7	30 x 30
6	132/48	14-03-2018	7	30 x 30

2. ALOS PALSAR Digital Elevation Model (ALOS DEM)

ALOS DEM is digital format of mathematic model that represents altitudes of earth surface. The ALOS DEM has been applied for many researches that related to topographical work and very useful for geological research, especially study geomorphological feature for structural geology. The ALOS DEM in this study received data from ALOS PALSAR RTC Corrected DEM with spatial resolution 12.5 x 12.5 m. were applied to identify detail morphotectonic evidences in the study area. The informative image detail is shown in Table 3.

Landsat 7 ETM+ images were enhanced the quality with the mixing false-colored composite image data of band 4 (red), 5 (green), and 7 (blue) shown in Figure 14. This enhanced Landsat imaged and shaded relief map from the ALOS DEM data (Figure 15) with sunlight angle 30° surface and used sunlight direction in azimuth system 313° were used for separating the different materials properties on surface.

จุฬาลงกรณ์มหาวิทยาลัย
CHULALONGKORN UNIVERSITY

In this study, shaded relief of study area show gray tone scale and dark tone level depending on the sunlight direction (azimuth) and the elevation the sunlight (sun angle) (Figure 15A). In case the sunlight decreases the angle, the intensity level of gray will be increased continually, darker until black color. ALOS DEM data were usefulness for geomorphological study, rock classification and structural geology.

Table 3 Image information from ALOS DEM applied in this study

No.	Path/Row	Date of acquisition	Spatial resolution (m)
1	05158/330	21-11-2010	12.5 x 12.5
2	05158/340	21-11-2010	12.5 x 12.5
3	05158/350	21-11-2010	12.5 x 12.5
4	05158/360	21-11-2010	12.5 x 12.5
5	05158/370	21-11-2010	12.5 x 12.5
6	05158/380	21-11-2010	12.5 x 12.5
7	05158/390	21-11-2010	12.5 x 12.5
8	11868/330	23-11-2010	12.5 x 12.5
9	11868/340	23-11-2010	12.5 x 12.5
10	11868/350	23-11-2010	12.5 x 12.5
11	11868/360	23-11-2010	12.5 x 12.5
12	11868/370	23-11-2010	12.5 x 12.5
13	11868/380	23-11-2010	12.5 x 12.5
14	20839/330	06-09-2010	12.5 x 12.5
15	20839/340	06-09-2010	12.5 x 12.5
16	20839/350	06-09-2010	12.5 x 12.5
17	20839/360	06-09-2010	12.5 x 12.5
18	20839/370	06-09-2010	12.5 x 12.5
19	20839/380	06-09-2010	12.5 x 12.5

จุฬาลงกรณ์มหาวิทยาลัย
Chulalongkorn University

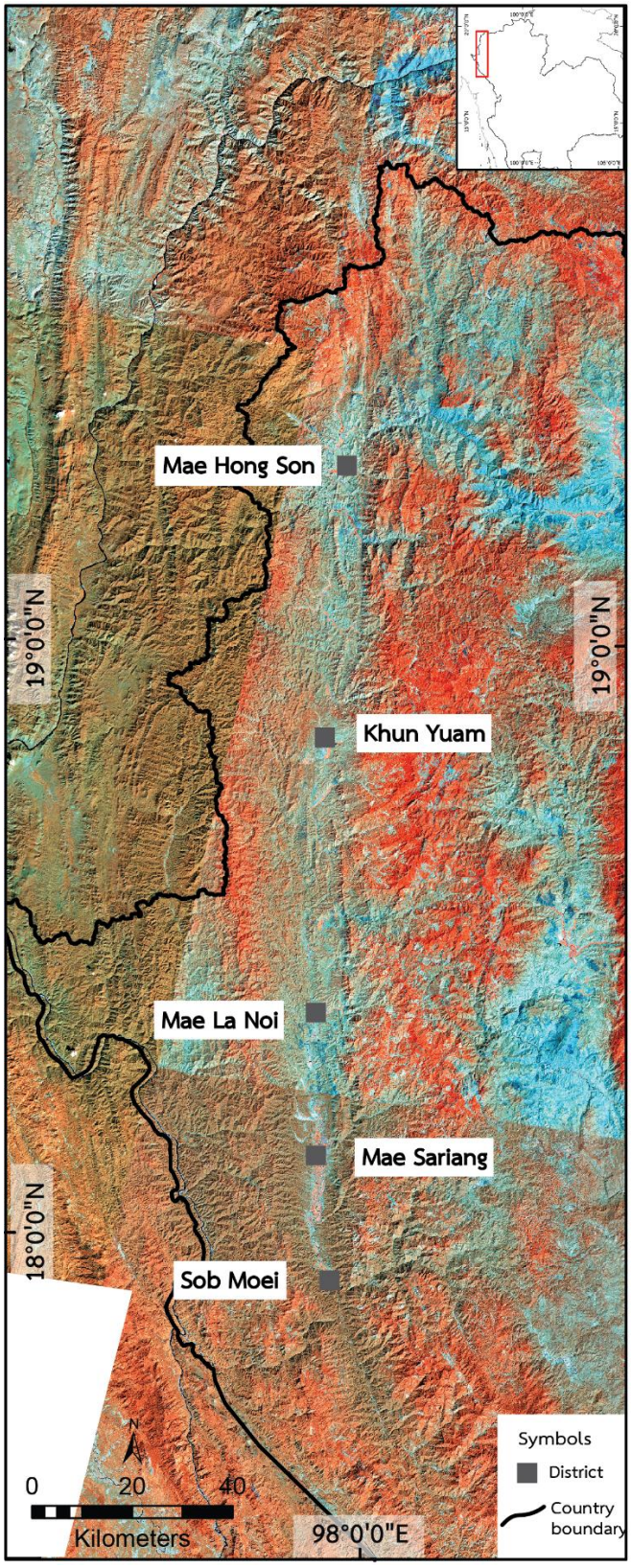

Figure 14 Enhancement Landsat 7 by the false-colored composite image data of bands 4 (red), 5 (green), and 7 (blue) showing physiographic features of the study area.

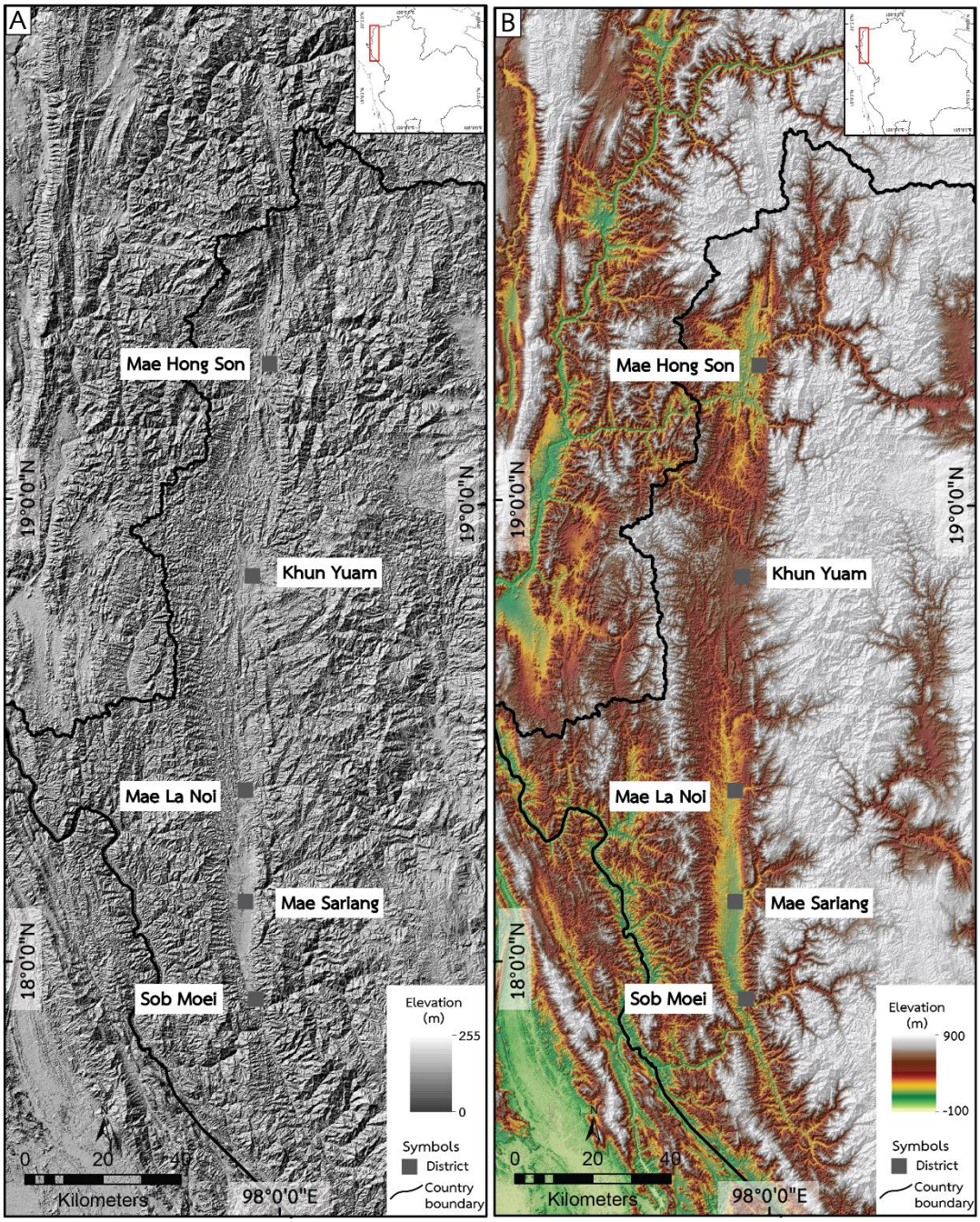

Figure 15 (A) Shaded relief (sunlight angle = 30°, sunlight direction = 313 and z factor = 2) and (B) Enhanced ALOS DEM map (sunlight elevation = 30°, sunlight direction azimuth = 313 and z factor = 1) show physiographic features of Mae Hong Son Province.

Morphotectonic landforms interpretation

Several remote sensing data sources (Landsat 7 ETM+, ALOS DEM and Google Earth) are analyzed for identifying the morphotectonic landforms (Figure 12) implying the possible active fault segments in the MHSF (Figure 16). The morphotectonic landforms in the study area were examined by visual justification with remote sensing data. The interpretation results for morphotectonic landforms show the appearance of several morphotectonic landforms including triangular facets, fault scarps, linear valley, hot spring, offset streams, and shutter ridges. Satellite images of the study area illustrate clearly the morphotectonic landforms in the MHSF as explained below.

Offset stream is a result of strike-slip fault movement by cutting through the stream, which originally flow straight line is moved laterally. The distance of lateral movement from the originally streamline can be referred to displacement of fault movement. Several offset streams can be found in the study area along the MHSF such as the offset stream of Samad river at Ban Pha Bong (Figure 17), Sa Surin river at Ban Mae Surin (Figure 18), Huai Mae Han river and Huai Mae Salab river at Mae Sariang (Figure 19).

Shutter ridge is a long and narrow mound that obstructs stream flow. The shutter ridge has affected of fault cutting through the hill ridge and appeared the ridge moved out from the originally mountain line and common evidences of strike-slip fault. The shuttle ridge can be found in the study area at Ban Sob Moei, southern part of the MHSF (Figure 20). In addition, linear valleys also found in this area. The linear valleys were generated from a transform faulting (strike-slip fault), which controls straight of the valley and stream channels as show in Figure 20.

จุฬาลงกรณ์มหาวิทยาลัย
Chulalongkorn University

Triangular facets are the result of vertical movement of normal fault and strike-slip fault, was affected by surface erosion until have the look like triangle cliff character. Several triangular facets can be found clearly along the MHSF at Ban Huai Pong (Figure 21), Ban Yod and Mae Tha Lu fault segments.

Fault scarp, the characterized slanting cliff is formed by fault cut through that area and can be generated by the movement of normal fault, reverse, and strike-slip faults. Commonly appear in the topography that showed steep cliff next to the basin and found in rows a trace moves distinctly. The results of above, mentioned processes can be indicated that the structures happen not long ago and if those structure leaned across sediment basin area, which Quaternary sediment deposited with age of about 10,000 years to present day, the traces line can be potentially active faults. Several fault scarps can be found clearly along the MHSF at Ban Yod and Khun Yuam fault segments.

จุฬาลงกรณ์มหาวิทยาลัย
Chulalongkorn University

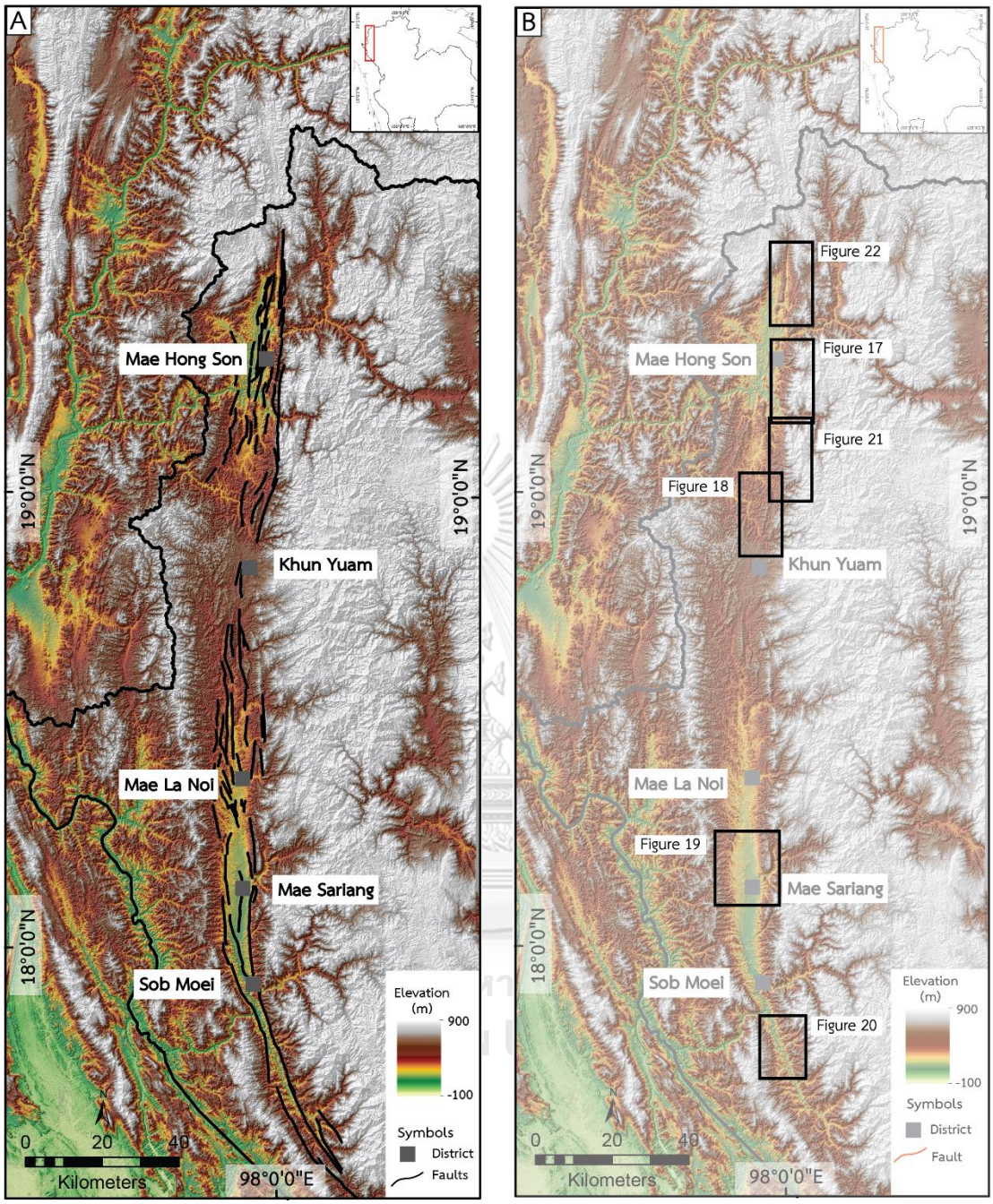

Figure 16 (A) Enhanced ALOS DEM data showing clearly the fault segments which oriented in north-south direction and cover Mae Hong Son province. (B) Boxes with number indicate selected areas for morphotectonic landforms using enhanced ALOS DEM and Google Earth images interpretation.

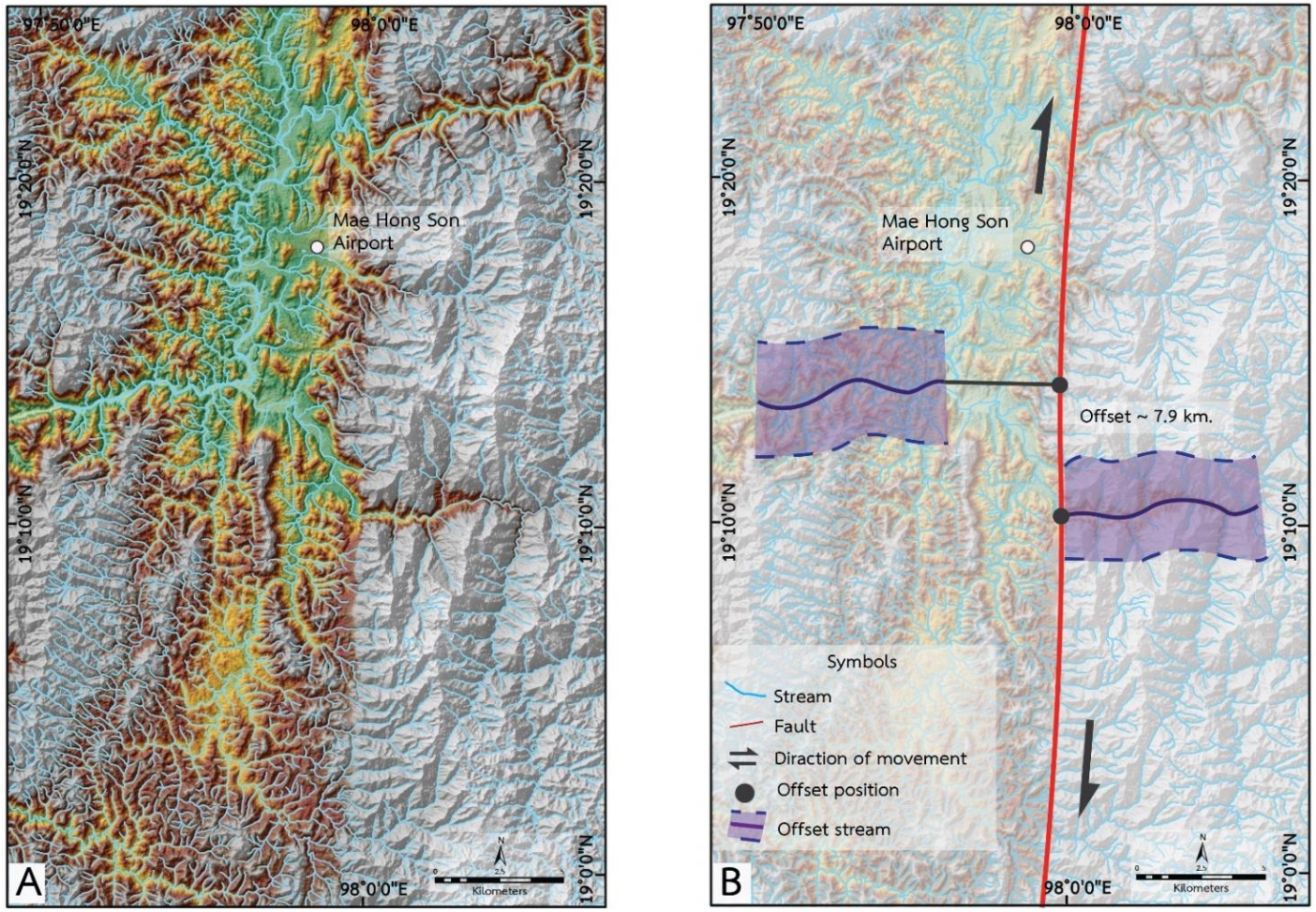

Figure 17 Detail interpreted map from ALOS DEM at Ban Pha Bong show offset stream of Sa Mad river is about 7.9 km. from right lateral strike-slip fault movement. Location shows in Figure 16B.

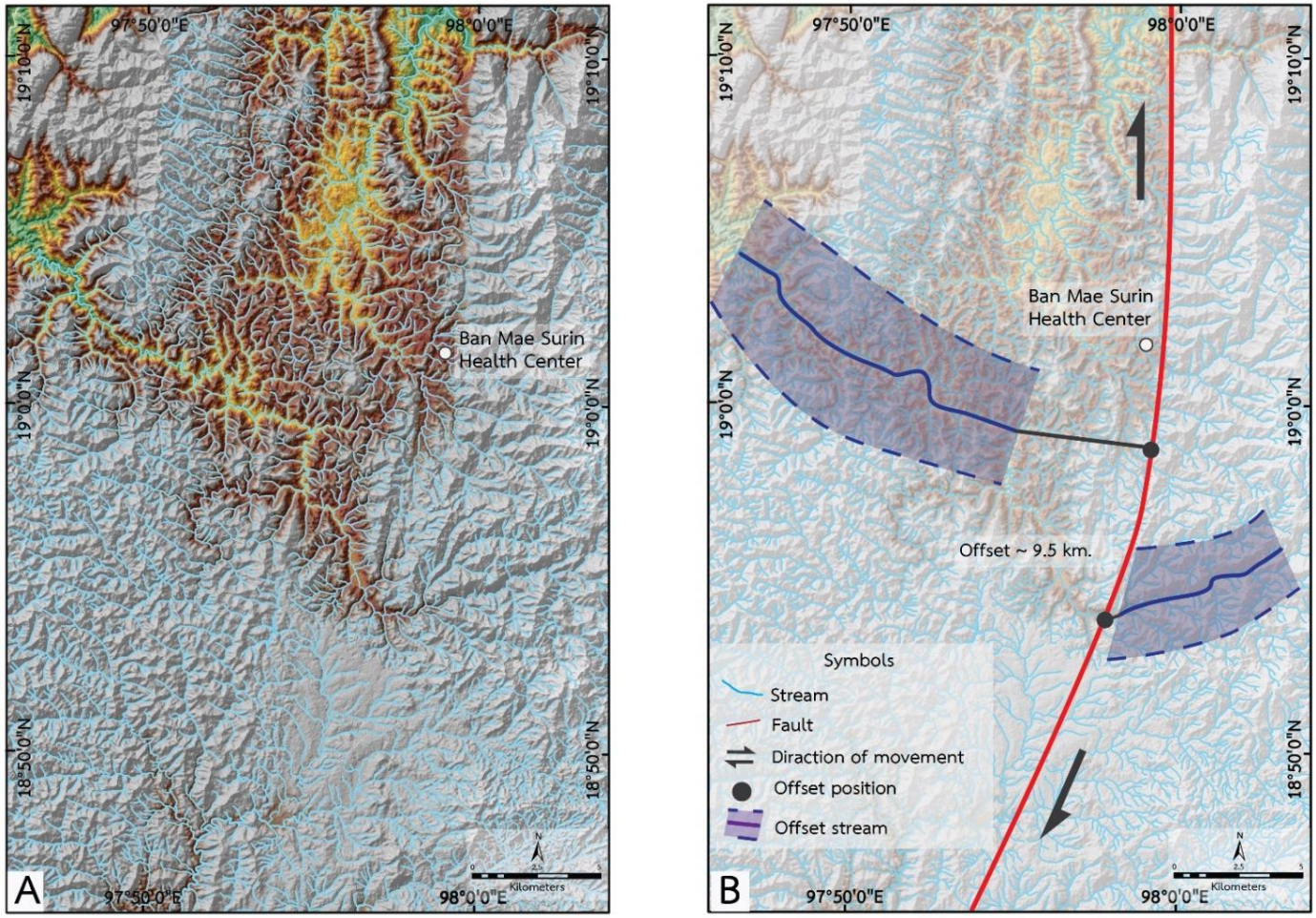

Figure 18 Detail interpreted map from ALOS DEM at Ban Mae Surin show offset stream of Sa Surin river is about 9.5 km. from right lateral strike-slip fault movement. Location shows in Figure 16B.

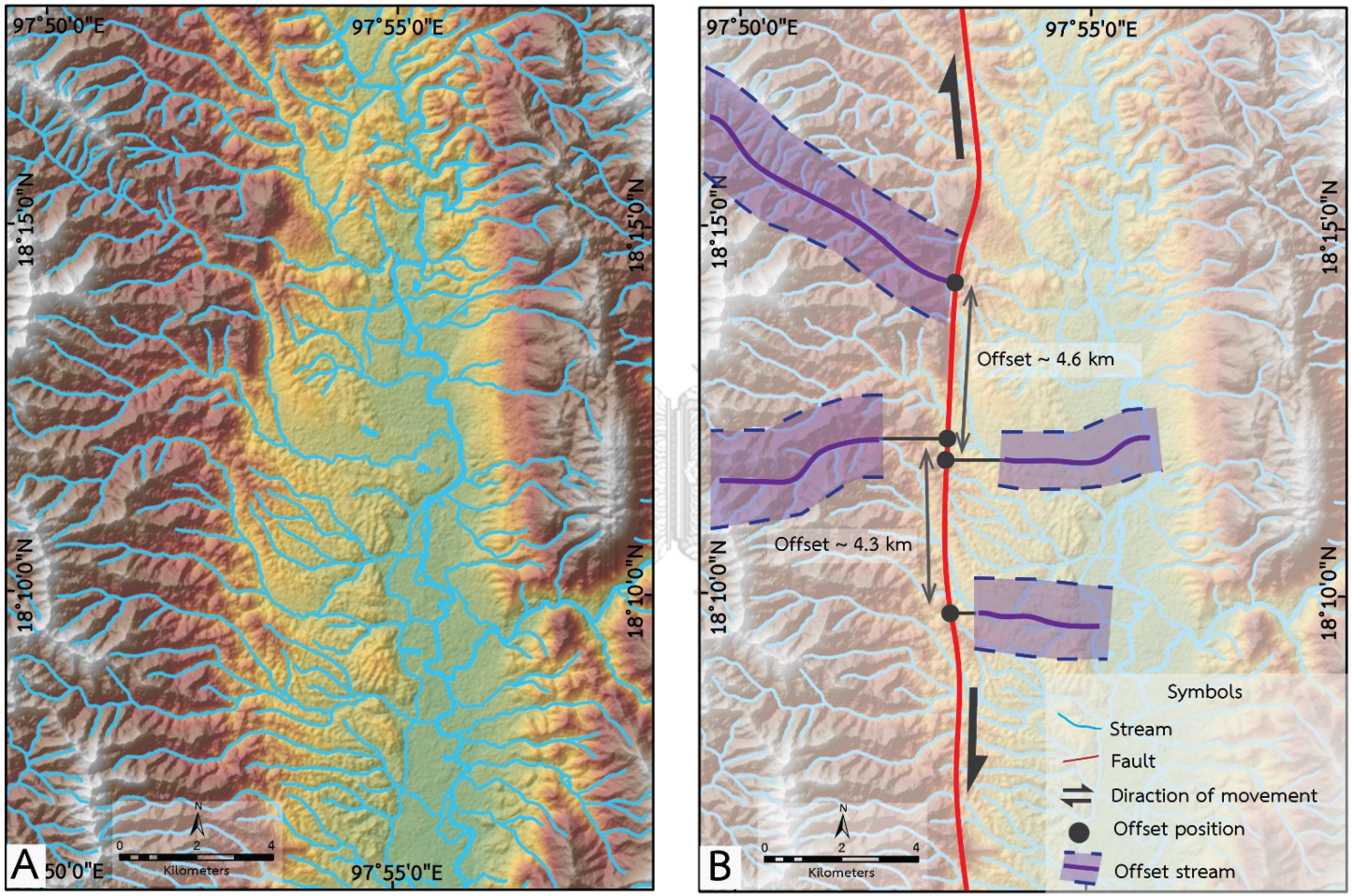

Figure 19 Detail interpreted map from ALOS DEM at Mae Sariang show offset stream of Huai Mae Han is about 4.6 km (north) and Huai Mae Salab is about 4.3 km (south) from right lateral strike-slip fault movement. Location shows Figure 16B.

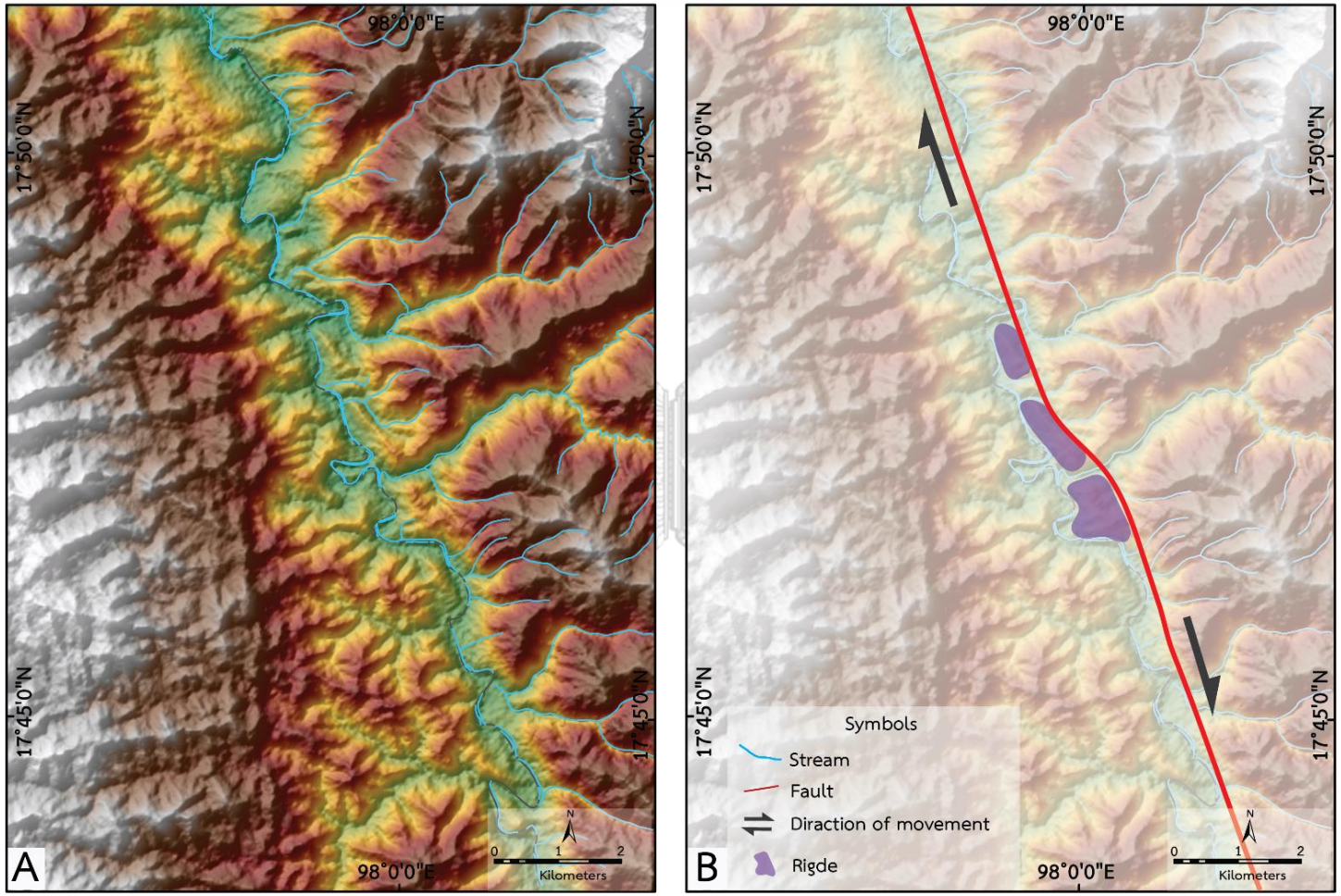

Figure 20 Detail interpreted map from ALOS DEM at Sob Moei show shuttle ridge which is the ridge moved out from the originally mountain from right lateral strike-slip fault movement. Location shows in Figure 16B.

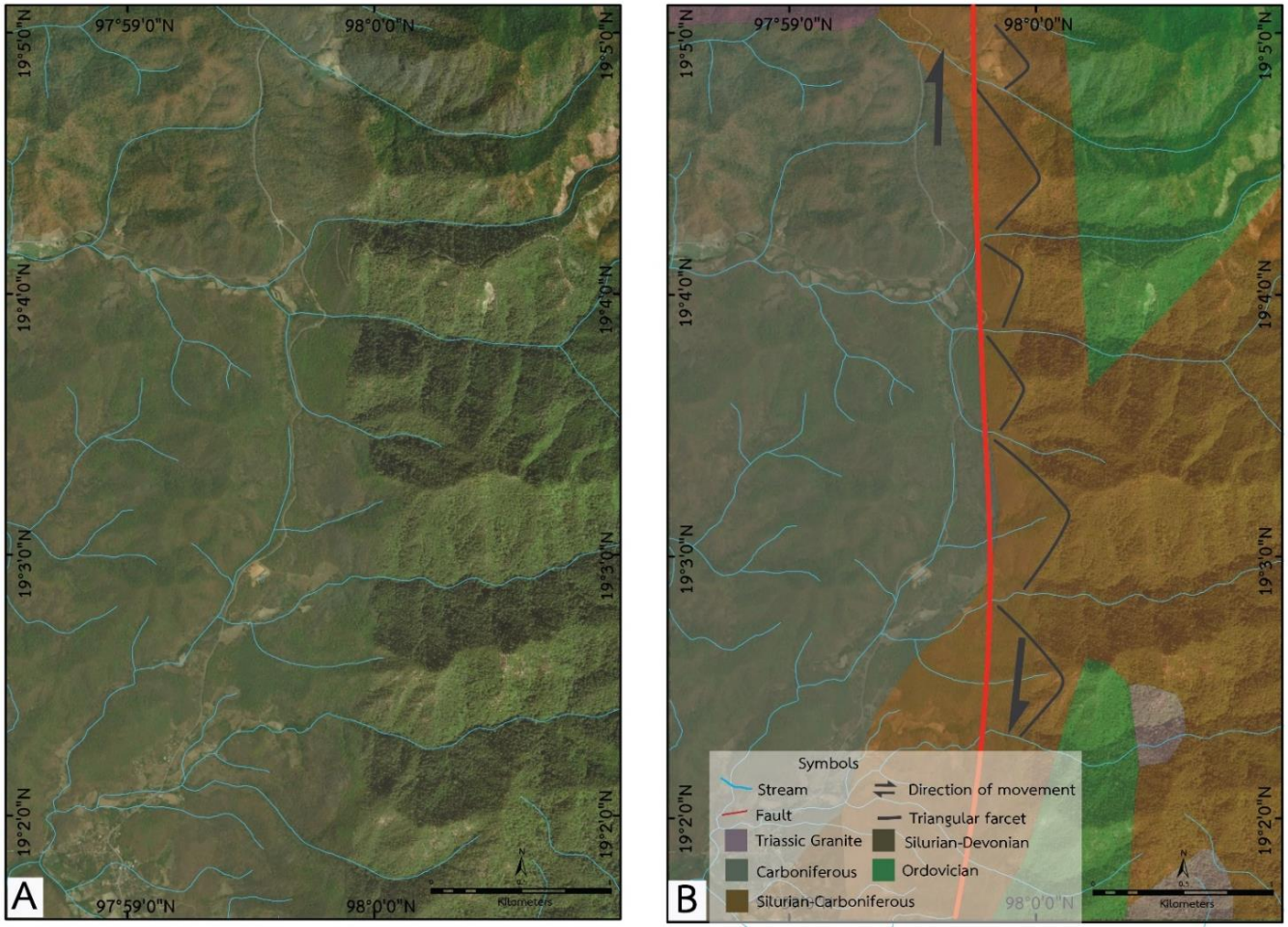

Figure 21 Detail interpreted map from Google Earth with geologic map at Ban Huai Pong show triangular facets from normal fault movement. Location shows in Figure 16B.

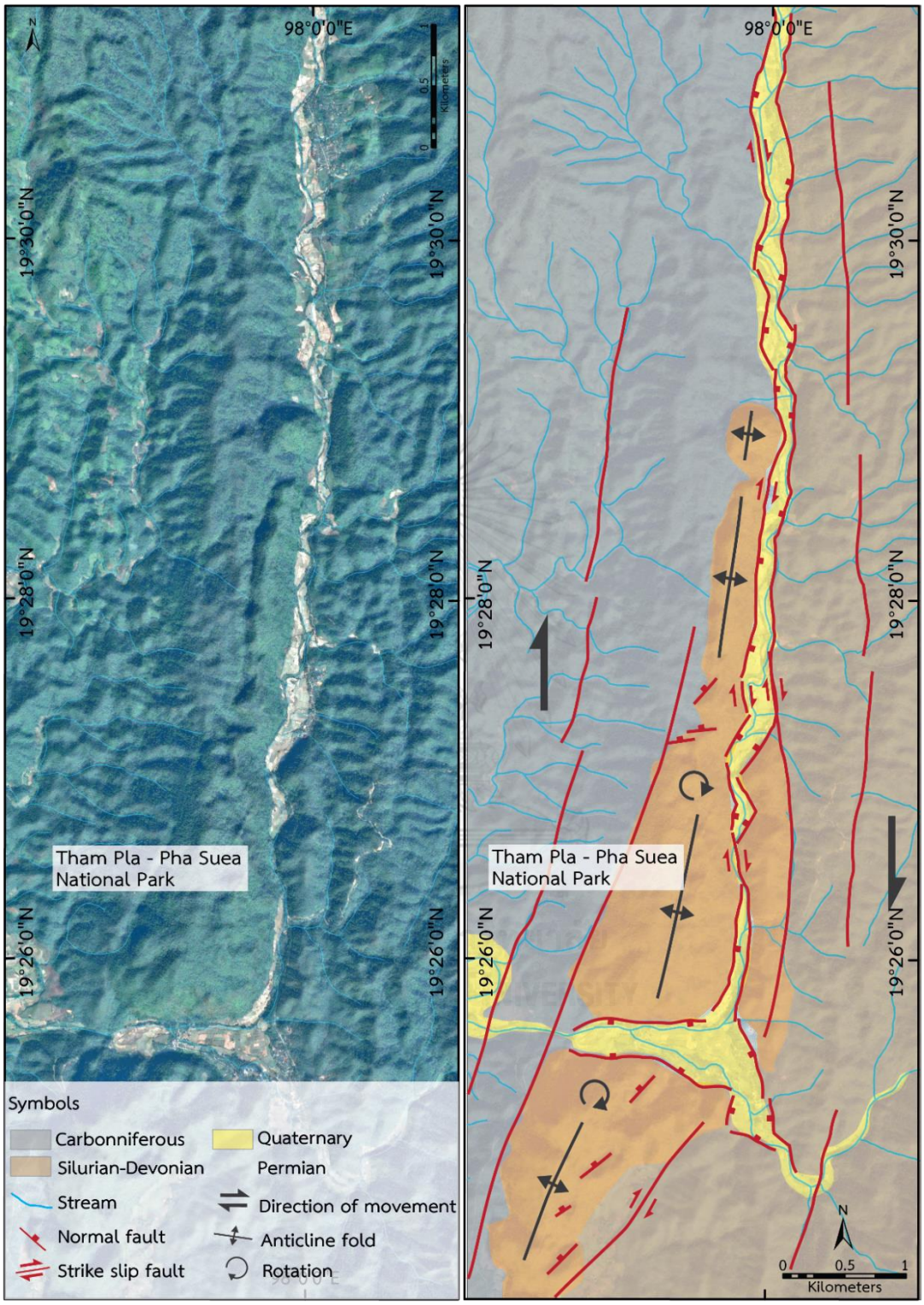

Figure 22 Detailed interpretion map from Google Earth with geologic map at Tham Pla – Pha Suea National Park show anticline folds with N-S fold axes and small basins that are occurred by subsidence parallel with the MHSF. Location shows in Figure 16B.

Lineament and fault segments

The processed satellite images show the image of the study are which easy to delineate of major structures and Cenozoic basins (Figure 15). The remote sensing data were applied for re-tracing lineaments and fault segments in the regional scale (Figure 16A) whereas satellite images of different types can support the morphotectonic evidence associated with surface faulting in more detail. Satellite images illustrate clearly the offset streams, triangular facets, linear valleys, shuttle ridges and fault scarps in the MHSF.

The interpretation base on ALOS DEM with the high resolution of 12.5 m for lineaments and fault segments. The result shows several neotectonic features including triangular facets, fault scarps, offset streams, and shutter ridges. Based on combined interpretation of DEM and Google Earth, the major trend of lineaments or fault lines are in the north-south direction and the minor trends of lineaments and faults lie in the northeast-southwest and northwest-southeast directions with short length than major trend. As shown in Figure 16A, most of lineaments which oriented in north-south direction situate along basin boundary composed of MHSB in the north and MSB in the south, whereas the lineaments in northeast-southwest and northwest-southeast direction situate in the area of basement rocks. The author considered these fault zones caused the opening of Cenozoic basins

Basins associated with the MHSF

The study of Cenozoic basins in the Mae Hong Son area uses regional Google Earth images and ALOS DEM data. They are well recognized in remote sensing images by relatively low-relief and gentle slopes to flat lying area (basin area) when compared with those of the older rocks (mountainous area) (Figure 16A) . The characteristic of topography in the study area is mainly mountain range in the western and eastern parts. The mountains lie in the north-south trend. From the interpretation it is suggested that sediment layers deposited in basins between mountain ranges both in the east and west were dissected by lineaments (or faults).

Based on Google Earth images and ALOS DEM data interpretation, the study area contains with two Cenozoic basins as the MHSB and MSB. Both basins have elongated shape and oriented in the north-south direction following the main structure which is bounded by fault lines (see Figure 16A). The MHSB and MSB orients in north-south direction, the width is about 7 km in both basins, but the length is about 30 km in MHSB and 60 km in MSB. If compare, MHSB has low relief and morphotectonic evidences are occurred in this basin is not sharp as the MSB. The upper part of the MHSB, from the characteristic of topography it is suggested that sediment deposited in the small basins that are occurred by subsidence along the fault line in north-south direction. The basins are parallel to the mountain ranges both in the west and the east.

To estimate the minimum total dip-slip displacement across the fault, a pre-kinematic paleotopographical datum was assumed to be defined by an enveloping surface bounded by modern topographic highs, based on the method of Ufimtsev (1990) and Dawers, H. Anders, and Scholz (1993). Projection of this enveloping surface towards an upwards projected fault eliminates compromising effects such as footwall crest erosion. Seven profiles were drawn across the MHSB and other seven profiles across the MSB immediately to the south (Figure 23 and Figure 24). Although subject to large uncertainties, the profiles show a maximum of 0.7 ± 0.1 km dip-slip displacement. Topographic profiles no. 1–7 across the northern part of the MHSF which is in the MHSB shows size of the basin, the basin is narrow and gradually widened from north to south. However, topographic profiles no. 8-14 across the southern part of the MHSF which is located in MSB shows the basin is narrow and gradually widened from north to south demonstrated by normal fault. In addition, profiles 13 and 14 shows the characteristic of a strike slip fault.

Displacement analysis of the MHSF along basin axis from the MHSB to the MSB indicated that the MHSB and the MSB are separated by the Khun Yuam Transfer Zone (KYTZ) (Figure 25). In the MHSB, the cumulative displacement on the eastern part rather than the western part and displacement on both sides decreasing toward Khun Yuam area, similarity has found in the MSB. From the graph of displacement analysis, the shape of the MSB is more symmetrical than the MHSB. Displacement analysis also shows understepping of fault from the MHSB and the MSB. The KYLZ is an area that is linked between the fault from MHSB and the fault from MSB. From topographic profile from Profile 7 (as shows in Figure 23), no obvious major faults on this profile but may be has minor faults but not clear.

จุฬาลงกรณ์มหาวิทยาลัย
Chulalongkorn University

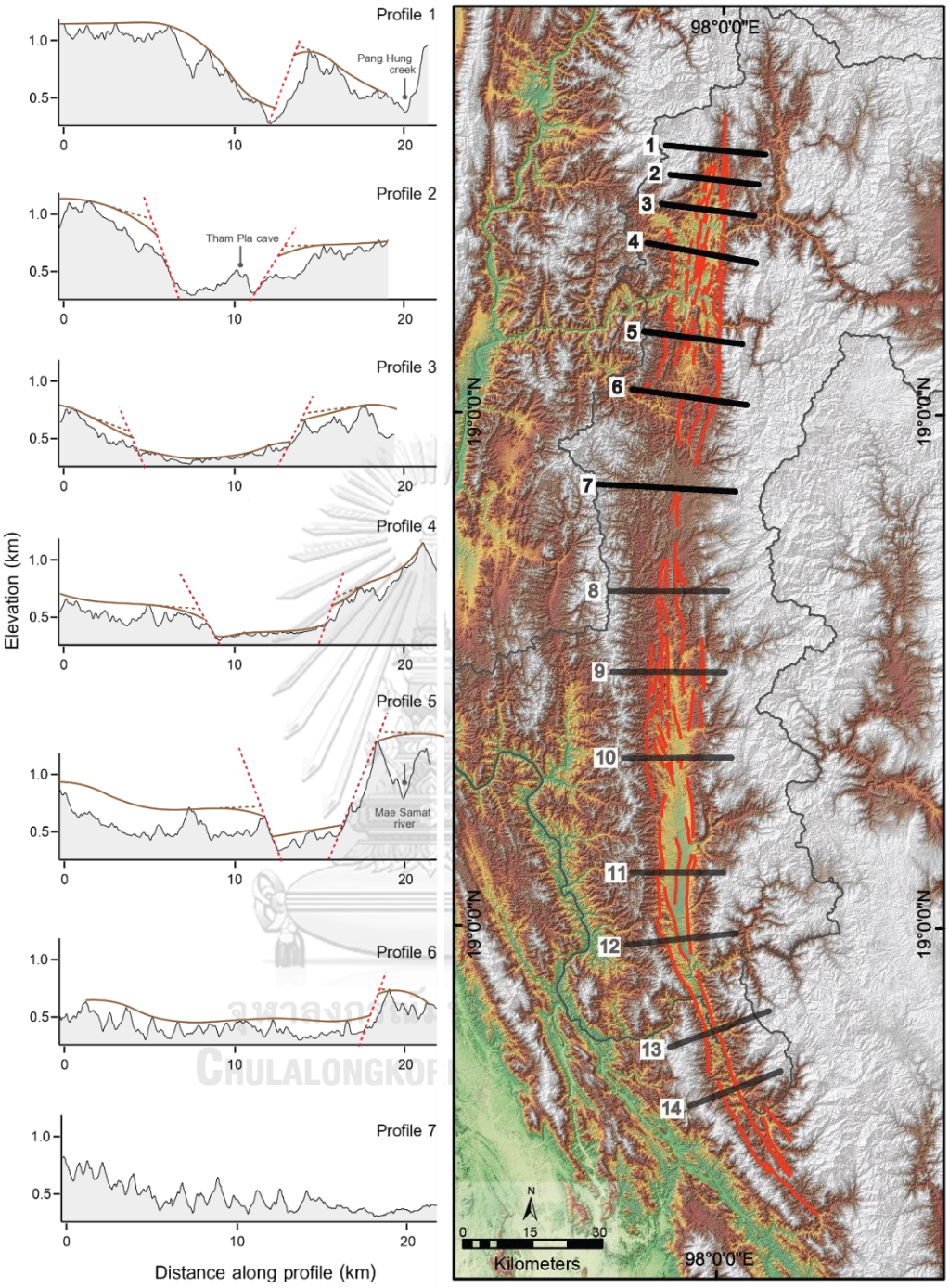

Figure 23 Topographic profile across the MHSF (Northern part). Profile locations shown in inset map. Brown lines show lower (dashed) and upper (dotted) of paleotopography and red line (dashed) show fault.

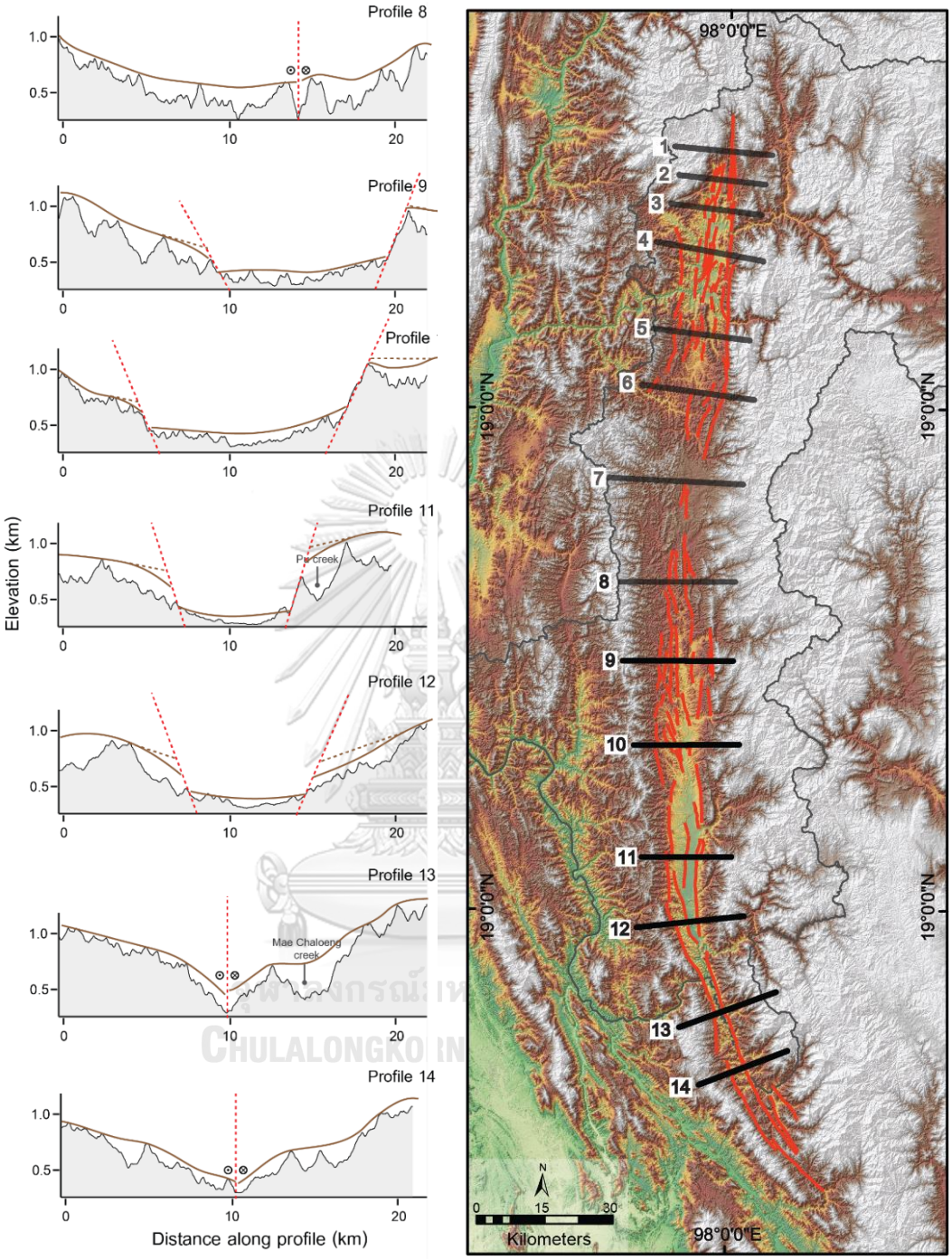

Figure 24 Topographic profile across the MHSF (southern part). Profile locations shown in inset map. Brown lines show lower (dashed) and upper (dotted) of paleotopography and red line (dashed) show fault.

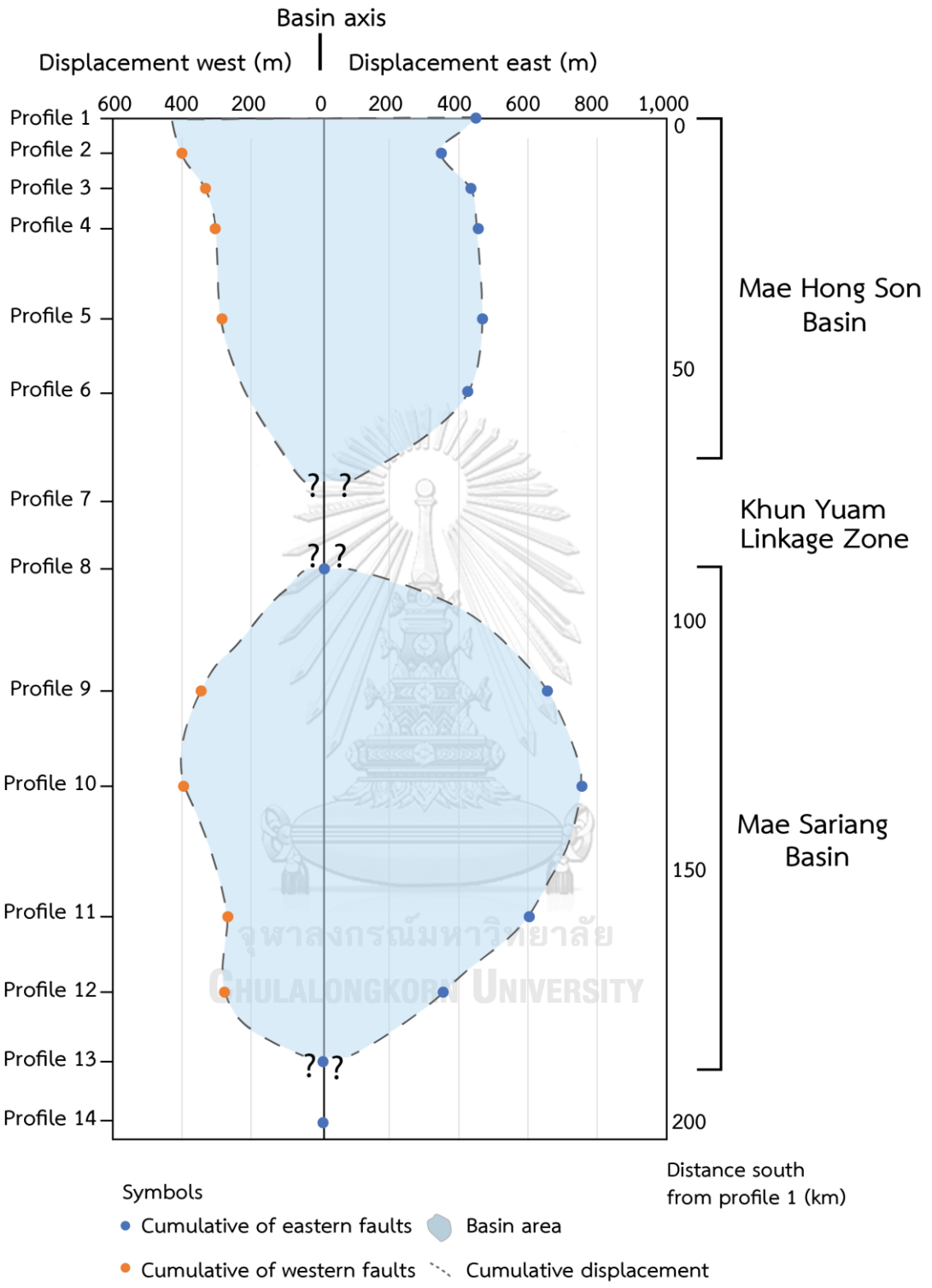

Figure 25 Graph showing total offsets down to west and east plotted along the length of the fault. Location shown in Figure 23 and Figure 24.

Determination of Maximum Credible Earthquakes

The Maximum Credible Earthquakes (MCEs) are estimated using the fault rupture length at the surface (SRL). Based on the equation proposed by Wells and Coppersmith (1994), Wells and Coppersmith (1994) also found the vertical slips are related to the earthquake magnitude. The SRL (or surface rupture length) used for the Mw calculation is the length of the longest fault segment in individual fault segments which were interpreted in this chapter. These relationships lead them to propose the empirical equations (3.1, 3.2, 3.3 and 3.4) as shown below:

$$M = 5.08 + 1.16 \log (SRL) \quad \text{(Eq 3.1) *}$$

$$M = 5.16 + 1.12 \log (SRL) \quad \text{(Eq 3.2) **}$$

$$M = 6.93 + 0.82 \log (AD) \quad \text{(Eq 3.3) ***}$$

$$M = 6.61 + 0.71 \log (MD) \quad \text{(Eq 3.4) ****}$$

Whereas Mw is moment magnitude, SRL is surface rupture length of fault segment (km), MD is maximum displacement and AD is average displacement

* Equation for all fault type

** Equation for strike-slip fault

*** Equation for normal fault

**** Equation for normal fault

จุฬาลงกรณ์มหาวิทยาลัย
CHULALONGKORN UNIVERSITY

Based on satellite image interpretation, several lines of morphotectonic evidence show that the fault segments belonging to the Mae Hong Son have the wide range of from 3.03 km (Phra That Chom Kiti segment) up to 28.55 km (Mae La Noi segment) (see Table 4). As a result, the determined fault segments of the MHSF zone can generate the credible earthquakes with the maximum around 5.64 to 6.77.

Table 4 Fifty-five fault segments of the MHSF with essential information of earthquake source parameters identified in this study.

No.	Fault Segment	SRL (km)	MCEs
1	Nai Soi	5.9	6.0
2	Pang Moo	9.3	6.2
3	Ban Luang	3.4	5.7
4	Mae Han	28.6	6.8
5	Pong Deang	4.7	5.9
6	Huai Dua	11.1	6.3
7	Huai Pong	19.1	6.6
8	Mae Surin	8.4	6.2
9	Pattana	3.5	5.7
10	Nong Mae La	7.9	6.1
11	Thung Pam	15.5	6.5
12	Mae Sa Nga	19.2	6.6
13	Khun Yuam	4.1	5.8
14	Huai Mae Su	6.7	6.0
15	Thum Keaw Ko Mol	10.0	6.2
16	Wat Wang Kun	8.7	6.2
17	Mae La Noi	13.0	6.4
18	Pong Doi Chang	13.8	6.4
19	Mae Ka Tuan I	3.0	5.6
20	Mae Ka Tuan II	4.1	5.8
21	Huai Kia	8.4	6.2
22	Mae Ngao	13.9	6.4
23	Na Doi	10.5	6.3
24	To Pae	10.3	6.3
25	Khun Yuam	3.5	5.7
26	Ban Pae	23.0	6.7
27	Huai Singh Nuea	5.9	6.0

จุฬาลงกรณ์มหาวิทยาลัย
Chulalongkorn University

Table 4 (cont.)

No.	Fault Segment	SRL (km)	MCEs
28	Mae Sariang	5.3	5.9
29	Pa Pae	5.2	5.9
30	Sao Hin	4.4	5.8
31	Tha Pha Pum Tai	6.4	6.0
32	Mae Tha Lu	8.8	6.2
33	Doi Wiang	8.1	6.1
34	Mae Heep	11.7	6.3
35	Mae Ra Murng	14.9	6.4
36	Phra That Chom Kiti	4.1	5.8
37	Kon Phung	9.8	6.2
38	Mae Hua	4.0	5.8
39	Thunh Laeng	4.2	5.8
40	Ban Yod	4.2	6.4
41	Pha Bong I	10.7	6.3
42	Pha Bong II	6.0	6.0
43	Mae Su	5.8	6.0
44	Mae La Noi	4.1	5.8
45	Huai Ha	23.4	6.7
46	Huai Pha	8.2	6.2
47	Mok Chum Pae	25.2	6.7
48	Huai Pong On	3.4	5.8
49	Kung Pao	8.0	6.2
50	Kung Mai Sak	23.8	6.7
51	Ta Su De	14.6	6.4
52	Mae Kao	4.7	5.9
53	Pa Pong	6.9	6.1
54	Doi Wiang Luang	12.5	6.4
55	Pa Phang	13.7	6.4

จุฬาลงกรณ์มหาวิทยาลัย
Chulalongkorn University

CHAPTER IV
PALEOEARTHQUAKE INVESTIGATIONS

The investigations on the paleoearthquake events using the evidences of offset stratigraphic units and deformed sediment layers that recorded in the trenching and the road-cut are the most important data. Therefore, the trenching studies across the fault segments of the MHSF are selected for a paleoearthquake investigation. Details of this study are shown below.

Field evidence of morphotectonic landforms

Field evidences of morphotectonic landforms during the field survey, geological mapping at the study area and its surrounding areas was made in order to disclose the appearance of active faults. This process focuses on geological investigations according to the method proposed by Keller and Pinter (1996) (Figure 12). The major important task is to compile all available information necessary for detailed geologic, tectonic and paleoearthquake investigations of the study area as well as interpretations on satellite images. Three trenches and one road-cut exposure were examined for field survey paleoearthquake study (Figure 26),

จุฬาลงกรณ์มหาวิทยาลัย
Chulalongkorn University

In the field at western side of Ban Yod appears east dipping triangular facets and fault scarp at foothill. The facet was developed in the western trend, suggesting a fault running parallel to the mountain front. The appearance of triangular facets along the Ban Yod segment is well developed as series of facet spurs, this indicates that the fault shows several movements. Additionally, there are significant morphotectonic landforms at Khun Yuam segment and Mae Tha Lu segment including fault scarp at the foothill together with offset and terrace which is developed by fault, respectively. Therefore, quarry and trenching studies across the fault segments of the MHSF are selected for a paleoearthquake study.

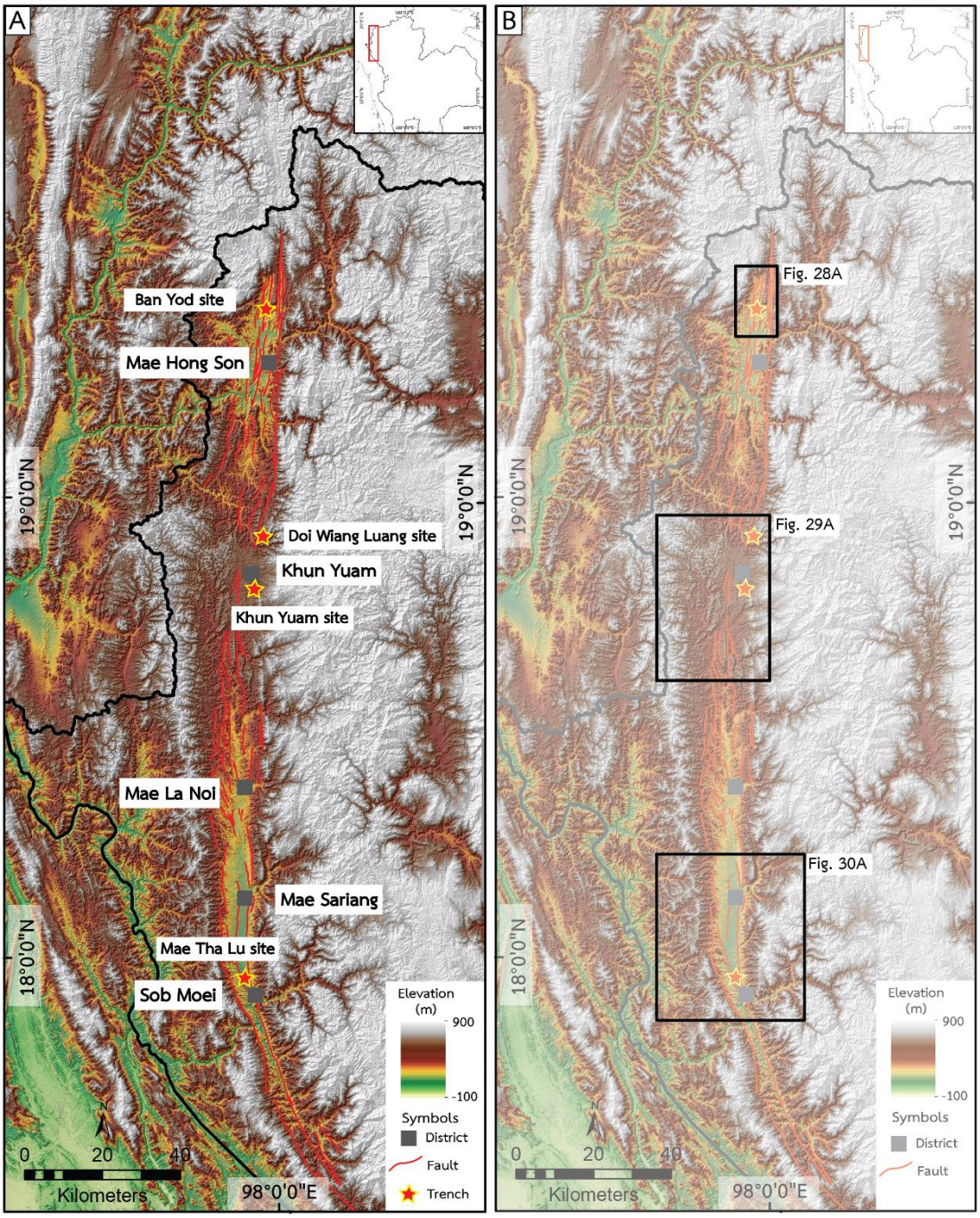

Figure 26 (A) Enhanced ALOS DEM Map showing the location of trenches and road-cut exposure which were examined for a paleoearthquake study. (B) Index map for detailed survey.

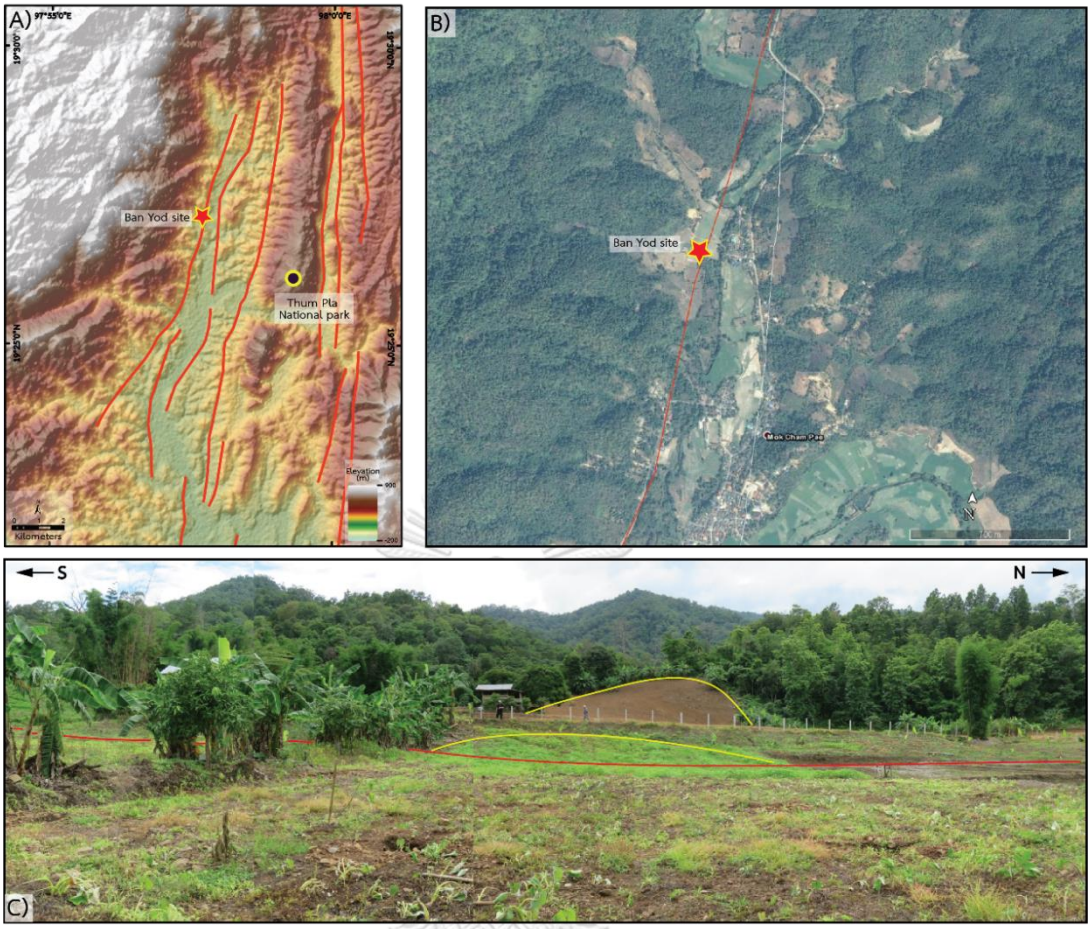

Figure 27 (A) Hill shade ALOS DEM and (B) Google Earth image show the location of the Ban Yod trench site, MHSB. C) Photograph of the north trending mountain range, showing the fault scarp and triangular facet covered mostly by tree. Note that red line is the fault line, and yellow triangular is triangular facet. Location shows in Figure 26B.

จุฬาลงกรณ์มหาวิทยาลัย
Chulalongkorn University

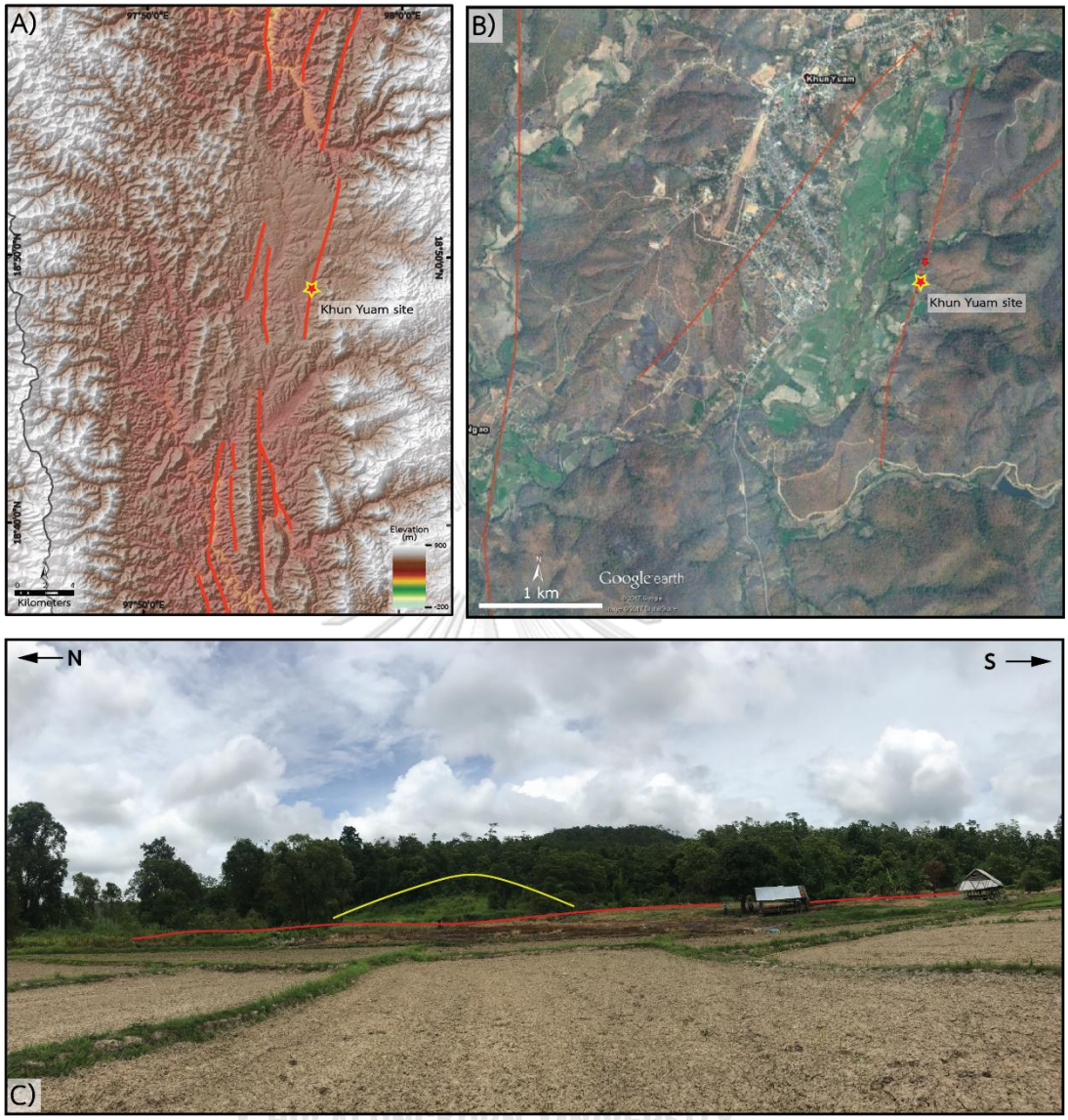

CHULALONGKORN UNIVERSITY

Figure 28 (A) Hill shade ALOS DEM and (B) Google Earth image show the location of the Khun Yuam trench site. C) Photograph of the north trending mountain range, showing the fault scarp covered mostly by tree. Note that red line is the fault line, and yellow triangular is fault scarp. Location shows in Figure 26B.

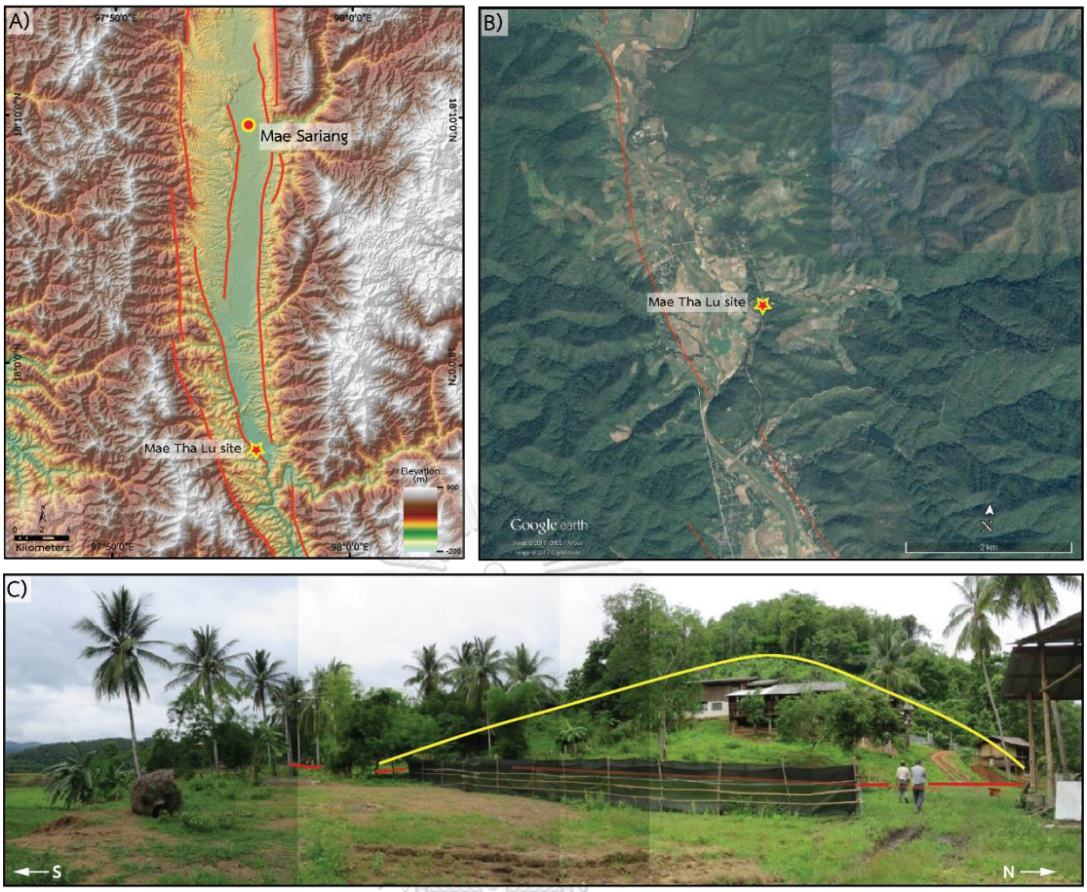

Figure 29 (A) Hill shade ALOS DEM and (B) Google Earth image show the location of the Mae Tha Lu trench site, MSB. C) Photograph of the north trending mountain range, showing the triangular facet covered mostly by tree. Note that red line is the fault line, and yellow triangular is triangular facet. Location shows in Figure 26B.

จุฬาลงกรณ์มหาวิทยาลัย
Chulalongkorn University

Paleoearthquake trenches

In as much as the reliable study is the supporting field evidences relevant to the fault segments concerned, it is necessary to study all the fault segments. The detailed Paleoearthquake investigation based on the integration of results from remote sensing interpretations, digital elevation models and geological maps as shown below.

1. Doi Wiang Luang road-cut outcrop

Quaternary faults cutting Cenozoic terrace deposits have been observed at the road-cut wall on the HW108 to the Khun Yuam District (location shown in Figure 26A). The road-cut outcrop was exposed a 15-m-long and 9-m-high. The Quaternary stratigraphy and structural geology of the road-cut wall are mapped in Figure 30 and Figure 31, the stratigraphic units and structural geology were identified based on sedimentological characteristics. The mapped faults strike N50°E–N72°E and dip 70°NW–80°SE. However, the stratigraphic units can be divided into seven units consisting of unit A-F and top soil. Details of individual units are described below;

Unit A is an alluvial unit consisting mainly of moderately sorted, brown to yellowish very fine to coarse sand. The thickness of the unit is about 1.5 m.

Unit B is an alluvial unit consisting of silty clay and clasts of feldspar and quartz. The thickness of the unit ranges from 50 cm to 1 m.

จุฬาลงกรณ์มหาวิทยาลัย
Chulalongkorn University

Unit C is an alluvial/colluvial unit comprised of brown to yellowish sand with gravel. Most clasts are subrounded with pebble sized of sandstone, siltstone, and quartz. The thickness of the unit ranges from 50 cm to 1.2 m.

Unit D is an alluvial unit comprised of light brown to yellowish gravel and sand. The clasts are clast supported which are subrounded of sandstone, siltstone, and shale. The thickness of this unit is 80 cm.

Unit E is an alluvial unit that contains reddish brown gravel and sand. These clasts are clast supported which are subangular to subrounded of sandstone and shale. The grain size of gravel ranges from pebble to cobble. The thickness of this unit is 2 m.

Unit F is an alluvial unit consists of gravel, sand, and clay. The clasts are mainly rounded and consist mostly of quartz and sandstone, with the maximum diameter is 6 cm. The thickness of this unit is 2.5 m.

Top soil is a dark clay layer, consists of organic rich silt/clay with some gravel and sand. It is approximately 20 cm thick.

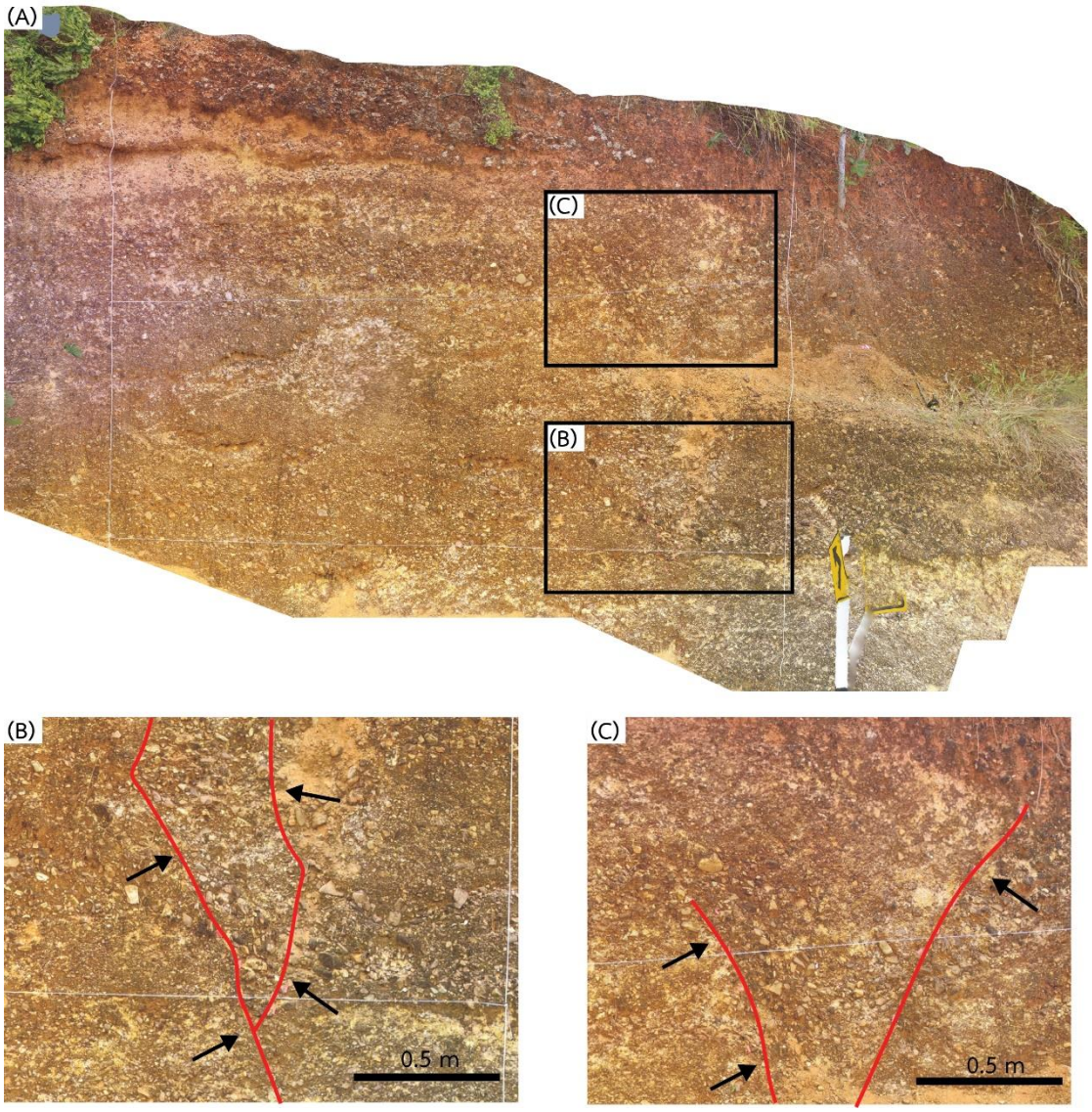

Figure 30 (A) Photograph of Doi Wiang Luang area. (B) and (C) Closed-up photographs show the fault traces were found on the wall. (Red lines).

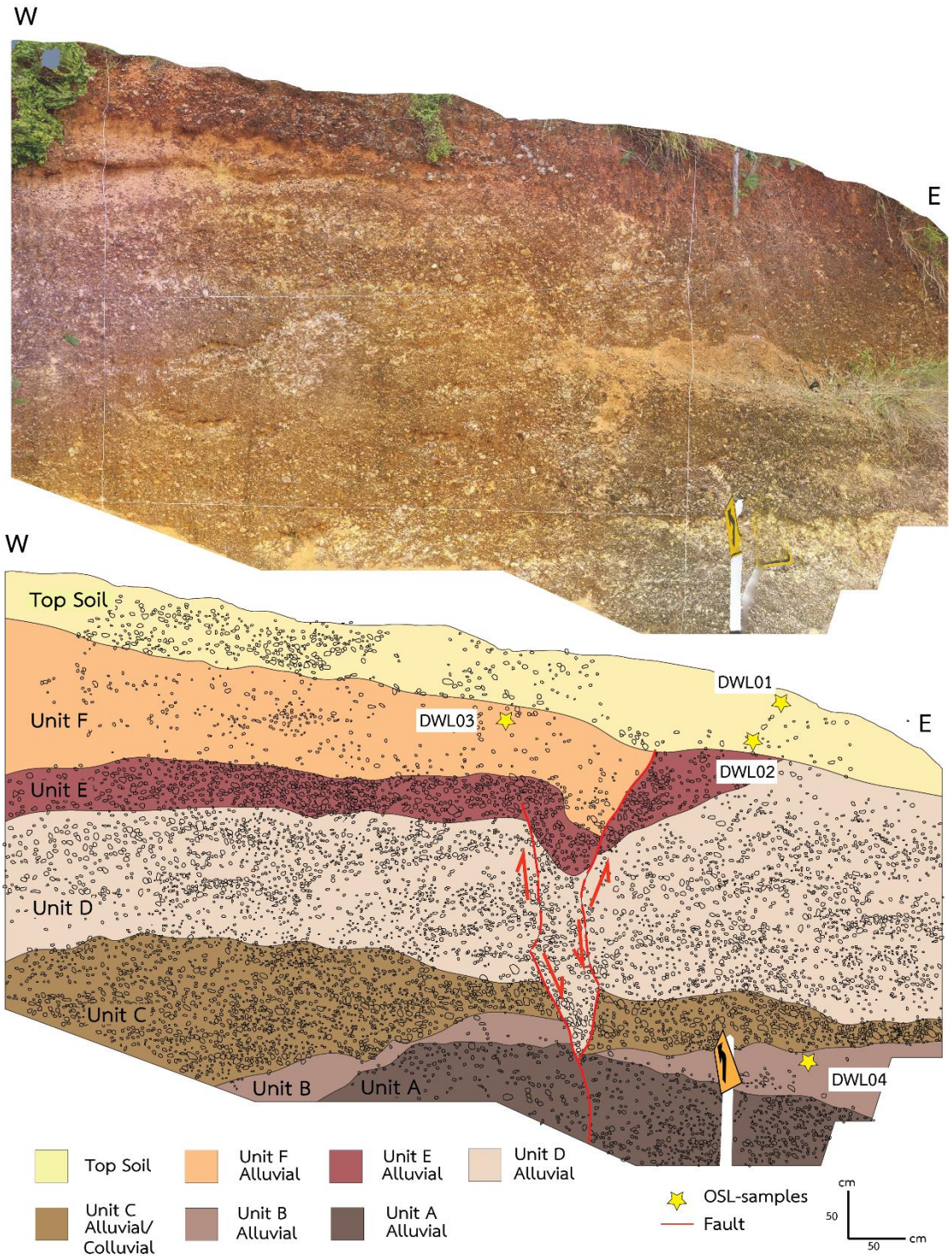

Figure 31 Road cut outcrop section and wall log section on the north wall at Doi Wiang Luang showing sediment stratigraphy, fault orientation and sample location for dating. Location shows in Figure 26A.

2. Mae Tha Lu trench

The Mae Tha Lu site is located along the frontal foothill, near Mae Sariang district. The trench was excavated a 14-m-long, 3-m-wide and 3.5-m-deep. Trench-wall exposures show one basement rock and 10 depositional units (A-I) and top soil which are exposed in both sidewalls (Figure 32 and Figure 33). Details of individual units are described below;

Basement rock is a shale that contains light brown and weathered. The orientation of bedding is 016/28.

Unit A is a colluvial unit that contains reddish brown gravel and sand. These clasts are clast supported which are subangular to subrounded of sandstone and shale. The grain size of gravel ranges from pebble to cobble. graded bedding (fining upward sequence), boulder of conglomerate, bedding of gravel 082/70

Unit B is a colluvial unit that contains clay with mottle Fe and Mn (more clay),

Unit C is an alluvial unit with matrix supported. This unit is mainly clay with gravel, almost fine grain, gravel can be found in the west of the trench, lateritic texture, more Fe and Mn concretion (black spot).

Unit D is a colluvial unit consist of gravel, sand, silt and gravel. The gravel ranges from pebble to cobble (gravel is sand and shale), fine grain, well-sorted to moderate-sorted (more clay in the lower part).

จุฬาลงกรณ์มหาวิทยาลัย
Chulalongkorn University

Unit E is an alluvial unit comprised of clay, silt with Fe or Mn concretion and gravel, gravel is not much (a few). Gravel; quartz, reddish brown, some show lateritic texture. Gravel disappeared to the west wall.

Unit F is an alluvial unit consisting mainly of sand and clay, a few gravels can be observed hear, reddish brown.

Unit G is an alluvial unit, matrix-supported, dark reddish brown, consists of gravel, sand, silt and clay, angular to sub-rounded, some clasts of gravel can be found on both walls.

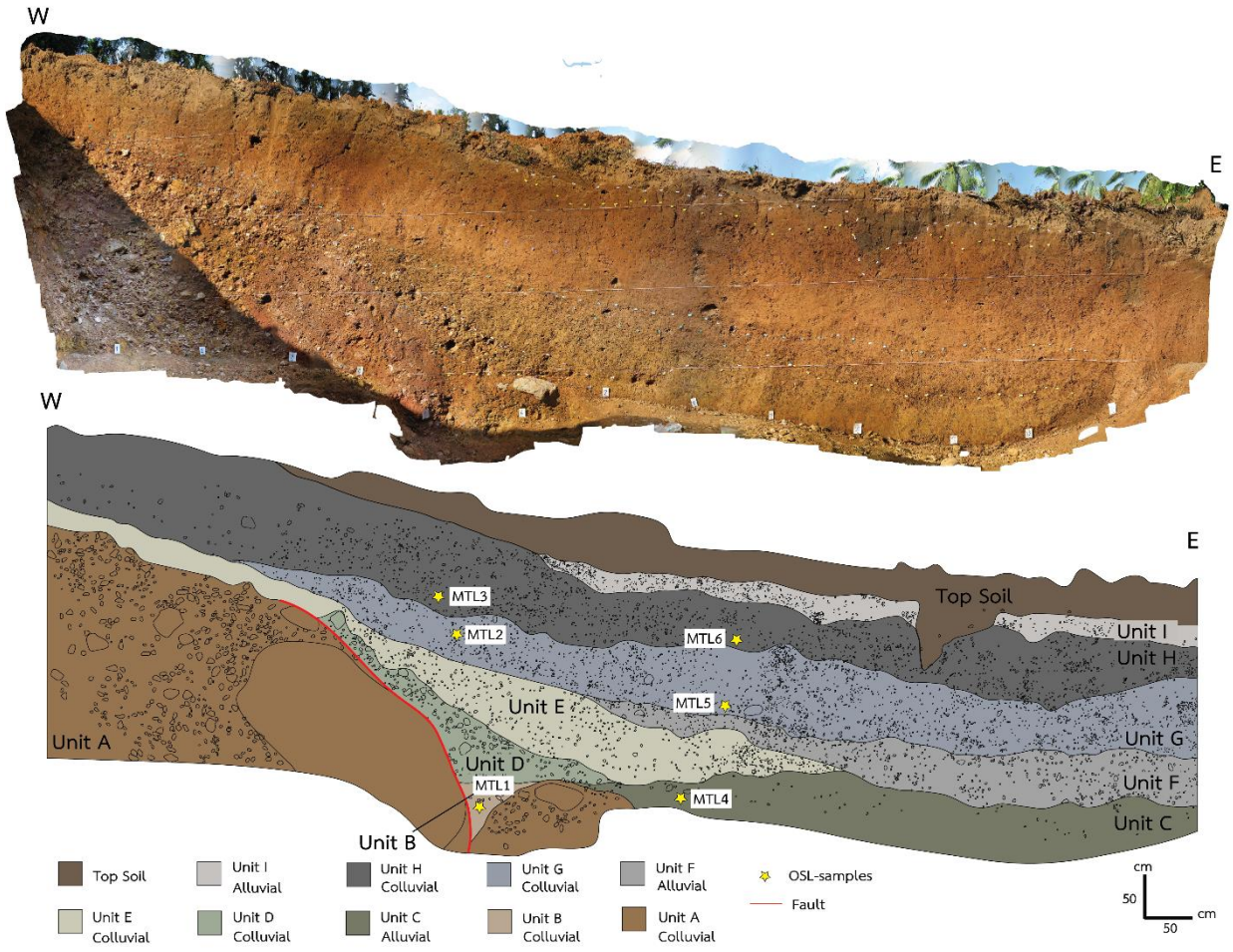

Figure 32 Paleoearthquake trench section and wall log section on the north wall at Ban Mae Tha Lu showing sediment stratigraphy, fault orientation and sample location for dating. Location shows in Figure 26A.

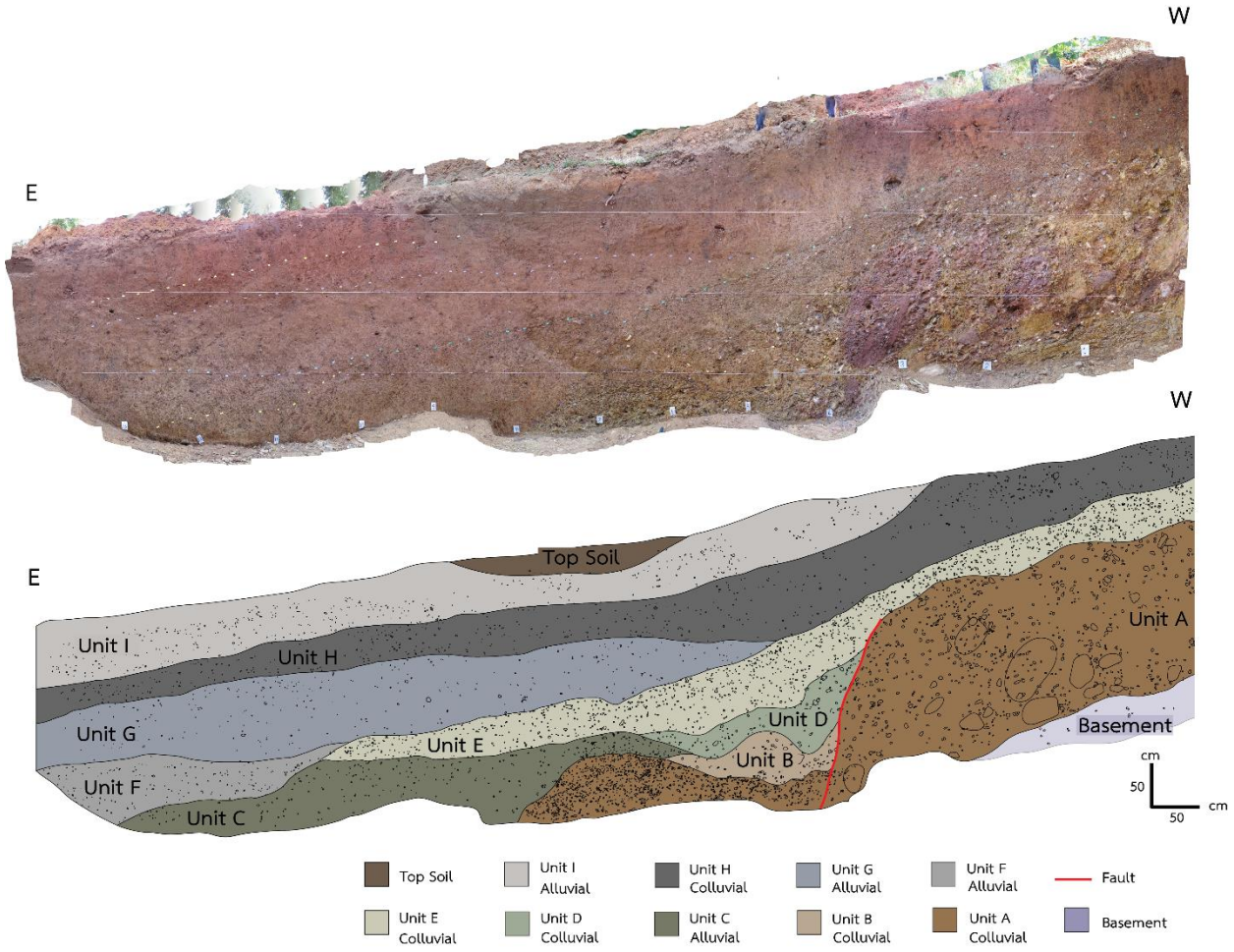

Figure 33 Paleoearthquake trench section and wall log section on the south wall at Ban Mae Tha Lu showing sediment stratigraphy and fault orientation. Location shows in Figure 26A.

Unit H is a colluvial unit with dark brown soil, mainly sand, silt and clay.

Unit I is an alluvial unit consisting mainly of sand and clay with some gravel.

Top soil is a dark clay layer, consists of organic rich silt/clay with some gravel and sand.

3. Khun Yuam trench

The Khun Yuam site is located along the frontal foothill, near Khun Yuam district. The trench was excavated a 18-m-long, 3-m-wide and 3.5-m-deep. Trench-wall exposures show 10 depositional units (A-I) which are exposed in both sidewalls (Figure 34 - Figure 36). Detail of individual units are described below;

Unit A is an alluvial unit with light brownish grey, mainly clay with a few of gravel

Unit B is an alluvial/ colluvial unit with gravel, sand, and clay. The gravel is pebble size (1.5 cm)

Unit C is a colluvial/alluvial unit that contains light brown to yellowish brown sand, silt and clay, and some gray to purple. The sediments in this unit are mainly clay with sand and sand lens.

Unit D is a colluvial unit that composed of gravel, sand, silt and clay. The grain size of gravel ranges from pebble to boulder (as much as 5x4 cm) and mainly of subangular to subrounded. The sediments in this unit are moderately to poorly sorted.

จุฬาลงกรณ์มหาวิทยาลัย
Chulalongkorn University

Unit E is a fluvial unit (channel sediment) that composed of sand, silt and clay. The grain size of gravel is pebble. At least 3 sequences of graded bedding can be observed here.

Unit F is an alluvial unit that contains orangish brown sand, silt and clay.

Unit G is an alluvial unit (channel deposits) that contains yellowish brown sand, silt and clay with some gravel. The grain size of gravel ranges from pebble to cobble. The lamination and chaositic structure could be found in the unit.

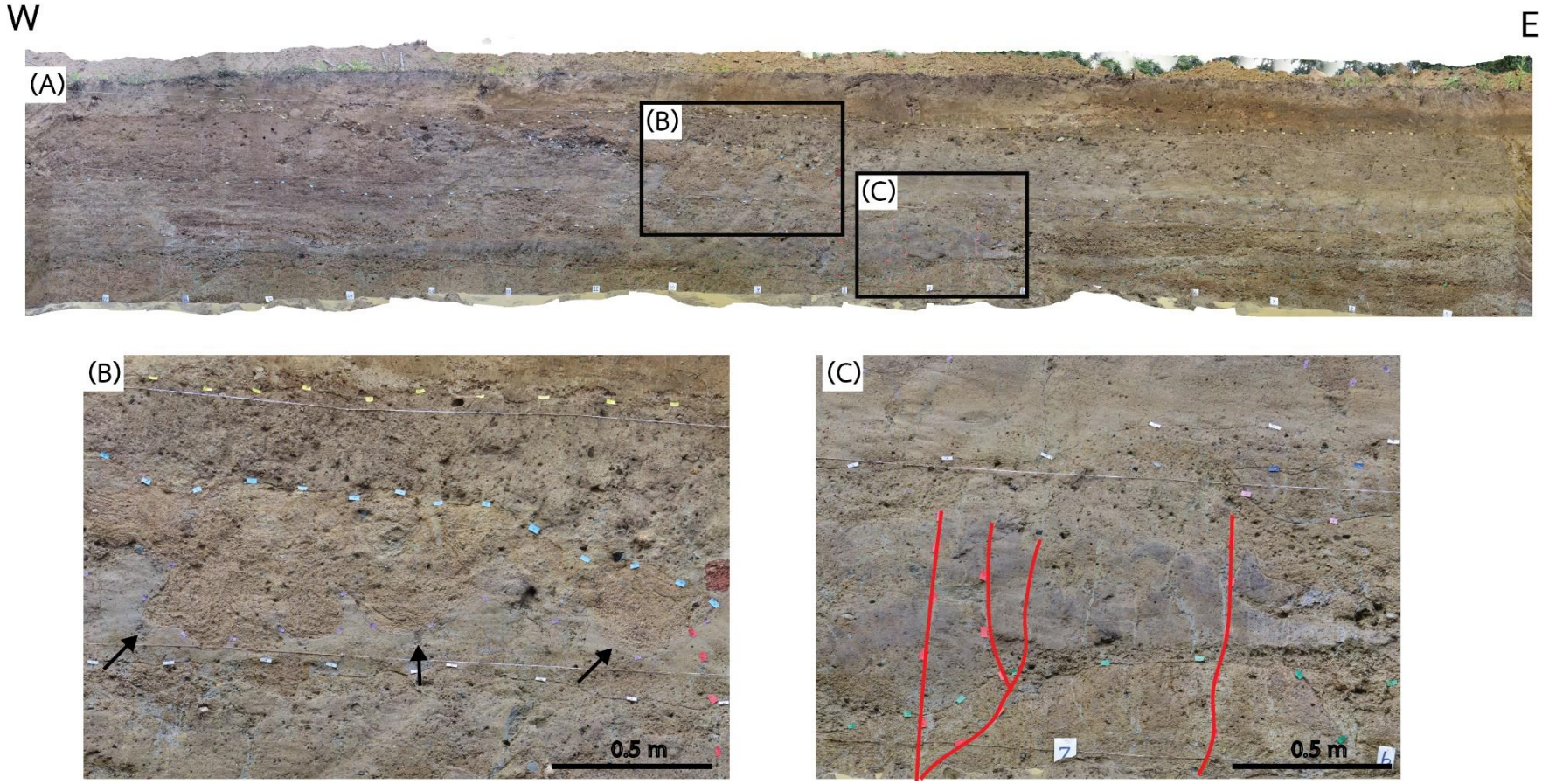

Figure 34 (A) Photograph of Khun Yuam area. (B) Closed-up photograph shows discontinuity of sediment layer that it is possibly a soft sediment deformation and (C) Closed-up photographs show the fault traces were found on the wall. (Red lines).

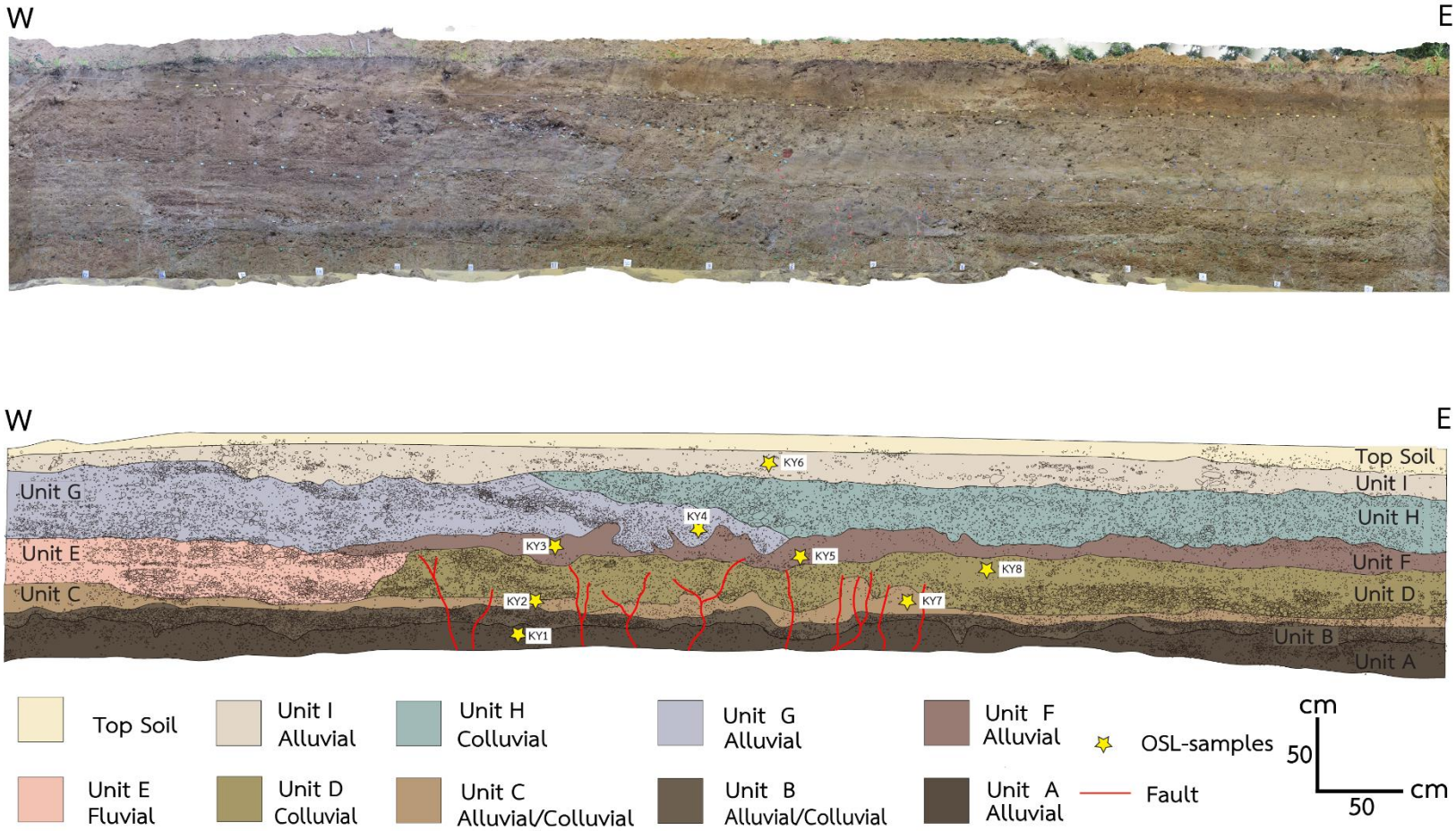

Figure 35 Paleoearthquake trench section and wall log section on the north wall at Ban Khun Yuam showing sediment stratigraphy, fault orientation and sample location for dating. Location shows in Figure 26A.

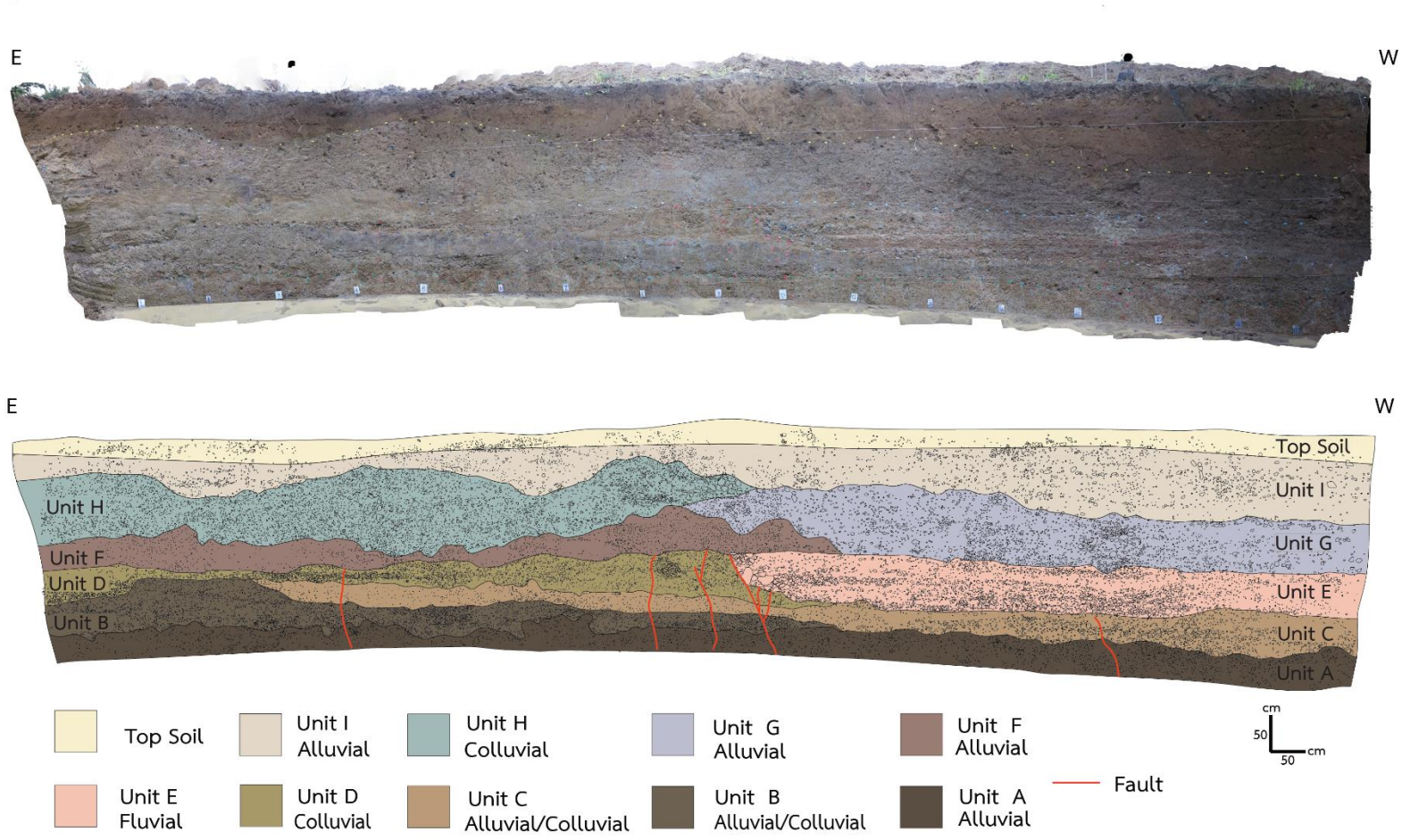

Figure 36 Paleoearthquake trench section and wall log section on the south wall at Ban Khun Yuam showing sediment stratigraphy and fault orientation. Location shows in Figure 26A.

Unit H is colluvial unit that composed of dark brown gravel, sand, silt and clay. These clasts are matrix supported and mainly composed of sand. Most clasts are angular to subrounded. The grain size of gravel ranges from pebble to cobble (as much as 12x12 cm), the gravel clasts are mainly shale, quartz and granite. The sediments in this unit are poorly to moderately sorted

Unit I is an alluvial unit clast of weather rock of sand spot, gravel spot, matrix: fine sand, clay.

Top soil: lamination can be observed in sand unit (fine to very course grain)

The sediment structure in unit F and unit G shows the deformation of the soft sediments, they are mostly ball and pillow structure from in unconsolidated sediment with low shear resistance as a result of tectonic or sedimentary processes called soft sediment deformation (SSD) (Allen, 1982). The SSD that found in the Khun Yuam trench (this study) possibly produced by seismic activity. However, this evidence also found in Ban Yod trench.

4. Ban Yod trench

The Ban Yod site is located along the frontal foothill, near Mae Hong Son Province. The trench was excavated a 19-m-long, 3-m-wide and 3-m-deep. Trench-wall exposures show 10 depositional units (A-I) which are exposed in both sidewalls (Figure 37 – Figure 39). Detail of individual units are described below;

จุฬาลงกรณ์มหาวิทยาลัย
Chulalongkorn University

Unit A, the oldest deposit exposed in trench is a colluvial unit that contains brownish grey gravel, sand, silt, and clay. These clasts are clast-supported gravel and the grain size of gravel ranges from pebble to cobble, mainly composed of sandstone, shale, and quartz. Most clasts are sub angular to rounded. The sediment in this unit are moderately sorted. Matrix is fine sand, and clay, and thickness of this unit varies from 0.5-1.25 meters.

Unit B is an alluvial unit that contains brownish grey consisting of gravel, sand and clay. The gravel is mainly composed of shale.

Unit C is a colluvial unit consisting of gravel, sand, silt, and clay. The unit is clast-supported and the grain size of gravel ranges from pebble to boulder (as much as 40 cm in diameter), and mainly of subangular to subrounded which a few gravels show subangular of sandstone and shale. The sediments in this unit are moderately sorted (gravel size). This unit is bigger than these of the lower unit.

Unit D is a colluvial unit consisting of sandstone, shale and quartz. The clast is clast supported and the grain size of gravel is varying, and maximum size is cobble which gravel size is smaller than these of the lower unit. Most clasts consist mainly of subangular to subrounded.

Unit E is a fluvio-lacustrine sediment that contains a few gravels within a dark grey clayey silt matrix. The gravels consist mainly of subangular of sandstone fragments. This unit has a lot of charcoal that can be found (carbonaceous soil).

Unit F is an alluvial unit with a light grey clay with fine sand layer. This unit shows laminations.

Unit G is a fluvial unit with a clast supported that consisting of gravel, sand silt and clay. Clast or nodule of sandstone can be observed in the unit. Most clasts of gravel are subangular and composed mainly of sandstone, shale and quartz. Lamination can be observed in sandstone clast. (sandstone: fine sand to very course sand)

จุฬาลงกรณ์มหาวิทยาลัย
CHULALONGKORN UNIVERSITY

Unit H is an alluvial/colluvial unit that composed of sand and clay with layer of gravel (sandstone size is fine grain)

Unit I is a colluvial unit that deposits in channel environment. The clasts are clast-supported gravel unit mainly consist of sandstone, shale and quartz. The gravels consist mainly of subrounded to rounded clast of sandstone and shale. At least 3 sequences of graded bedding can be observed. Upper part of this unit contains of dark clay.

Top soil is a dark soil unit, mainly composed of sandstone and clay (paleosurface) or small lens

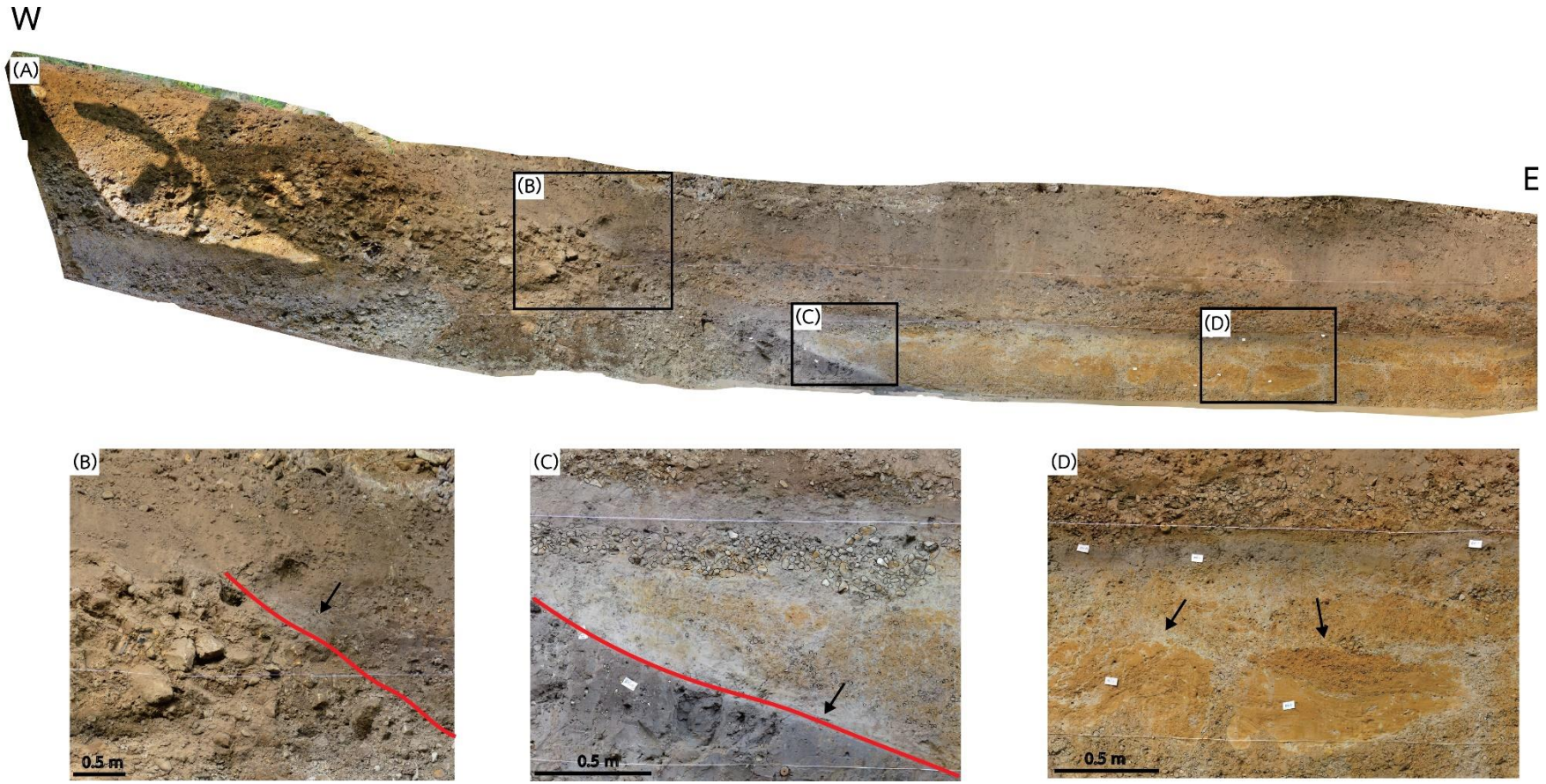

Figure 37 (A) *Photograph of* Ban Yod *area. (B) and (C) Closed-up photographs show the fault traces were found on the wall (Red lines).* (D) Closed-up photograph shows discontinuity of sediment layer that it is possibly a soft sediment deformation.

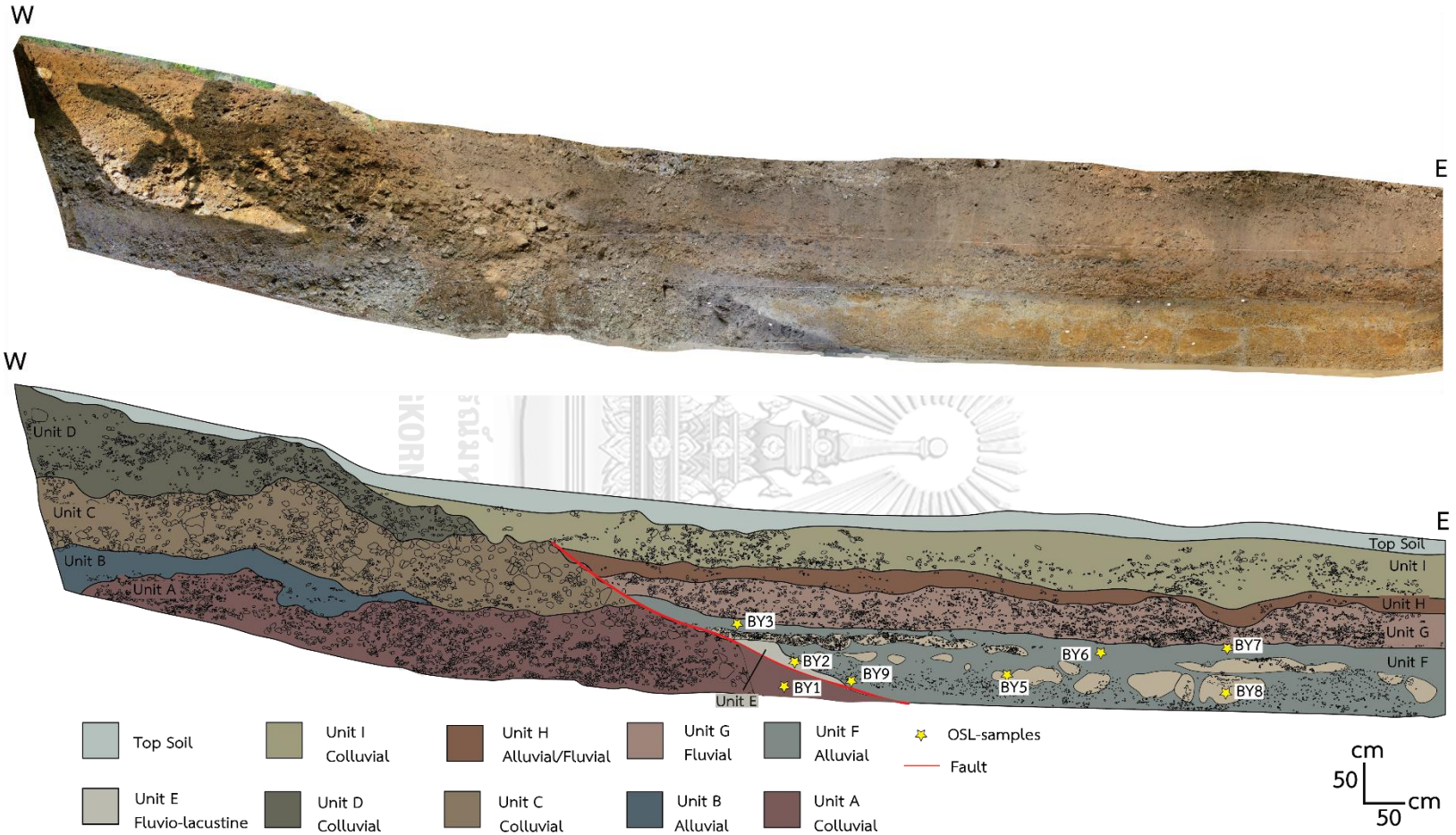

Figure 38 Paleoearthquake trench section and wall log section on the north wall at Ban Yod showing sediment stratigraphy, fault orientation and sample location for dating. Location shows in Figure 26A.

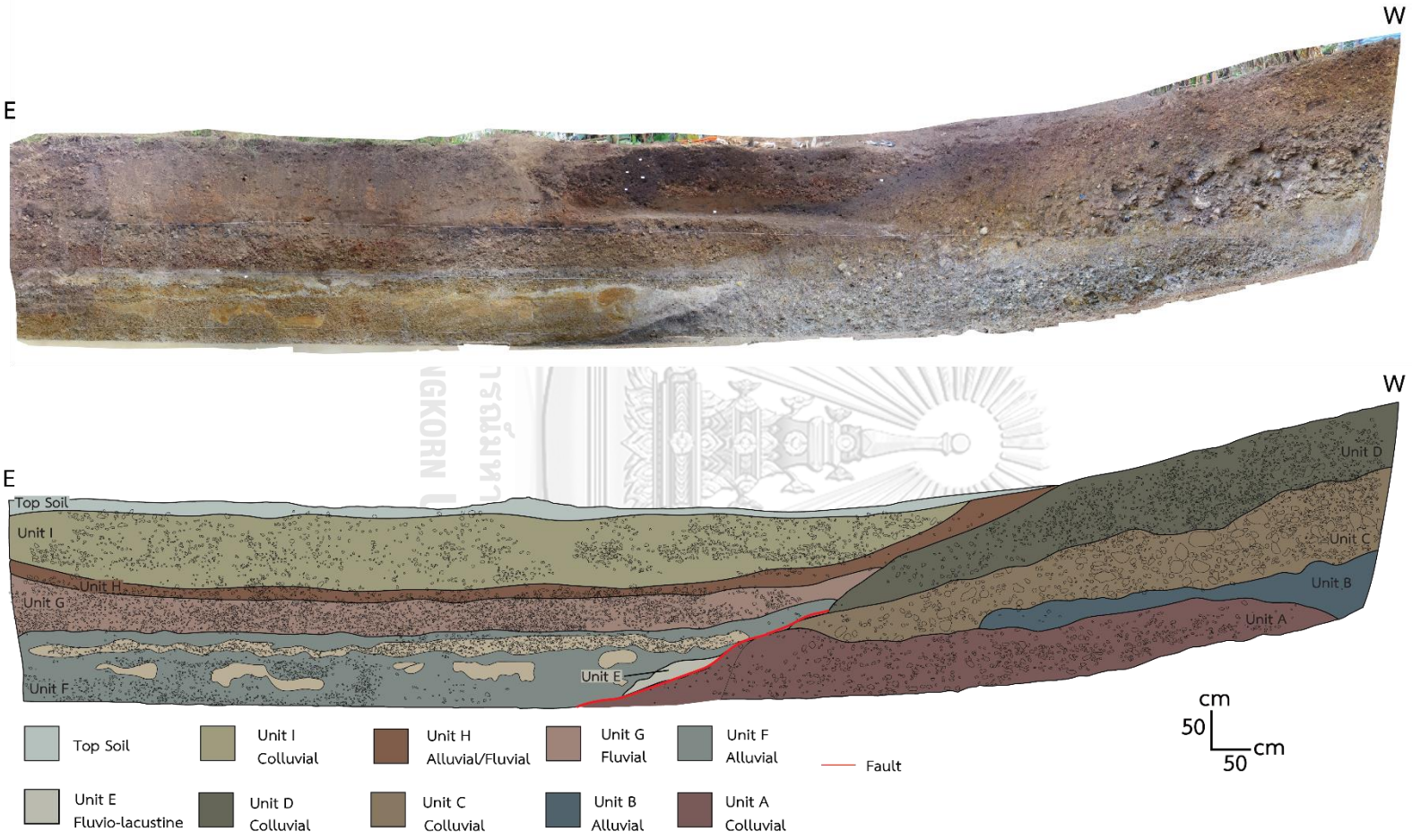

Figure 39 Paleoearthquake trench section and wall log section on the south wall at Ban Yod showing sediment stratigraphy and fault orientation. Location shows in Figure 26A.

Optical Stimulated Luminescence (OSL) dating

The OSL dating is a chronological method that has been applied extensively in archaeology and geology. It is a radiometric dating that is bases on the time-dependent accumulation of electron traps inside the crystal lattice of minerals (such as quartz and feldspar) (Duller, 2008). The OSL dating method follows that of Frankel et al. (2015) commencing at collecting suitable geological samples related to active fault, treatment of quartz-enriched samples for dating, and analyzing both of including equivalent dose evaluation (ED) and annual dose evaluation (AD) of quartz concentrates.

In this part, the procedure of OSL dating are proposed by Frankel et al. (2015). The procedures commence from collecting suitable sediment samples related to active fault, treatment of quartz-enriched samples for dating, and analyzing both of equivalent and annual doses of quartz concentration (Figure 40). The methodology of analysis composed of 2 main procedures, including ED and AD. Ultimately, based on OSL process from Frankel et al. (2015) , age of quartz bearing sediments can be determined using the simple equation:

$$Age = \frac{\textbf{Paleodose (De)}}{\textbf{Annual dose (AD)}} \quad \text{..... (Eq 4.1)}$$

Water content analysis

26 sediment samples were dried by baking to 80° C in a dark room. Water content is also measured for all samples being dated because it is the one significant parameter for annual dose determination. The formula of water content calculation is shown in equation 4.2.

$$\textbf{Water content} = \frac{\textbf{(weight of a wet sample} - \textbf{weight of a dried sample)x 100}}{\textit{weight of a dried sample}} \quad \text{..... (Eq 4.2)}$$

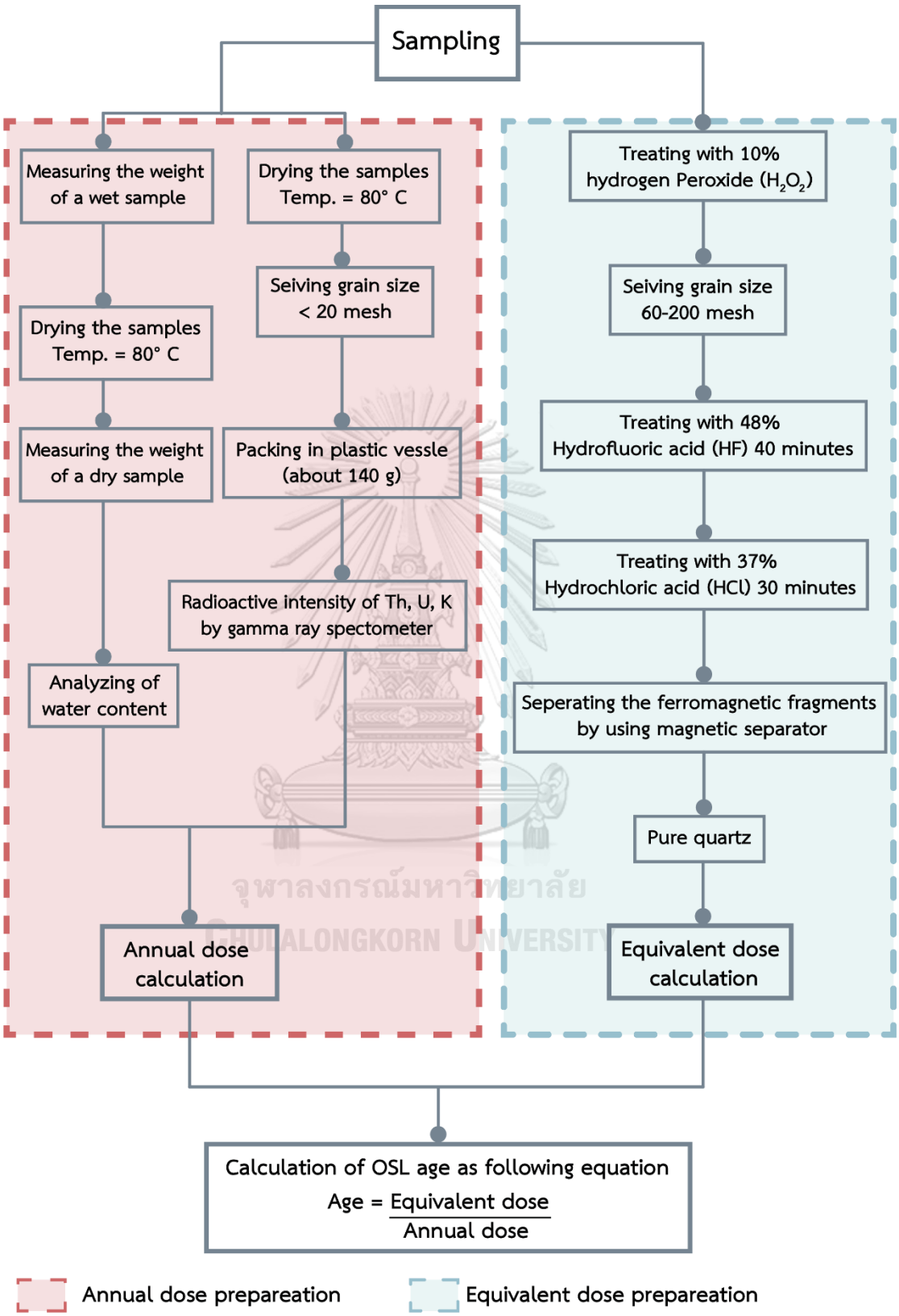

Figure 40 Chart of annual dose and equivalent dose for OSL dating, (modified after Frankel et al. (2015))

Annual Dose Evaluation

After getting dried sample, each sediment sample was shattered by using a rubber-hammer and sieved to isolate the grain size fraction. Sediments which grain size pass through 20 mesh (<841μm) were collected about 140 g and was separated to keep in plastic containers for annual dose determination.

Generally, sediments are exposed continuously to ionizing radiation, which originates from their radioactive contents, plus a small fraction from cosmic rays (Aitken, 1985). There are essentially 3 radioactive elements which contribute to the natural dose rate (annual dose) i.e., uranium (U), thorium (Th) and potassium (K). The decay of uranium and thorium results in α, β and γ radiations whereas potassium emits β and γ normally, the natural dose rates of sediment are of the order of mGy/year.

The annual dose to the sample is computed from the concentrations of K, U and Th by the method described by Bell (1979) and Aitken (1985), as shown in equation 4.3.

Annual dose = (AD) = Dα+Dβ+Dγ+Dc.....(Eq 4.3)

Where α = Alpha irradiation content,

β = Beta irradiation content,

γ = Gamma irradiation content, and

C = Cosmic ray irradiation content.

จุฬาลงกรณ์มหาวิทยาลัย
CHULALONGKORN UNIVERSITY

Measurement of Uranium, Thorium, and Potassium Contents shows the schematic preparation and procedure for measurement of U, Th, and K contents by neutron activation analysis (NAA).

Paleodose or Equivalent Dose Evaluation

Remnant part from annual dose collection is carefully re-sieved and the material passed through sieves to isolate the grain size fraction between 60 and 200 mesh (74-250μm) according to Aitken (1985). Both portions were kept in beakers for purifying quartz grain and equivalent dose determination, respectively. In the annual

dose, a sample portion is ready and skips to the measurement step but in both of two portions for equivalent dose determination is necessary to participate in chemical treatment.

In this OSL dating procedure, the quartz grains were selected as suggest by Aitken (1985) for representation of the OSL signal of the sediment sample. The main objective of chemical treatment is, therefore, to extract quartz grains from sediment samples before the OSL signal measurement procedure. The detailed steps of the chemical treatment are as follows:

a) Treating the sample with 10% hydrogen peroxide (H_2O_2) to remove some organic materials.

b) Chemically cleans the sample in treated with 37% HCl for 15-30 minutes and re-wash several times with distilled water to eliminate carbonates and deep-rooted organic materials.

c) Etching the sample in 48% HF for 40 minutes and re-wash it several times with distilled water. HF is used to dissolve the plagioclase, and

d) After washing with water and drying in the red-light room, the dried sample was then separated to remove minerals e.g., Fe, zircon, and metallic minerals by using an isodynamic separator (Frant'z isodynamic magnetometer). After purified sample, it is ready for equivalent dose determination.

จุฬาลงกรณ์มหาวิทยาลัย
Chulalongkorn University

Evaluation of equivalent dose commences with measurement of OSL intensities on 3 sample portions: 1) natural sample portion, 2) residual sample portion and 3) artificial irradiation sample portion. The OSL emission of quartz was measured in red-light room by the Riso TLD dosimeter at Department of Geology Faculty of Science, University of Cincinnati, USA (Figure 41). About 20 mg of sample was filled in aluminum planchettes and placed on a molybdenum heater. The filter system applied in this study is a blue filter (Toshiba IRA-10). The light emission is amplified and measured by photomultiplier and recorded simultaneously with the temperature added to the sample.

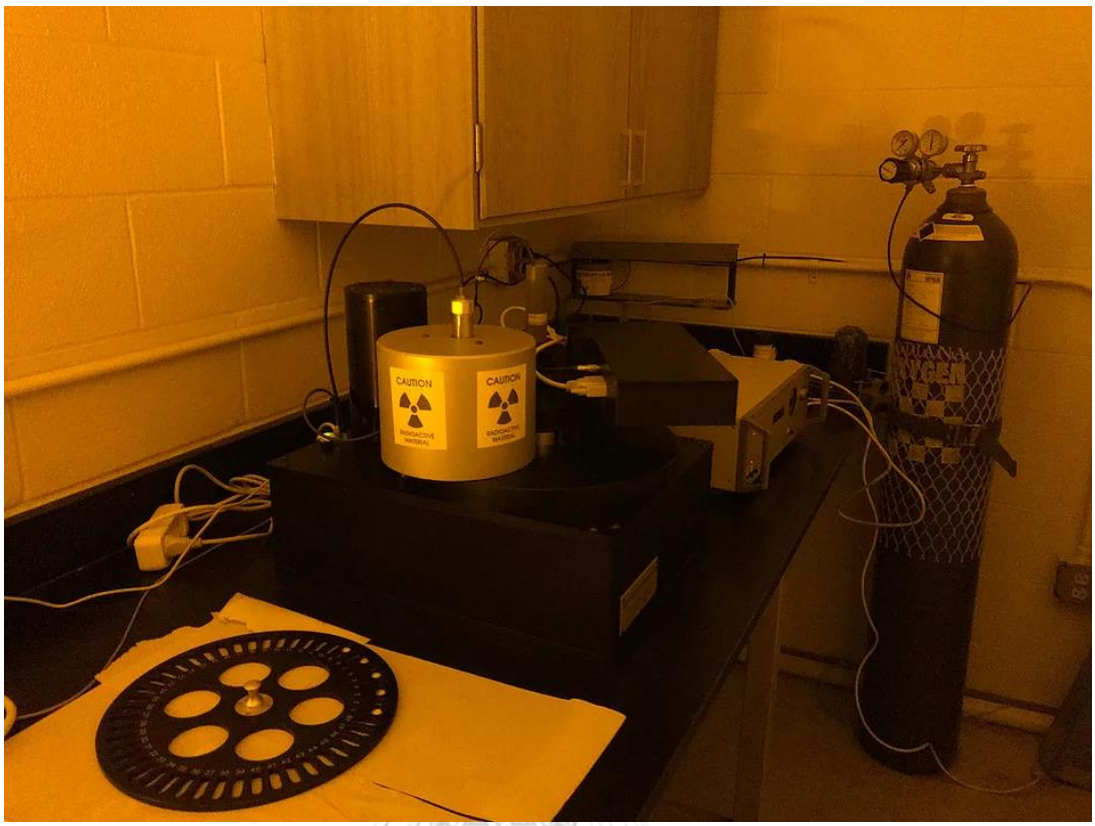

Figure 41 The Riso TLD dosimeter installed at Department of Geology Faculty of Science, University of Cincinnati, USA.

จุฬาลงกรณ์มหาวิทยาลัย
Chulalongkorn University

Dating results

26 samples were selected from Ban Mae Tha Lu, Ban Yod and Khun Yuam trenches and road-cut wall at Doi Wiang Luang (as shown in Figure 42 - Figure 45) for OSL dating. The results are 26 samples shown in Table 5. For AD analysis, the samples contain U contents varying from 0.18 to 7.14 ppm, Th contents from 4.25 to 41.63 ppm, and K contents from 0.32% to 4.44%. In general, water contents of samples are between 16.65 and 68.66%. The AD of samples varies from 0.64 to 4.78 mGy/Y, and the ED range from 5.15 to 348.20 Gy (see determination in appendix). The OSL ages are between 1,200 and 176,000 years.

Table 5 Summary of OSL dating results of extracted sediments from study area, Mae Hon Son Province, northern Thailand, containing radioisotope concentrations, moisture contents total dose rate, equivalent dose estimates and absolute ages.

Sample No.	U (ppm)	Th (ppm)	K (%)	W (%)	AD (Gy/ka)	ED* (Gy)	Age (yr)	Error (yr)
KY1	7.14	32.12	3.46	68.66	4.24	143.67	33,900	2,300
KY2	6.73	27.98	2.08	63.64	3.37	31.97	9,500	650
KY3	6.25	30.20	2.02	61.15	3.44	21.85	6,400	460
KY4	5.52	20.97	3.52	49.43	4.17	16.99	4,000	310
KY5	3.59	41.63	1.53	51.35	3.47	9.34	2,700	210
KY6	3.23	38.07	4.44	61.75	4.78	5.88	1,200	150
KY7	3.25	40.78	1.95	49.67	3.68	14.26	3,900	290
KY8	3.10	30.71	1.30	51.09	2.79	8.13	2,900	200
BY1	1.43	9.08	0.91	37.10	1.47	18.72	12,700	960
BY2	1.53	7.73	0.68	34.19	1.29	41.42	32,000	2,400
BY3	1.05	4.25	0.32	58.37	0.68	7.26	10,600	620
BY5	0.70	8.52	1.45	42.92	1.63	16.33	10,000	940
BY6	0.74	8.27	1.36	34.65	1.67	7.79	4,600	390

จุฬาลงกรณ์มหาวิทยาลัย
Chulalongkorn University

Table 5 (cont.)

Sample No.	U (ppm)	Th (ppm)	K (%)	W (%)	AD (Gy/ka)	ED* (Gy)	Age (yr)	Error (yr)
BY7	0.18	7.30	1.39	46.39	1.43	5.15	3,600	300
BY8	1.35	5.97	0.49	64.98	0.86	40.96	47,900	2,800
BY9	0.50	8.31	1.40	43.44	1.55	13.54	8,700	680
MTL1	1.24	9.31	1.73	39.56	1.98	348.20	176,000	15,000
MTL2	1.80	15.55	1.93	21.51	2.93	102.11	34,800	2,900
MTL3	1.99	13.88	1.54	39.68	2.22	55.36	25,000	2,000
MTL4	1.09	19.03	3.11	56.47	2.97	119.63	40,000	3,100
MTL5	1.48	18.41	2.76	16.65	3.22	64.12	16,500	1,500
MTL6	1.80	13.84	1.44	32.28	2.23	51.31	23,000	1,700
DWL1	0.99	23.61	1.67	45.49	2.57	34.85	13,500	1,000
DWL2	1.15	17.78	1.64	55.17	2.12	67.38	31,800	2,300
DWL3	1.07	18.79	1.30	52.43	1.97	67.38	34,200	2,400
DWL4	0.93	17.93	2.97	59.56	2.77	213.73	77,300	9,400

* Remark: ED grow and growth curves show in Appendix.

จุฬาลงกรณ์มหาวิทยาลัย
Chulalongkorn University

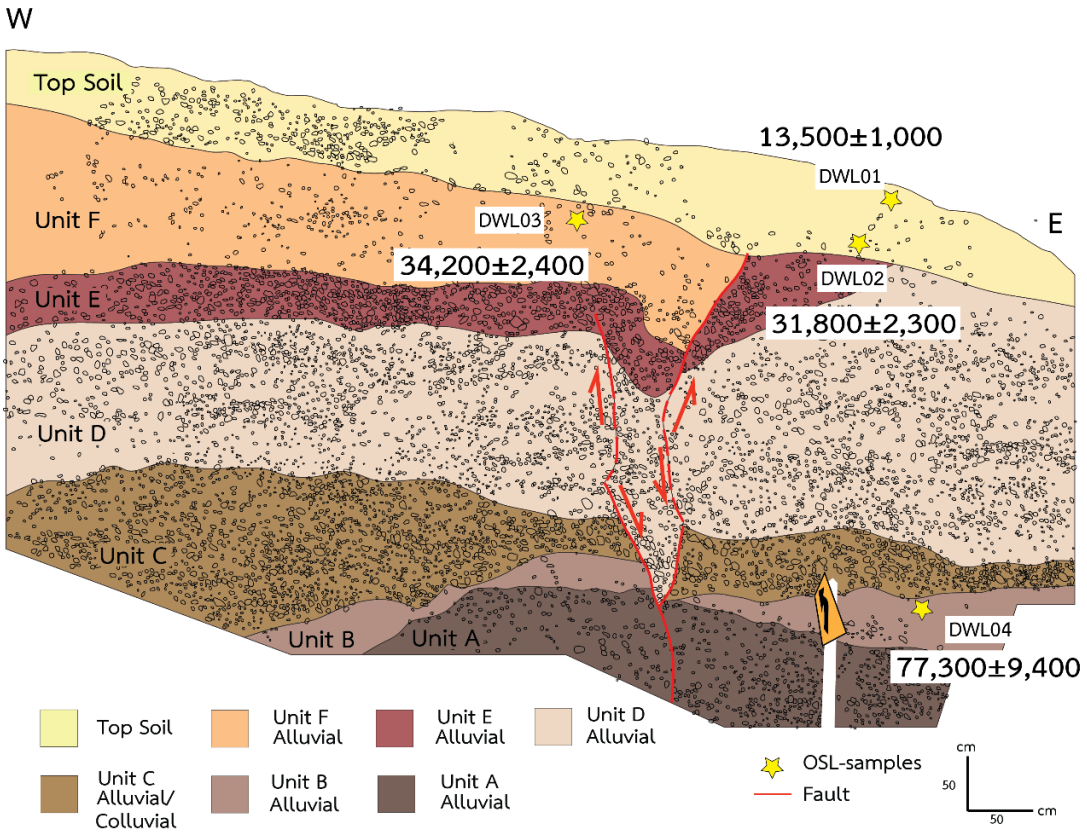

Figure 42 Trench-log stratigraphy and photograph show fault orientation and OSL ages of sediment layers on road-cut wall of Doi Wiang Luang site. Location shows Figure 26A.

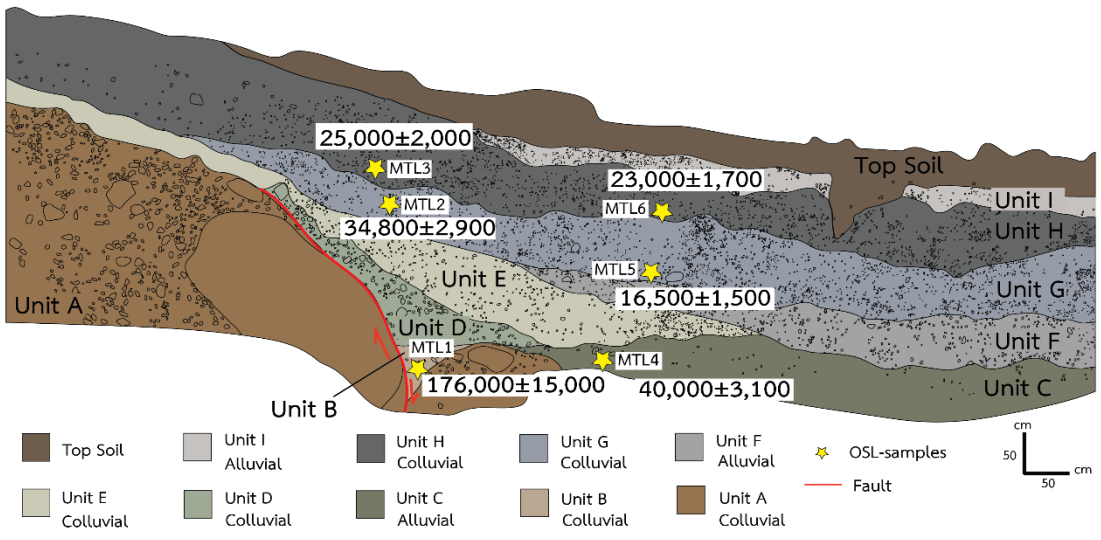

Figure 43 Trench-log stratigraphy and photograph show fault orientation and OSL ages of sediment layers on north wall of Mae Tha Lu site. Location shows Figure 26A.

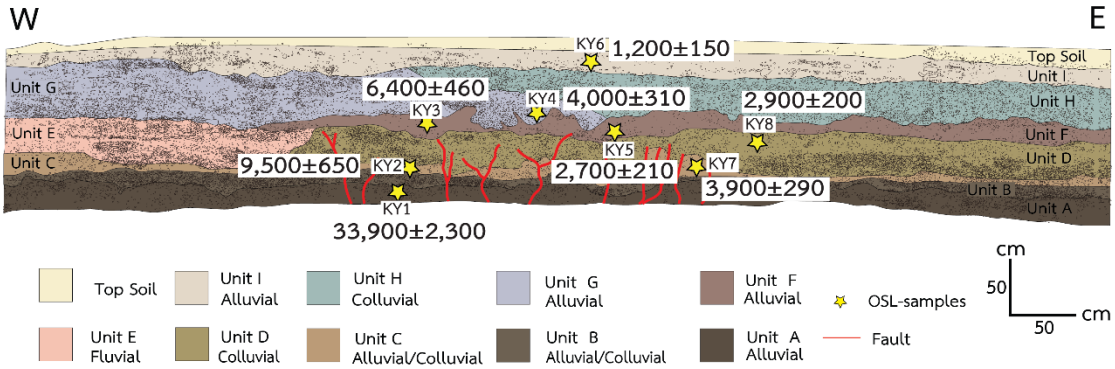

Figure 44 Trench-log stratigraphy and photograph show fault orientation and OSL ages of sediment layers on north wall of Khun Yuam site. Location shows Figure 26A.

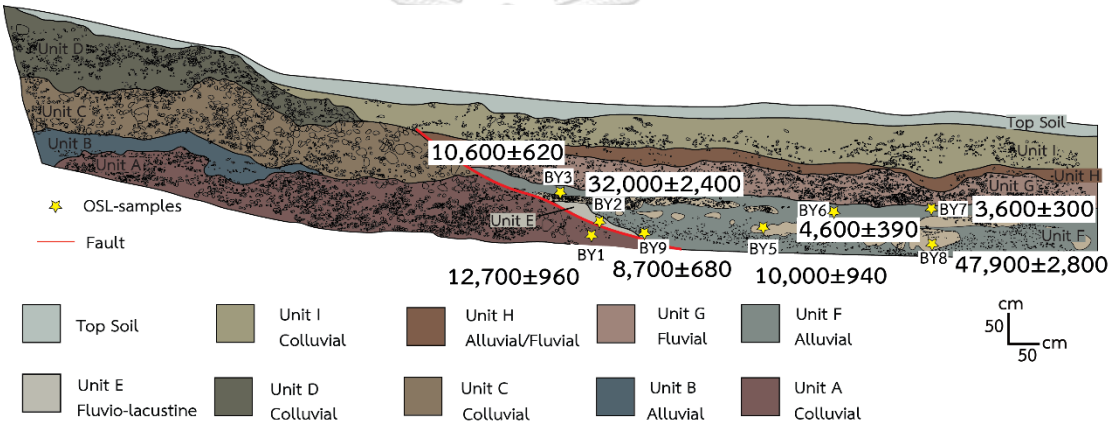

Figure 45 Trench-log stratigraphy and photograph show fault orientation and OSL ages of sediment layers on north wall of Ban Yod site. Location shows Figure 26A.

จุฬาลงกรณ์มหาวิทยาลัย
Chulalongkorn University

The stratigraphic unit and OSL dating from Doi Wiang Luang road-cut wall shows in Figure 42. Four samples were collected for OSL dating (DWL1, DWL2, DWL3, and DWL4). The OSL ages indicated that the sediments in the road-cut wall were deposited from ca. 77,300 yr BP to present year. Base on the stratigraphic unit and OSL dates, two paleoearthquake events occurred at ca 34,300 yr BP and 22,000 yr BP, respectively.

The stratigraphic unit and OSL dating from Mae Tha Lu trench show in Figure 43. Six samples were collected for OSL dating (MTL1, MTL 2, MTL 3, MTL4, MTL5, and MTL6). The OSL ages indicated that the sediments in the trench wall were deposited from ca. 176,000 yr BP to present year. Base on the stratigraphic unit and OSL dates, one paleoearthquake event occurred at ca 48,000 yr BP.

The stratigraphic unit and OSL dating from Khun Yuam trench show in Figure 44. Four samples were collected for OSL dating (KY1, KY2, KY3, KY4, KY5, KY6, KY7, and KY8). The OSL ages indicated that the sediments in the trench wall were deposited from ca. 33,900 yr BP to present year. Base on the stratigraphic unit and OSL dates, two paleoearthquake events occurred at ca 30,000 yr BP and 3,000 yr BP, respectively.

จุฬาลงกรณ์มหาวิทยาลัย
Chulalongkorn University

The stratigraphic unit and OSL dating from Ban Yod trench show in Figure 45. Four samples were collected for OSL dating (BY1, BY2, BY3, BY4, BY5, BY6, BY7, BY8, and BY9). The OSL ages indicated that the sediments in the trench wall were deposited from ca. 47,900 yr BP to present year. Base on the stratigraphic unit and OSL dates, three paleoearthquake events occurred at ca 30,000 yr BP, 8,000 yr BP, and 3,000 yr BP, respectively.

CHAPTER IV
Discussion

In this chapter, morphological interpretation results of the MHSF (MHSF) and the influence of pre-existing fabrics on fault kinematics and basin geometry are discussed. A three-dimensional (3D) conceptual structural model of the MHSF is proposed with implication for basin evolution related to strike-slip faults in northern Thailand. Then, paleoearthquake events and recurrence interval of the MHSF from Chapter IV are discussed with previous works for better understanding of Present-day kinematic behavior the MHSF and other active faults in Thailand.

Influence of pre-existing fabrics on fault kinematics and basin geometry

The MHSF is located on the boundary between the Inthanon zone and the Sibumasu block, which formed a narrow N-S-trending weak zone within the basement rocks (Hisada et al., 2004). Continuous collision between the Eurasian and Indian plates during the Oligocene possibly caused reactivation of this pre-existing fabric under a N-S compression (Shi et al., 2018). The influence of pre-existing fabrics on fault kinematics and fault patterns during the Cenozoic has been studied in other parts of Thailand e.g. Gulf of Thailand (Morley et al., 2011), Phetchabun Basin (Pongwapee, Morley, and Won-in, 2018). Also, analogue modelling of intraplate strike-slip tectonics indicates the effect of crustal weak zones on strike-slip fault-zone segmentation (Dooley and Schreurs, 2012). Therefore, the orientation of the MHSF and the geometry of the MHSB and the MSB might reflect the control of the reactivated pre-existing fabrics. These two basins are aligned along the MHSF in N-S direction and are structurally separated by Khun Yuam Linkage Zone (KYLZ), which is described for the first time in this chapter.

จุฬาลงกรณ์มหาวิทยาลัย
Chulalongkorn University

Following the definition of pull-apart basins by Aydin and Nur (1982), they measured the dimensions of 62 active pull-apart basins in 2-dimention from all over the world and found that the relationship between the length (l) and width (w) of pull-apart basins shows a well-defined linear correlation exists between length and width, with a ratio of approximately 3. According to the result, the MSB is a very elongated basin, with the dimension of 64.82 km in length and 8.96 km in width (l/w= 7.23) and the MHSB is elongated basin, with the dimension of 35.95 km in length and 6.97 km in width (l/w= 5.16) (Figure 46). From the studying of Hisada et al. (2004), the MHSF represents the boundary between the Inthanon zone and Sibumasu block in N-S direction and reactivated along this suture. Therefore, it is possible that the high ratio (l/w) of the MHSB and the MSB possibly related to the prior structure and created by the MHSF.

In Mae Hong Son area as shown in the Figure 16- Figure 22, the MHSB is a fault–controlled Cenozoic basin which may have formed by the development of two major sets of faults along the western and eastern margins of the basin. The faults which are mainly oblique normal faults. Several lines of morphotectonic evidence including many sets of offset streams and linear valleys suggest that these faults potentially are still active although there is a less likely chance to create big earthquake in this region (Pailoplee and Charusiri, 2016).

In Mae Sariang area, faults are similar to those recognized in the MHSB in that they are mainly oblique normal faults. The faults are characterized by linear valleys, offset streams, shuttle ridge and scarplets. The faults are in the N-S direction in the northern portion and deviate to NW- SE in the southern portion and some sets are in the basin. The basin is about 64.82 km long and its rims are controlled by two faults. It seems likely that the fault line in the east is more prominent than that in the west. Therefore, the faults in the eastern side are more subsided or less uplifted than those in the west, suggesting that the vertical movement component becomes more prominent than that of the horizontal component.

The zone located high elevation between the MHSB and the MSB is defined as the Khun Yuam Linkage Zone (KYLZ) (Figure 47). In the KYLZ, displacement analysis results (shown in Figure 23 and Figure 24) show decreasing vertical displacement of the MHSF towards the Khun Yuam district. This suggests that the MHSF was initiated by two separated fault segments underneath the MHSB and the MSB, which each later propagated towards the KYLZ and formed overlapping low-displacement fault pattern. Implication for earthquake potential in the linkage zone that is dominated by low-displacement faults is of future works.

It can be expected that most MHSF segments converge downwards to the weak zone in the middle crust (Searle and Morley, 2011). Morphological interpretation from this study suggests that the MHSF and its related basins may form as a result of dextral shear of the crustal boundary with lateral displacement up to 200 km.

จุฬาลงกรณ์มหาวิทยาลัย
Chulalongkorn University

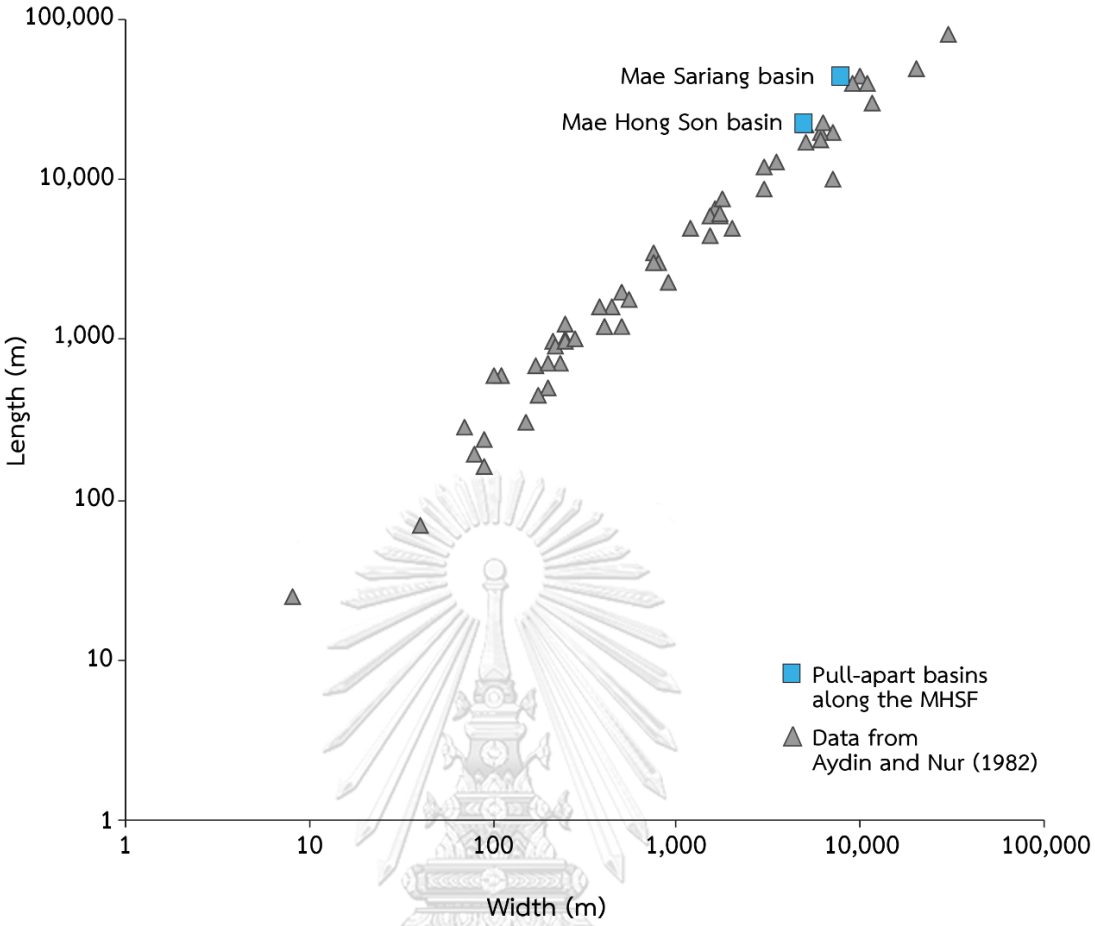

Figure 46 Length versus width plot for natural pull-apart basins (data from Aydin and Nur (1982)) and pull-apart basins in Mae Hong Son area from this study.

จุฬาลงกรณ์มหาวิทยาลัย
Chulalongkorn University

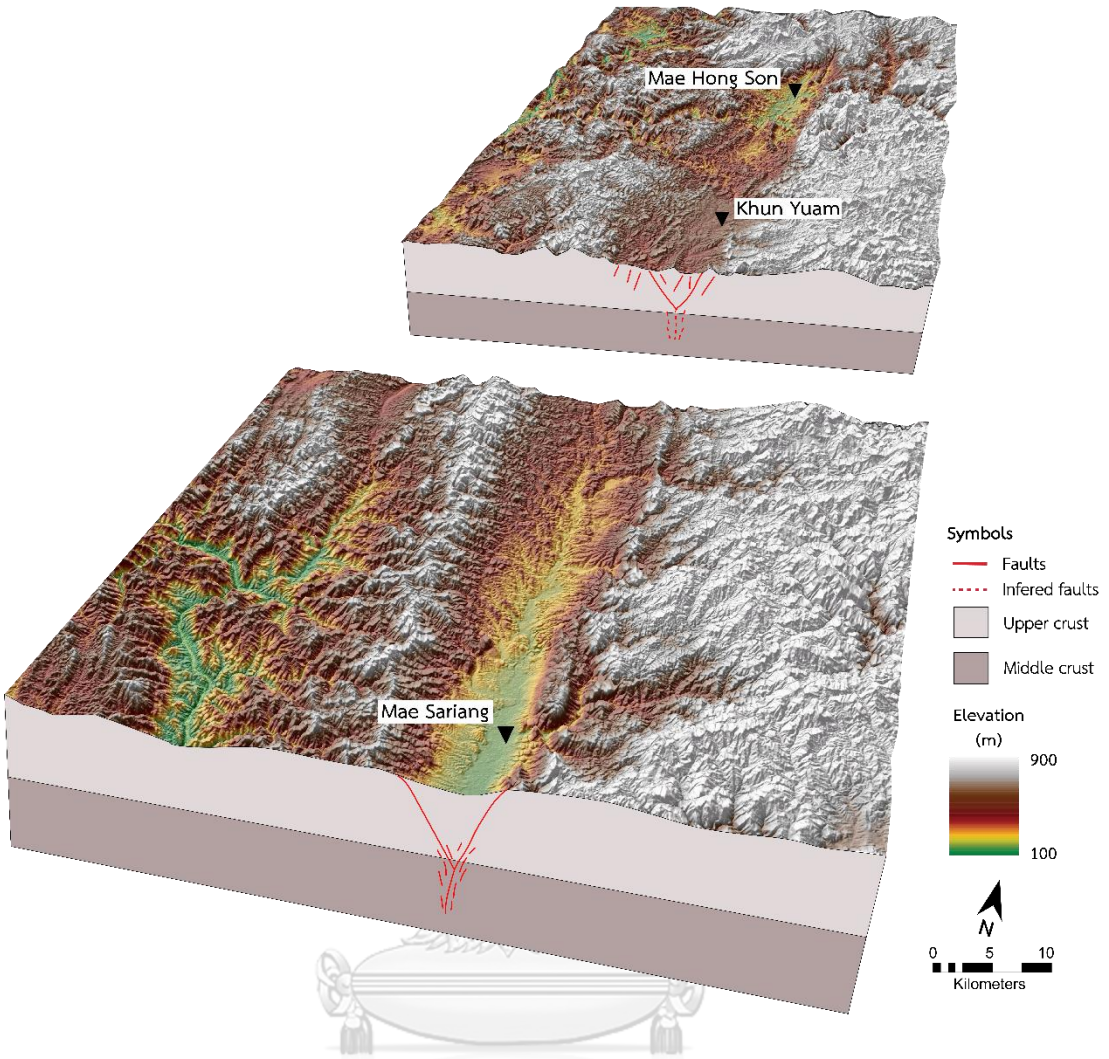

Figure 47 Simplified model explaining the neotectonics of the MHSF, high elevation area between the MHSB and the MSB is defined as the Khun Yuam Linkage Zone (KYLZ).

จุฬาลงกรณ์มหาวิทยาลัย
Chulalongkorn University

Paleoearthquake events and recurrence interval of MHSF

Based on field and geochronological data from DMR (2007), Wiwegwin et al. (2014), and this study, nine paleoearthquake events have been identified along the MHSF, as shown in Figure 48. The evidence for these paleoearthquake events consists of offsets of stratigraphic units in the road-cut and trench walls. Detailed discussion of individual paleoearthquake events are discussed below.

The first paleoearthquake event of the MHSF may be related to the offset sedimentary layers on the Phra That Chom Kitti segment (Figure 48), as reported by Wiwegwin et al. (2014). The fault cuts through a sedimentary unit that was deposited at ca. 89,720 yr BP, and the movement must therefore be younger than this unit. However, geochronological dates are available to constrain the timing of the cessation of fault movement. Thus, based on the OSL and TL age from Wiwegwin et al. (2014), the timing of the event is roughly constrained as having occurred at ca. 78,000 yr BP.

The second paleoearthquake event of the MHSF may be related to movement on the Ban Pae segment (reported by DMR., 2007). The fault cuts through a sedimentary unit that was deposited at ca. 69,740 yr BP. (Figure 48), and hence must be younger than the unit. Thus, the timing of the event as having occurred at ca. 68,000yr BP, based on the OSL age from DMR (2007).

จุฬาลงกรณ์มหาวิทยาลัย
Chulalongkorn University

The third paleoearthquake event of the MHSF may be related to movement on the Mok Chum Pae segment. The fault cuts sediment layers deposited during the period of 58,670–57,670yr BP. Thus, the timing of the event as having occurred at ca. 58,000 yr BP, based on the OSL age from Wiwegwin et al. (2014).

The fourth paleoearthquake event of the MHSF is possibly related to movement on the Phra That Chom Kitti segment (reported by Wiwegwin et al. (2014)). The fault cuts sediment layers deposited during the period 53,300–41,240 yr BP. This event also found on the Mae Tha Lu segment, may be related to movement

of the fault that cuts unit A before the sediment layers deposited during the period of 37,193- 43,369 yr BP. (unit B). Thus, the timing of the event as having occurred at ca. 48,000 yr BP.

The fifth paleoearthquake event of the MHSF may be related to the offset sedimentary layers on the Doi Wiang Luang segment (Figure 32). The fault cuts through a sedimentary unit (unit B) that was deposited at ca. 77,283 yr BP and cuts through unit B-E. The movement must be younger than unit F that was deposited at ca. 34,929 yr BP. Thus, based on the OSL ages, it is possible that this fault was active before ca. 34,300 yr BP. This paleoearthquake event also found in the Phra That Chom Kitti segment that reported by Wiwegwin et al. (2014).

The sixth paleoearthquake event of the MHSF may be related to the offset sedimentary layers on the Khun Yuam, Ban Yod and Phra That Chom Kitti segments (Wiwegwin et al. (2014)) (Figure 48). Based on the OSL ages, it is possible that this fault was active before ca. 30,000 yr BP.

The seventh paleoearthquake event of the MHSF may be related to the offset sedimentary layers on the Doi Wiang Luang segment and also Mae La Noi segment that reported by Wiwegwin et al. (2014) (Figure 48). Based on the OSL ages, it is possible that this fault was active before ca. 22,000 yr BP.

จุฬาลงกรณ์มหาวิทยาลัย
CHULALONGKORN UNIVERSITY

The eight paleoearthquake event of the MHSF occurred at ca. 8,000 yr BP, may be related to the offset sedimentary layers on the Ban Yod segment, Mae La Noi segment and Mok Chum Pae segment (Wiwegwin et al. (2014)) (Figure 48).

The last paleoearthquake event occurred at about 3,000 yr BP, based on the result of the OSL ages at Khun Yuam and Ban Yod segments (Figure 48). However, evidence for this youngest faulting event is clear in the trench (see Figure 44 and Figure 45 in Chapter IV).

Summary of earthquake events is shown in Figure 48, based upon the results of discussion with earlier dating data and this study that the recurrence interval of the MHSF is approximately 5,000 yrs. By contrast, the recurrence interval of the MHSF of previous study which is purposed by Wiwegwin et al., 2014 may be on 10,000 years. Therefore, it is possible that the recurrence interval of the MHSF was ca. 5,000 years based on nine paleoearthquake events of this study and previous study.

Determination on slip rates

The slip rate in this study was determined from the lateral offset of streams of the recent fault movement and the age of latest earthquake from paleoearthquake investigation. For example, the average or mean offset of the stream at Mae Tha Lu segment is ca. 4 m. and using the age as 48,000 yr BP of the last earthquake which found from the trench, an average slip rate on Mae Tha Lu segment is ca. 0.09 mm/yr.

The average slip rate can also be estimated from the equation Slip rate = D/R (where D is the slip per event and R is the recurrence interval). The vertical offset in the trench wall at Khun Yuam segment is ca. 20 cm. and Doi Wiang Luang segment is ca. 75 cm. and the recurrence interval is ca. 5,000 yr. Thus, an average slip rate on Khun Yuam segment and Doi Wiang Luang segment is ca. 0.04 mm/yr. and 0.15 mm/yr, respectively.

จุฬาลงกรณ์มหาวิทยาลัย
Chulalongkorn University

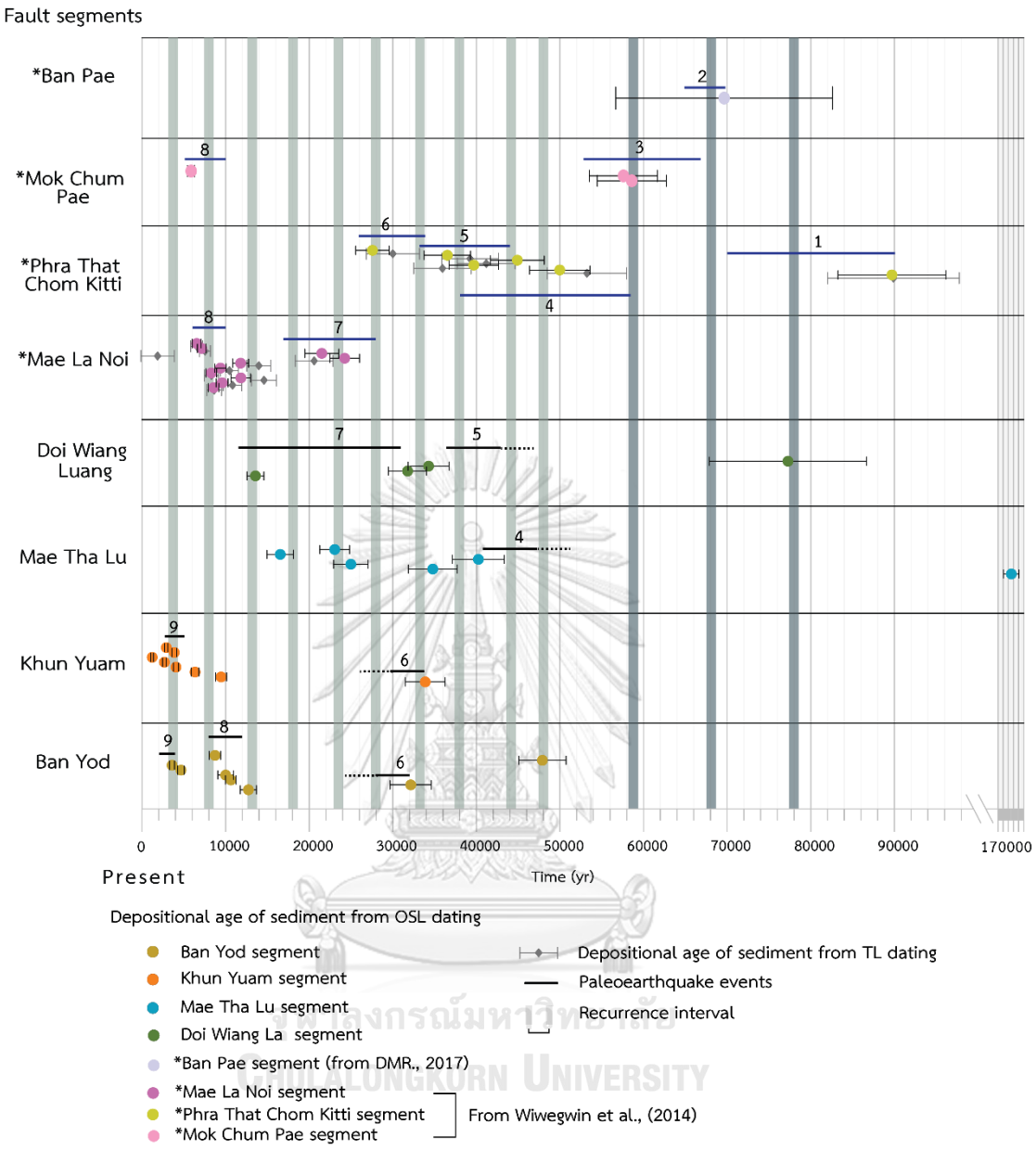

Figure 48 Diagram showing the depositional ages of sediments in the road-cut wall and trenches from the OSL ages and paleoearthquake events.

Evolution of the basins along the MHSF

All the results described and analyzed from this study may be sufficient for determining evolution of basin, based upon tectonic syntheses, the slip rate of fault and basin geometry. However, the MSB is investigated for describing the evolution of basin in the southern part of the MHSF. The basin is interpreted as pull apart basin. Lacassin, Replumaz, and Leloup (1998) reported the upper and lower bound for average slip rate is 5 Ma and 20 Ma, respectively. The Mengxing Fault was applied to determine the age of the basin because the fault is an active fault that closed to the MHSF and still active. Therefore, the maximum slip rate of the fault is ca. 4.8 mm/yr. and minimum slip rate of the fault is ca. 1.2 mm/yr. Moreover, the estimated lateral displacement of the MSB is ca. 12 km. Consequently, if assume that the MHSF has been moving at a constant rate, the age of this pull apart basin possibly began to open in maximum age ca. 10 Ma. and minimum age ca. 2.5 Ma. (Early Miocene – Late Pliocene) (Figure 49). The comparative plots show the MSB related to the development of rift basins and dextral movement of the Mae Ping Fault which is purposed by Morley et al. (2007) and the dextral movement of northern Thailand (Morley, Charusiri, and Watkinson, 2011). Thus, the MSB possibly occurred at the same time as other basins in northern Thailand.

จุฬาลงกรณ์มหาวิทยาลัย
Chulalongkorn University

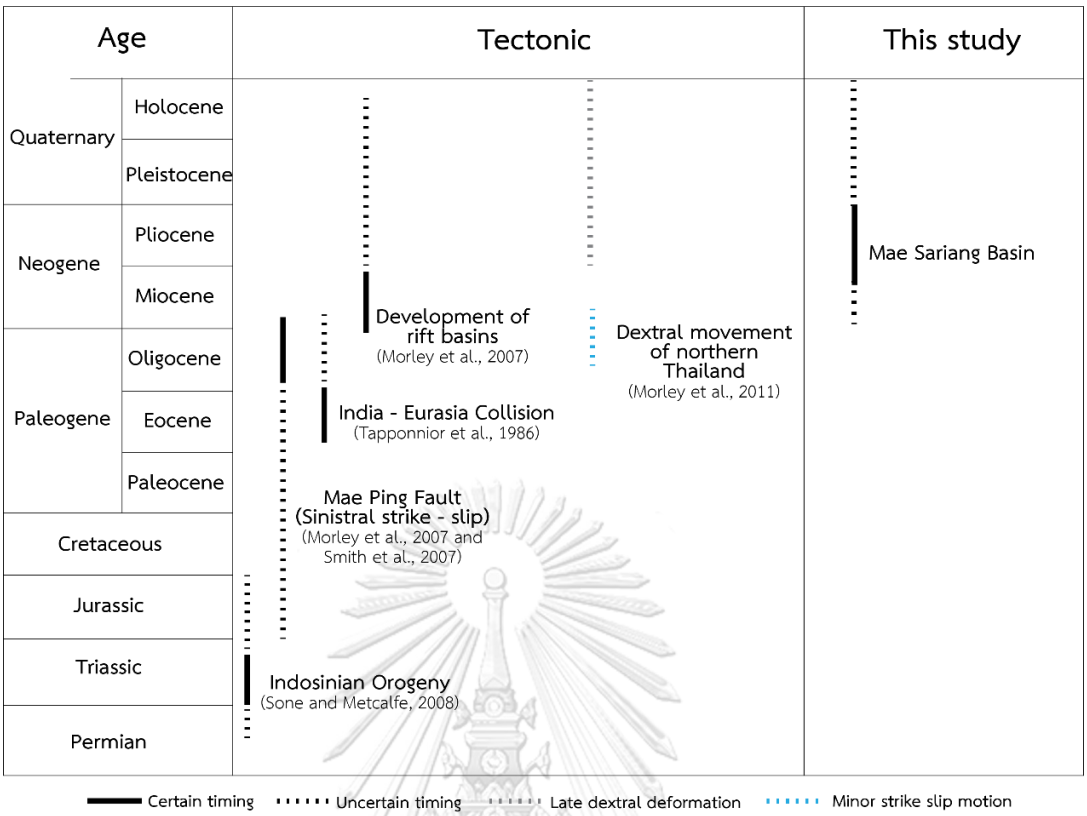

Figure 49 Comparative chart of the regional tectonic events (modified from Kaewpradit., 2018 and Morley et al., 2011) and the evolution of the MSB from this study.

จุฬาลงกรณ์มหาวิทยาลัย
Chulalongkorn University

CHAPTER V
CONCLUSION

Based on the results of remote-sensing interpretation (Landsat 7 TM, ALOS DEM, ASTER) integrated with those of the detailed topographic and field surveys as well as those of OSL-dating of fault related sediments, and basin analysis, and the conclusions are shown as followings:

1. Orientation of the MHSF is mainly the north-south with some northwest-southeast and northeast-southwest directions. Morphotectonic landforms along the MHSF include offset streams, triangular facets, shuttle ridges, linear valleys and fault scarps. The sense of movement of the MHSF is a right lateral strike- slip with normal movement,

2. Nine major paleoearthquake events along the MHSF occurred about 78,000, 68,000, 58,000, 48,000, 35,000, 30,000, 25,000, 8,000 and 3,000 years ago. Therefore, long recurrence interval is approximately 10,000 years and short recurrence interval is approximately 5,000 years. The MHSF was triggered by the earthquakes with a maximum paleoearthquake magnitude of Mw 6.77, estimated by the surface rupture length of about 28.55 km, slip rate is ca. 0.04-0.15 mm/yr,

3. Based on the morphotectonic landforms and basin analysis, there are two north-south trending basins along the MHSF i.e., the MHSB in the north and the MSB in the south. Between those two basins (Khun Yuam area) shows high elevation which is inferred as the linkage zone that developed the lateral movement, and

4. The MHSB and the MSB along the MHSF were developed during Early Miocene to Late Pliocene as the pull apart basins related with the development of rift basins and dextral movement of the Mae Ping Fault.

จุฬาลงกรณ์มหาวิทยาลัย
CHULALONGKORN UNIVERSITY

REFERENCES

Aitken, A. J. 1985. Thermolunescence Dating. Newyork, Academic Press.

Aydin, A., and Nur, A. 1982. Evolution of pull-apart basin and their scale independence. Tectonics 1: 91-105.

Baum, F., Von Braun, E., Hahn, L., Hess, A., Koch, K.-E., Kruse, G., Quarch, H., and Siebenhuner, M. 1970. On the geology of northern Thailand. Beihefte zum Geologischen Jahrbuch 102: 23.

Bell, W. T. 1979. Thermoluminescence dating: Radiation dose-rate data. Archaeometry 21: 243–245.

Bunopas, S. 1981. 1981, Paleogeographic history of Western Thailand and adjacent parts of Southeast Asia - A plate tectonics interpretation, Doctoral dissertation, Victoria University of Wellington, New Zealand. Doctoral dissertation, Victoria University of Wellington, New Zealand

Charusiri, P., Daorerk, V., and Supajanya, T. 1996. Applications of remote-sensing techniques to geological structures related to earthquakes and earthquake-prone areas in Thailand and neighbouring areas: A preliminary study. J. Scientific Res. Chula. Univ. 21(1), 14–3

Charusiri, P., Kosuwan, S., Lumjuan, A., and Wechbunthung, B. 1998. Review of active faults and seismicity in Thailand.

Charusiri, P., Rhodes, B. P., Saithong, P., Kosuwan, S., Pailopli, S., Wiwegwin, W., Doarerk, V., Hinthong, C., and Klaipongpan, S. 2007. Regional tectonic setting and seismicity of Thailand with reference to reservoir construction.

Chuaviroj, S. 1991. Geotectonic of Thailand.

Cunningham, W. D., and Mann, P. 2007. Tectonics of strike-slip restraining and releasing bends. Geological Society, London, Special Publications 290: 1-12

Dawers, N., H. Anders, M., and Scholz, C. 1993. Growth of normal faults: Displacement-length scaling. Geology 21

Department of Mineral Resourses. 2007. Geologic Map of Mae Hong Son 1: 1,000,000. Department of Mineral Resources. Bangkok (with English explanation).

จุฬาลงกรณ์มหาวิทยาลัย
Chulalongkorn University

Department of Mineral Resourses. 2018. Active Faults Map in Thailand.

Department of Mineral Resourses. 2016. Seismic Hazard Map of Thailand.

Dooley, T. P., and Schreurs, G. 2012. Analogue modelling of intraplate strike-slip tectonics: A review and new experimental results. Tectonophysics 574-575: 1-71.

Duller, G. A. T. 2008. Luminescence Dating: guidelines on using luminescence dating in archaeology. Swindon: English Heritage.

Fenton, C. H., Charusiri, P., and Wood, S. H. 2003. Recent paleoseismic investigations in northern and western Thailand. Annals of Geophysics 46(5): 957-981.

Frankel, K. L., Owen, L. A., Dolan, J. F., Knott, J. R., Lifton, Z. M., Finkel, R. C., and Wasklewicz, T. 2015. Timing and rates of Holocene normal faulting along the Black

Mountains fault zone, Death Valley, USA. Lithosphere 8: 3-22.

Hinthong, C. 1997. The Study of Active Faults in Thailand. Report of EANHMP. An Approach to Natural Hazards in the Eastern Asia:

Hisada, K.-I., Sugiyama, M., Ueno, K., Charusiri, P., and Arai, S. 2004. Missing ophiolitic rocks along the Mae Yuam Fault as the Gondwana–Tethys divide in north-west Thailand. The Island Arc 13: 119-127.

Keller, E. A., and Pinter, N. 1996. Active tectonics: Earthquake, uplift, and landscape. New Jersey: Prentice-Hall.

Morley, C. K., Charusiri, P., and Watkinson, I. M. 2011. Structural geology of Thailand during the Cenozoic. In M. F. Ridd, A. J. Barber, and M. J. Crow (eds.), The Geology of Thailand, pp. 273-334. The Geological Society, London.

Morley, C. K., Smith, M., Carter, A., Charusiri, P., and Chantraprasert, S. 2007. Evolution of deformation styles at a major restraining bend, constrains from cooling histories, Mae Ping Fault Zone, western Thailand. Geol. Soc. Lond. Spec. Publ 290: 325–349.

Nutalaya, P., Sodsri, S., and Arnold, E. P. 1985. Series on seismology Vol. II – Thailand. Technical report, Southeast Asia Association of Seismology and Earthquake Engineering Project, USGS

จุฬาลงกรณ์มหาวิทยาลัย
Chulalongkorn University

Pailoplee, S., and Charusiri, P. 2016. Seismic hazards in Thailand: A compilation and updated probabilistic analysis. Earth, Planets and Space 68: 14.

Pongwapee, S., Morley, C. K., and Won-in, K. 2018. Impact of pre-existing fabrics and multi-phase oblique extension on Cenozoic fault patterns, Wichianburi sub-basin of the Phetchabun rift, Thailand. Journal of Structural Geology 118: 340-361.

Searle, M., and Morley, C. 2011. Tectonics and Thermal evolution of Thailand in the regional context of South-East Asia. Geology of Thailand. pp. 539-571.

Shi, X., Wang, Y., Sieh, K., Weldon, R., Feng, L., Chan, C.-H., and Liu-Zeng, J. 2018. Fault slip and GPS velocities across the Shan Plateau define a curved southwestward crustal motion around the eastern Himalayan syntaxis. Journal of Geophysical Research: Solid Earth 123: 2502–2518.

Tapponnier, P., Peltzer, G., Armijo, R., Le Dain, A., and Coobbold, P. 1982. Propagating Extrusion Tectonics in Asia: New insights from simple experiments with plasticine. Geology 10: 611-616.

Ufimtsev, G. F. 1990. Morphotectonics of the Mongolia-Siberian mountain belt. Journal of Geodynamics 11: 309-325.

Wang, Y., Sieh, K., Tun, S. T., Lai, K.-Y., and Myint, T. 2014. Active tectonics and earthquake potential of the Myanmar region. Journal of Geophysical Research: Solid Earth 119: 3767-3822.

Wiwegwin, W., Hisada, K.-I., Charusiri, P., Kosuwan, S., Pailopli, S., Saithong, P., Khaowiset, K., and Won-In, K. 2014. Paleoearthquake investigations of the Mae Hong Son Fault, Mae Hong Son region, northern Thailand. Journal of Earthquake and Tsunami 8(2): 35.

จุฬาลงกรณ์มหาวิทยาลัย
Chulalongkorn University

APPENDIX

จุฬาลงกรณ์มหาวิทยาลัย
Chulalongkorn University

OSL grow and growth curves

KY1

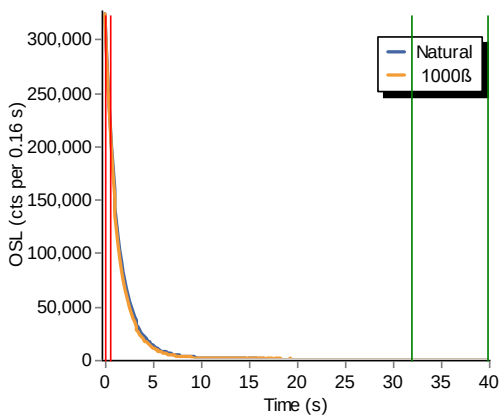

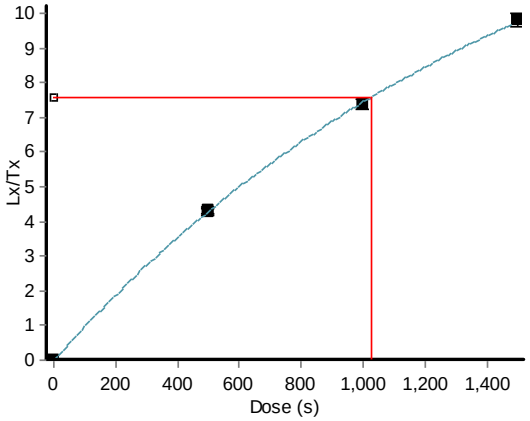

KY2

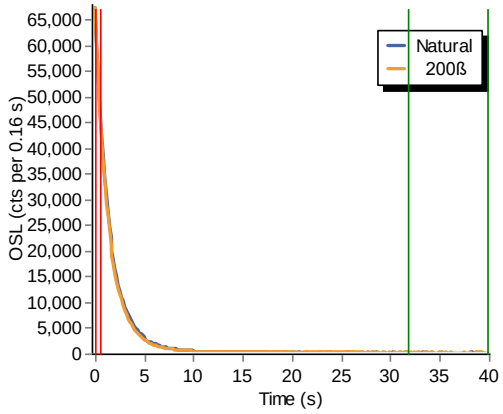

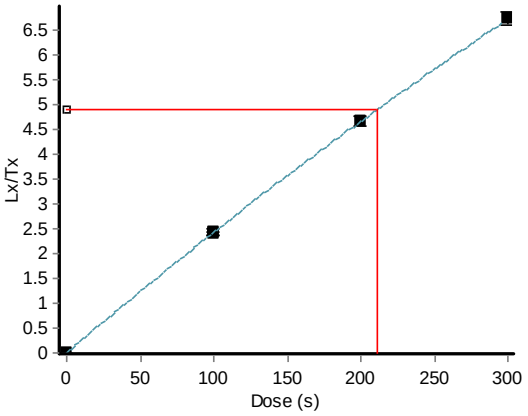

KY3

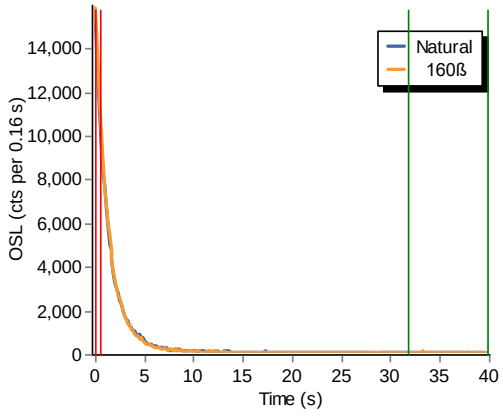

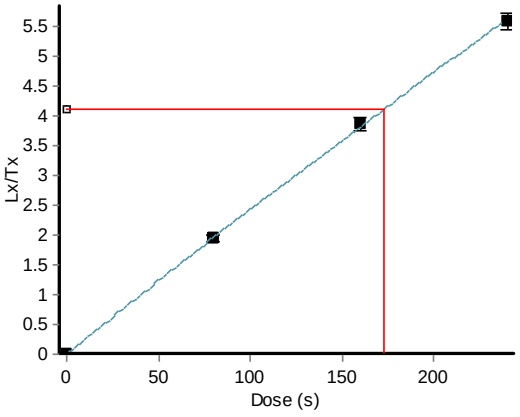

KY4

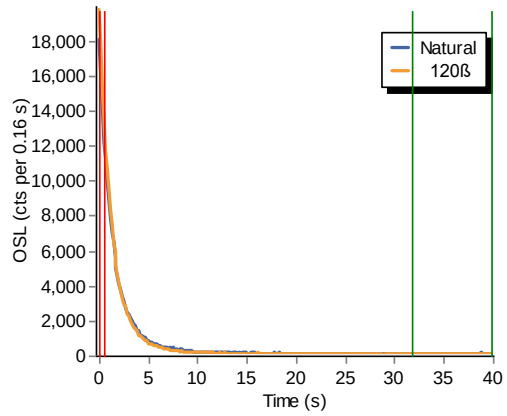

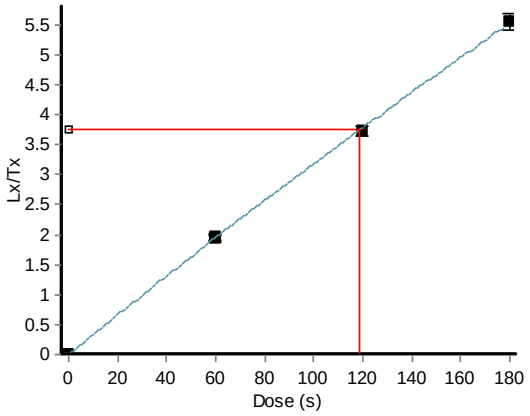

KY5

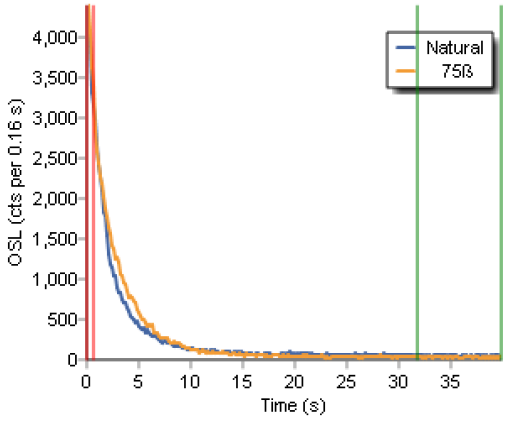

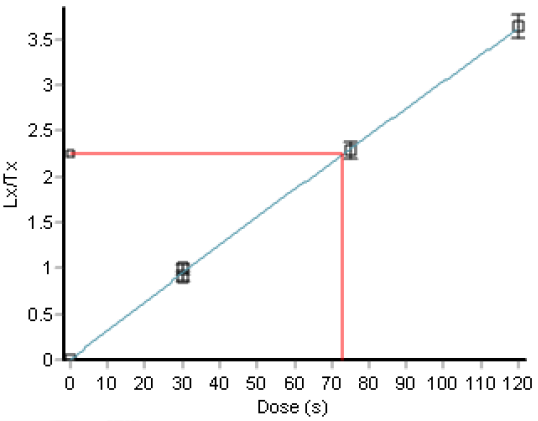

จุฬาลงกรณ์มหาวิทยาลัย
Chulalongkorn University

KY6

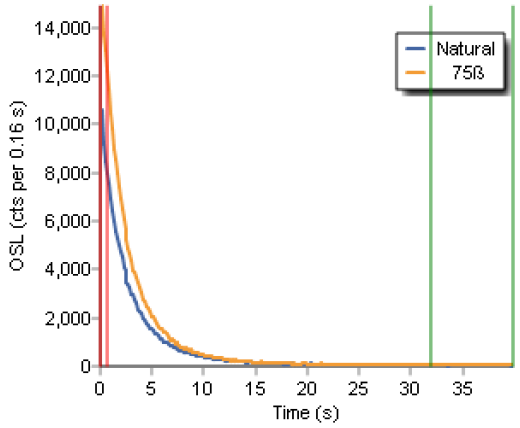

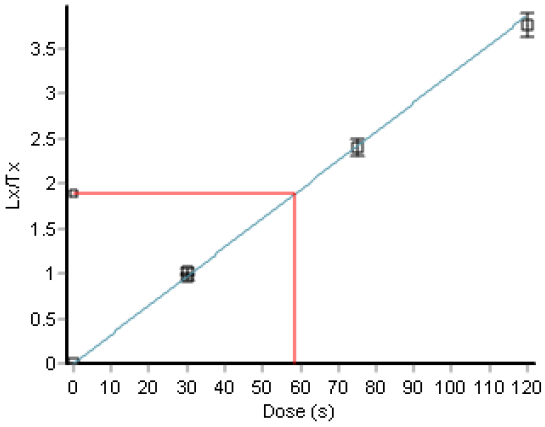

KY7

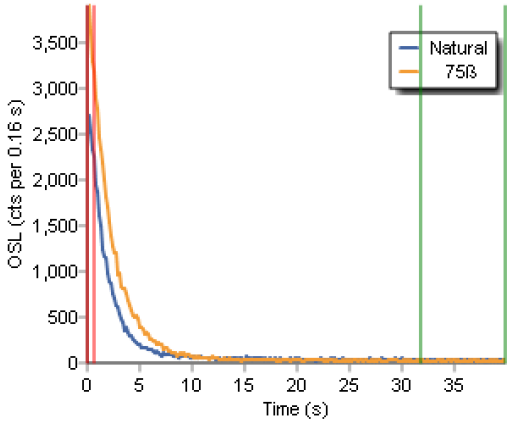

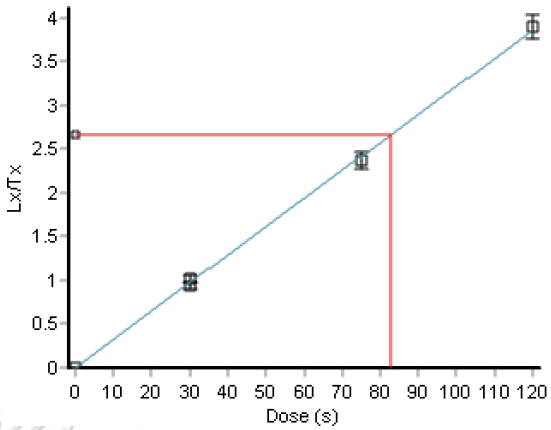

KY8

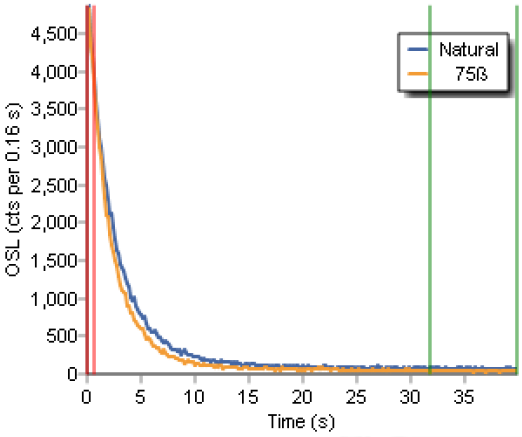

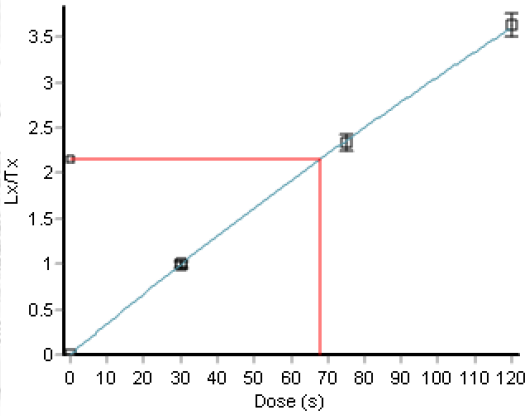

จุฬาลงกรณ์มหาวิทยาลัย
Chulalongkorn University

BY1

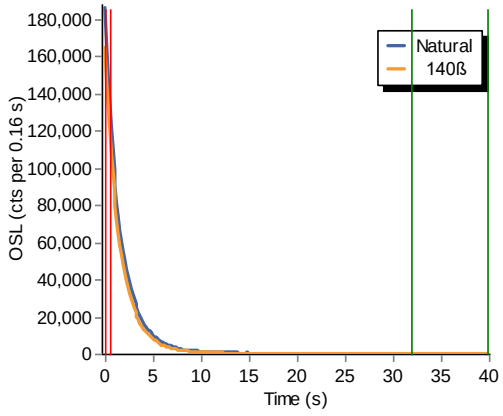

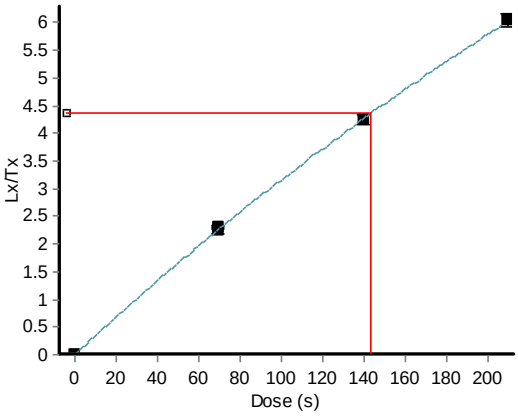

BY2

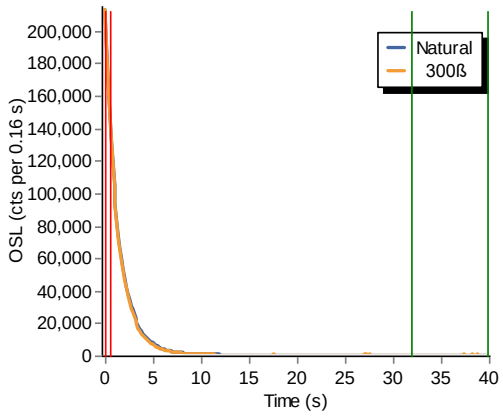

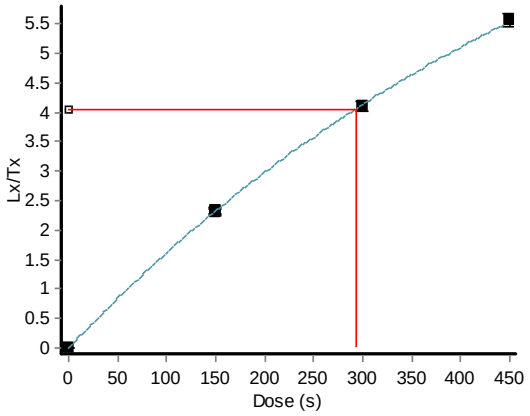

BY3

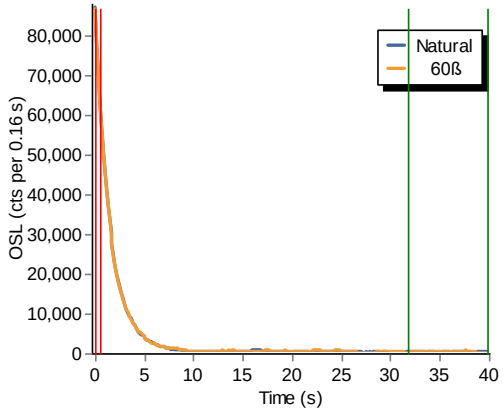

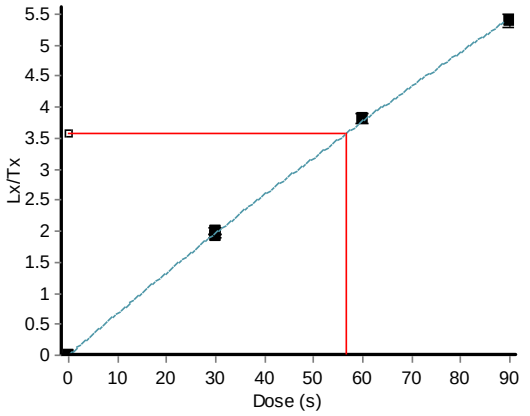

จุฬาลงกรณ์มหาวิทยาลัย
Chulalongkorn University

BY5

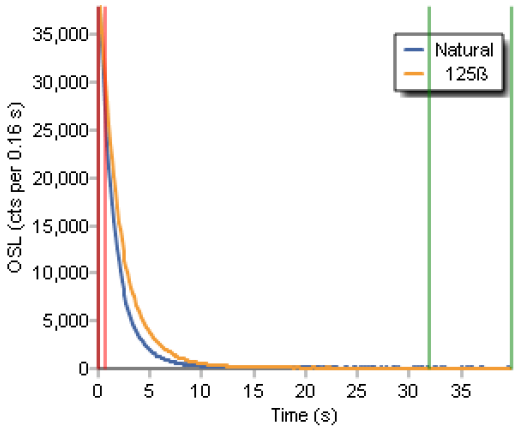

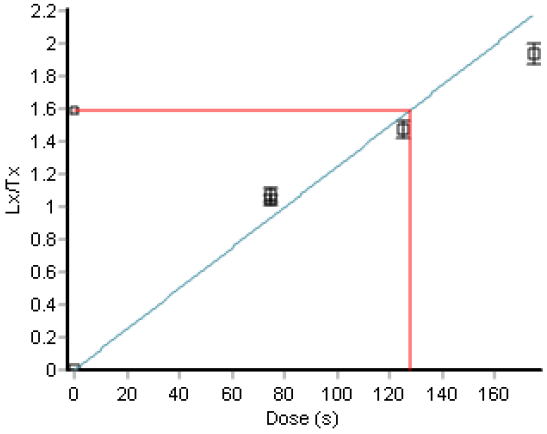

BY6

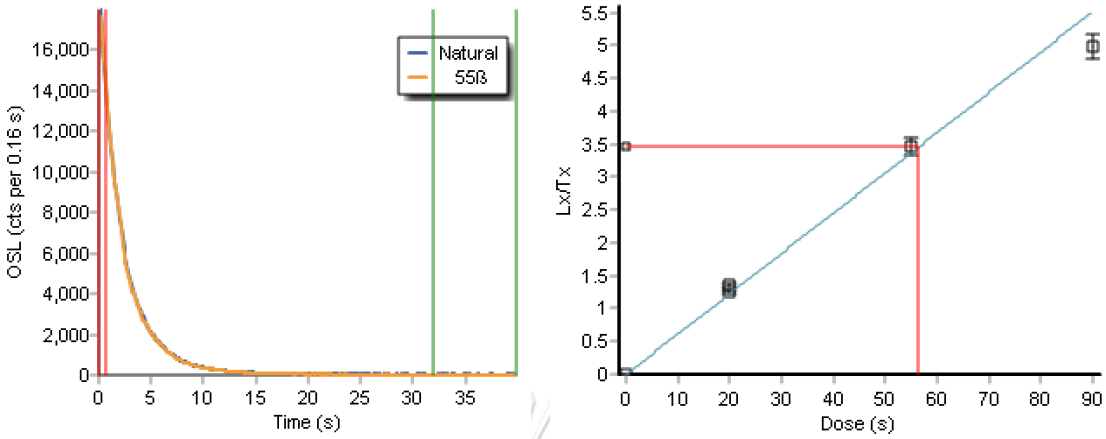

BY7

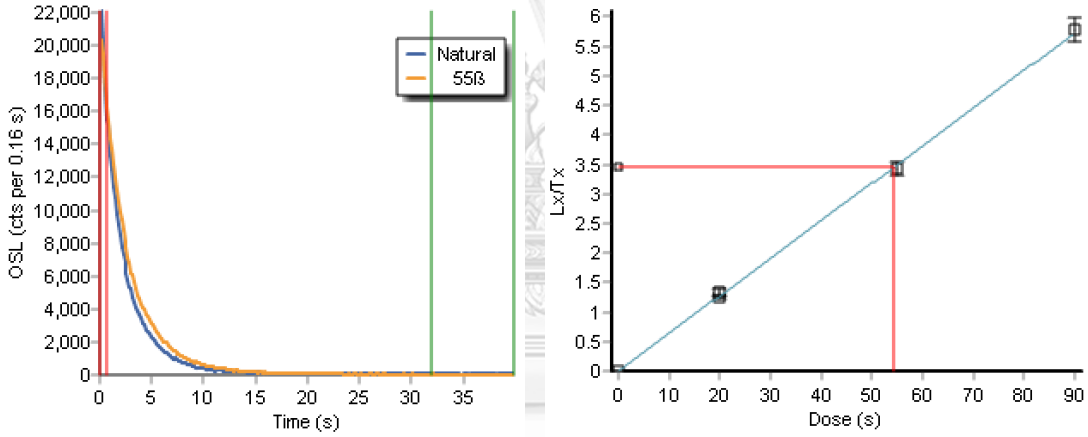

จุฬาลงกรณ์มหาวิทยาลัย
Chulalongkorn University

BY8

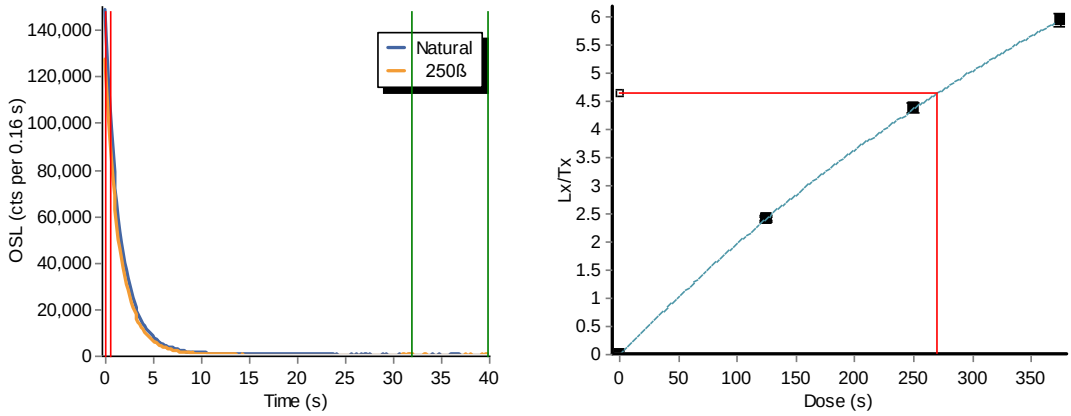

BY9

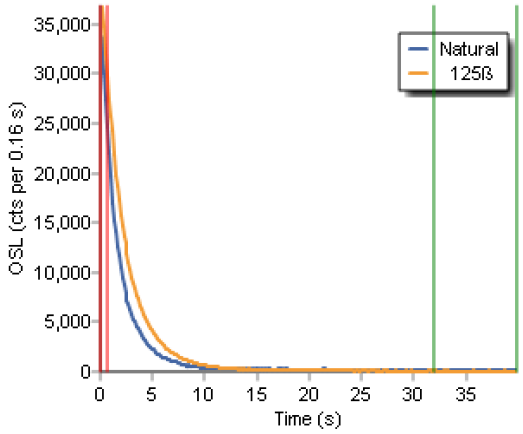

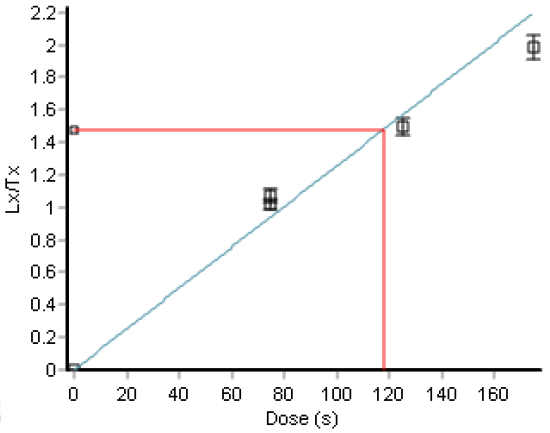

DWL1

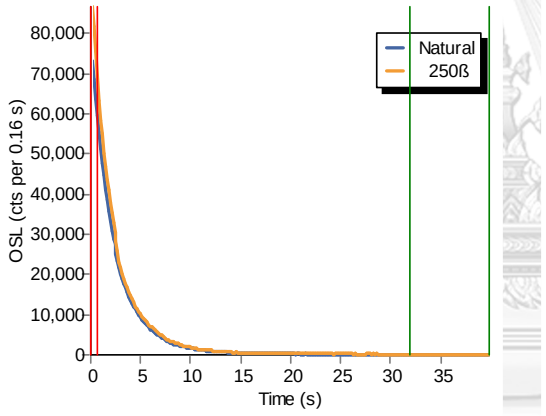

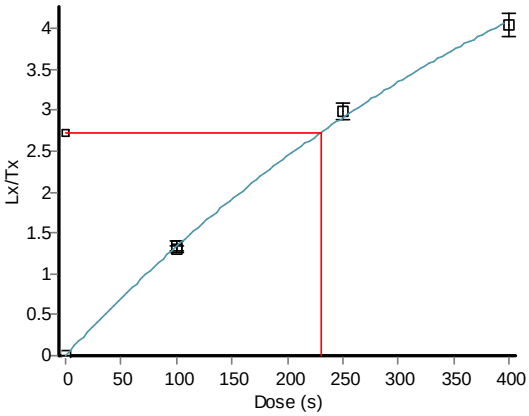

จุฬาลงกรณ์มหาวิทยาลัย
Chulalongkorn University

DWL2

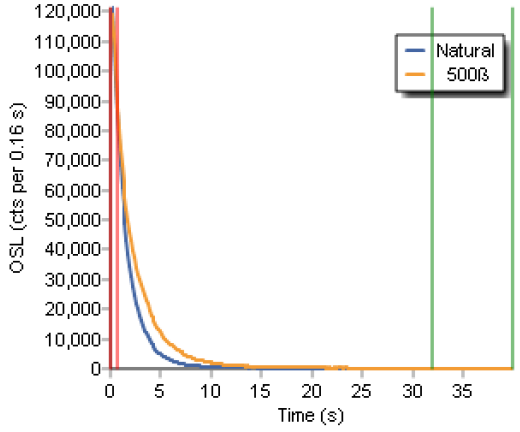

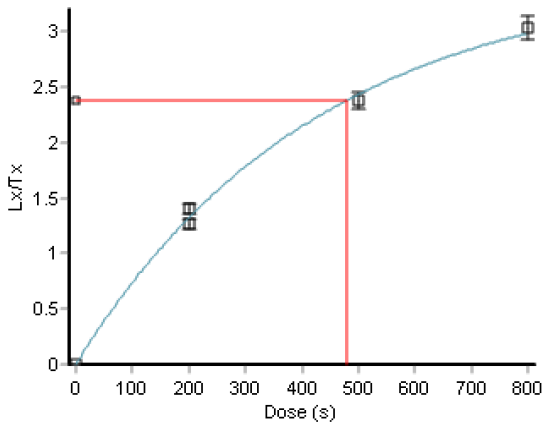

DWL3

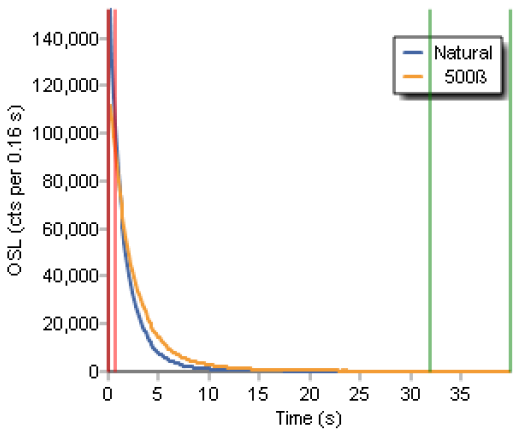

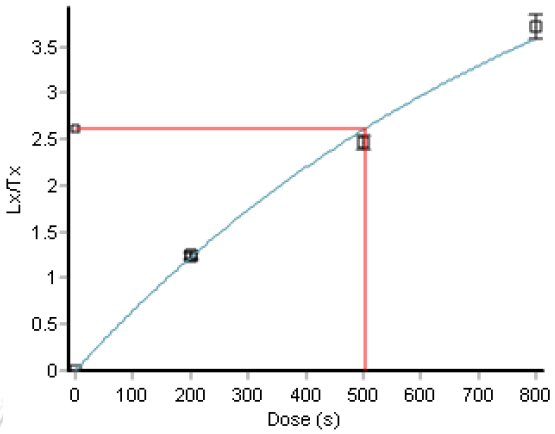

DWL4

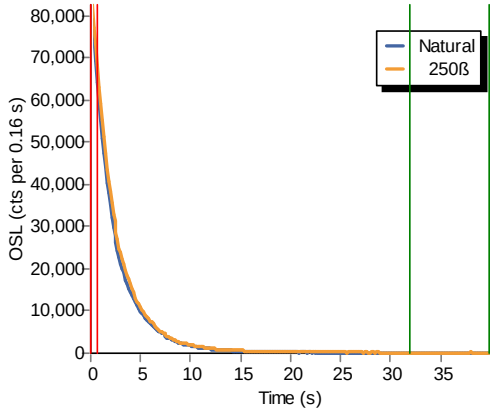

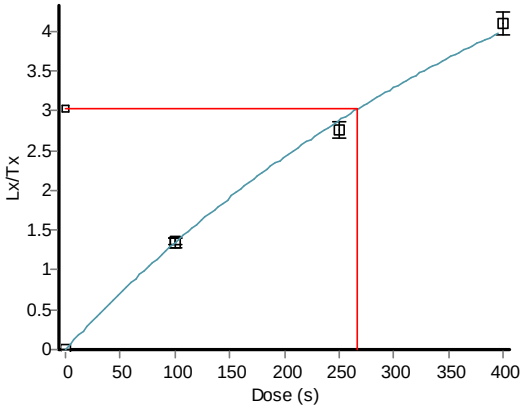

จุฬาลงกรณ์มหาวิทยาลัย
Chulalongkorn University

MTL1

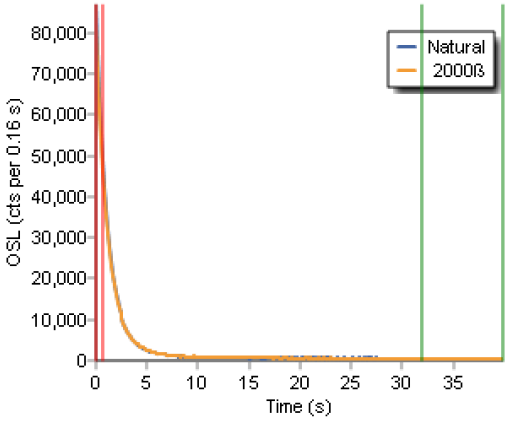

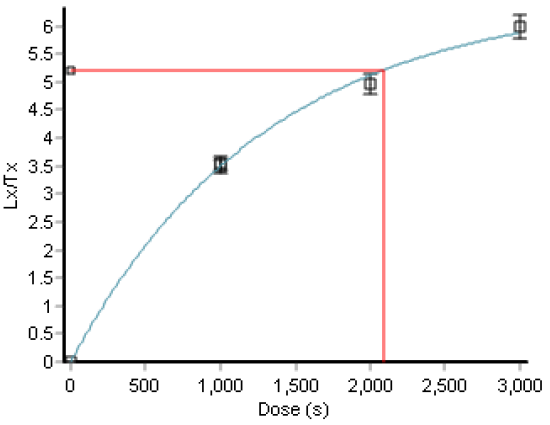

MTL2

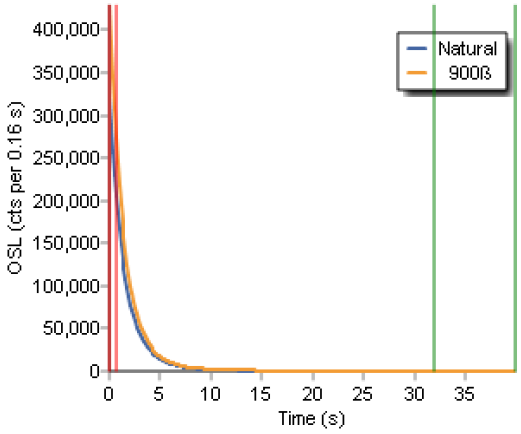

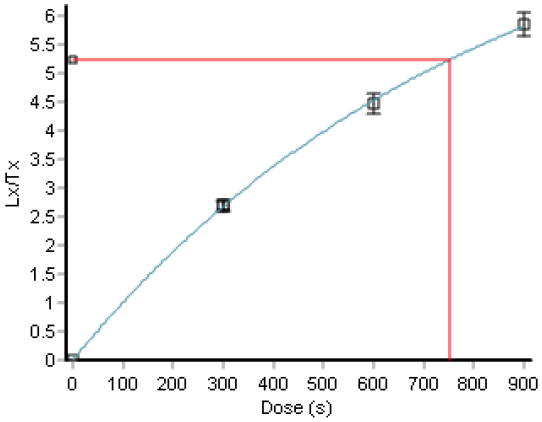

MTL3

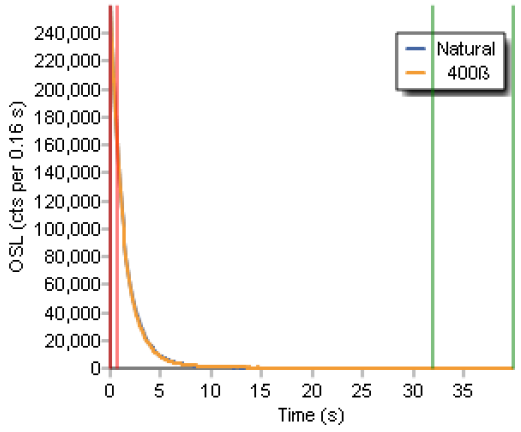

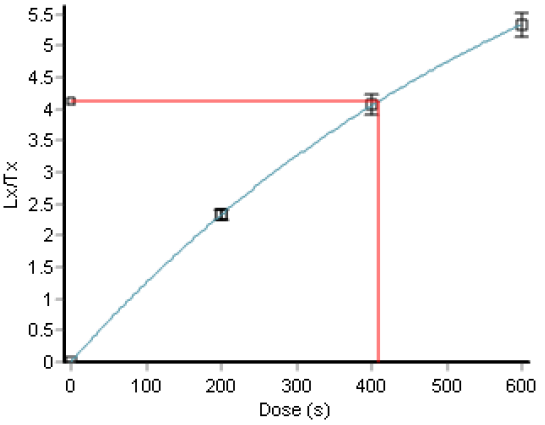

จุฬาลงกรณ์มหาวิทยาลัย
Chulalongkorn University

MTL4

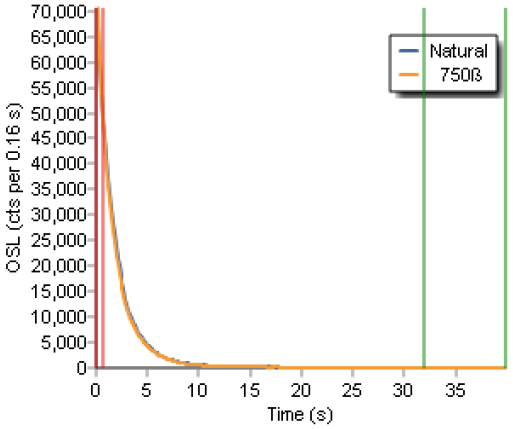

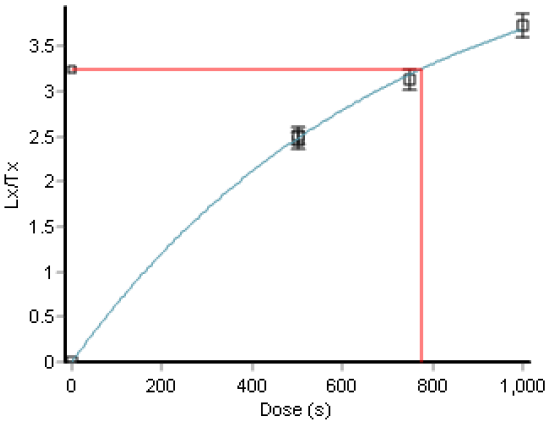

MTL5

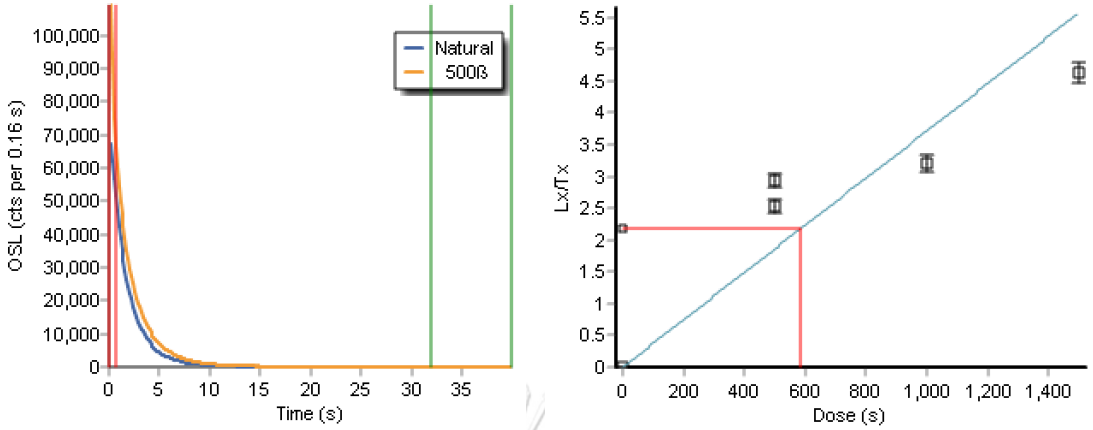

MTL6

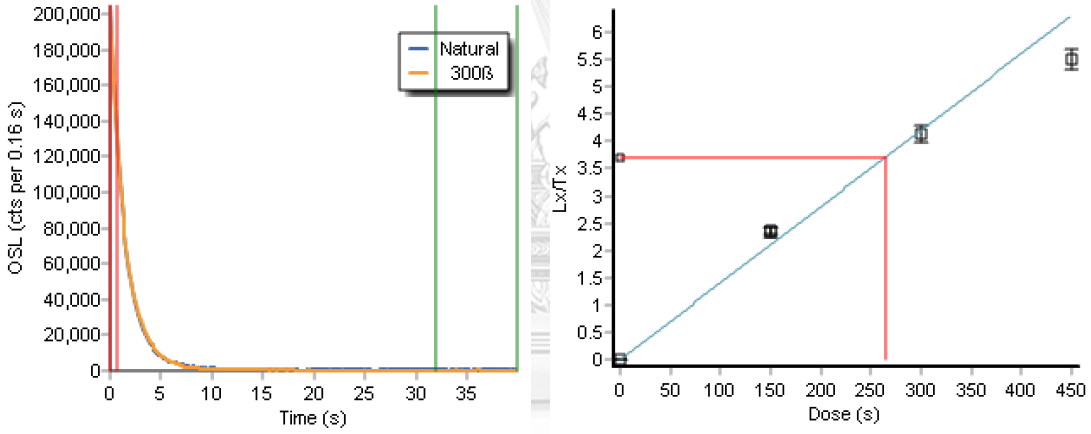

จุฬาลงกรณ์มหาวิทยาลัย
Chulalongkorn University

Radial plotter of ED

BY1

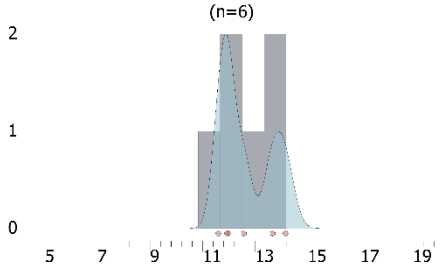

Density plot

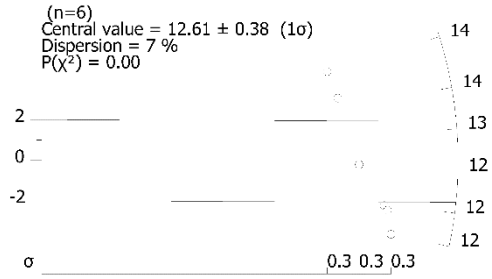

Radial plot

BY2

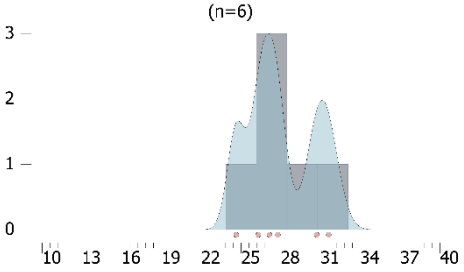

Density plot

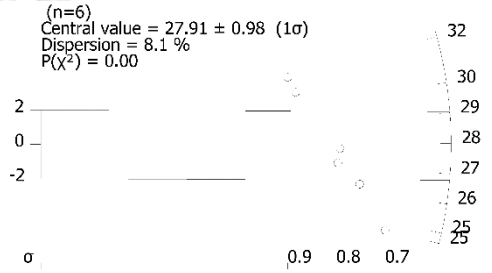

Radial plot

จุฬาลงกรณ์มหาวิทยาลัย
Chulalongkorn University

BY3

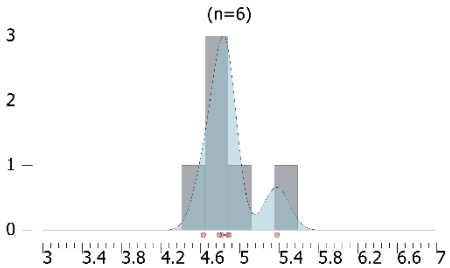

Density plot

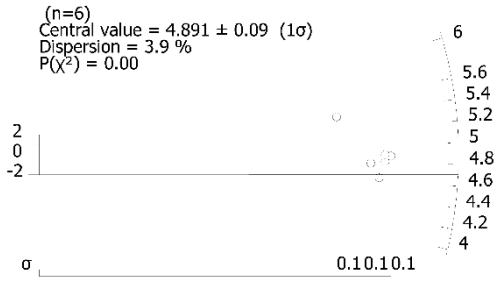

Radial plot

BY5

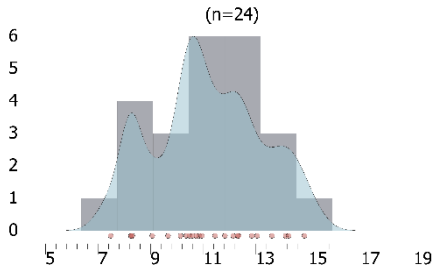

Density plot

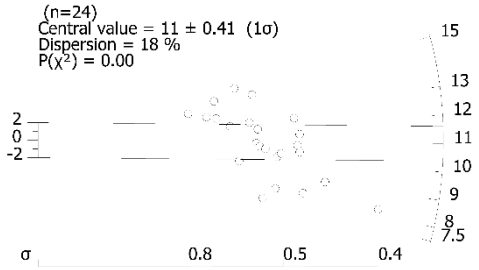

Radial plot

BY6

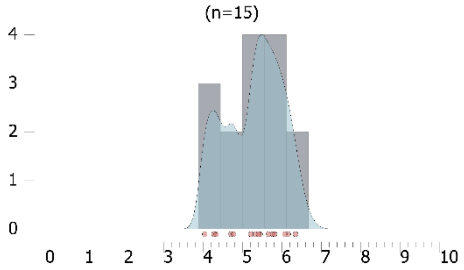

Density plot

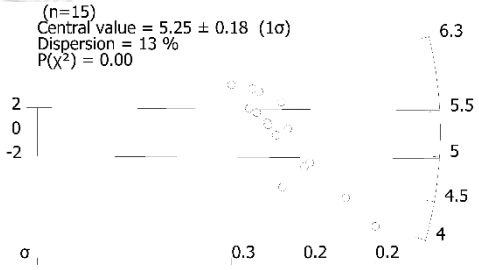

Radial plot

จุฬาลงกรณ์มหาวิทยาลัย

BY7

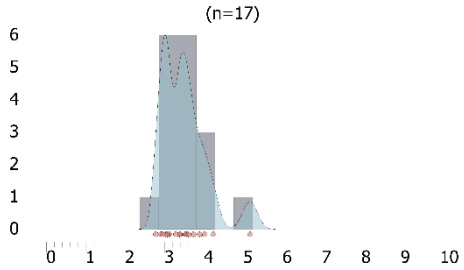

Density plot

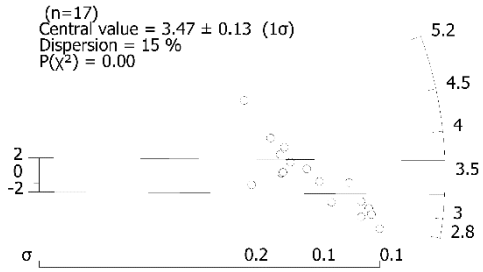

Radial plot

BY8

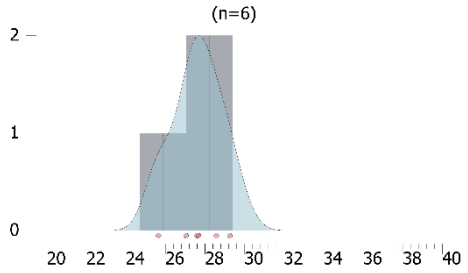

Density plot

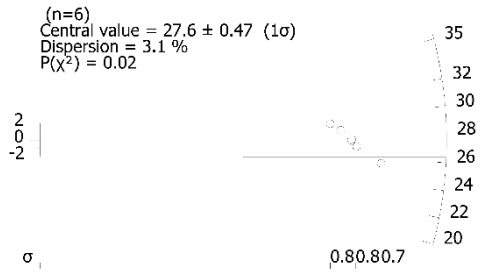

Radial plot

BY9

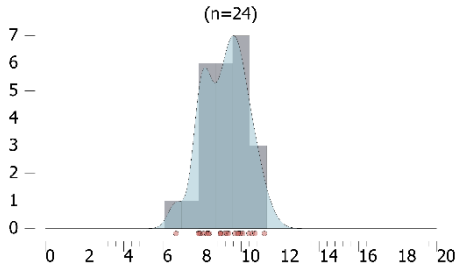

Density plot

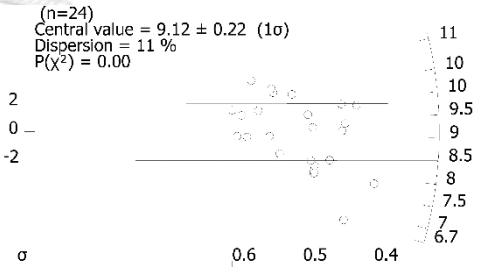

Radial plot

จุฬาลงกรณ์มหาวิทยาลัย

DWL1

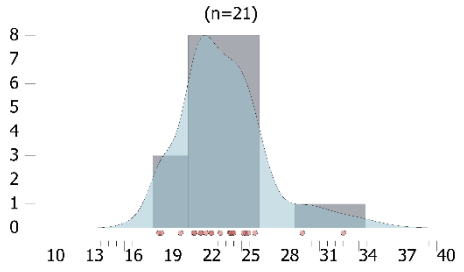

Density plot

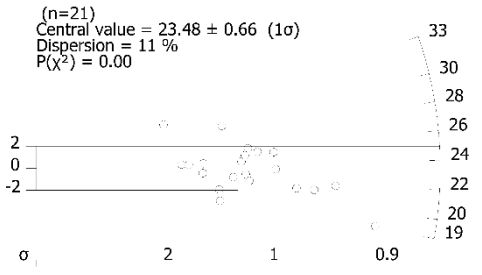

Radial plot

DWL2

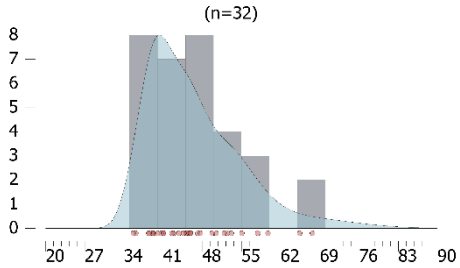

Density plot

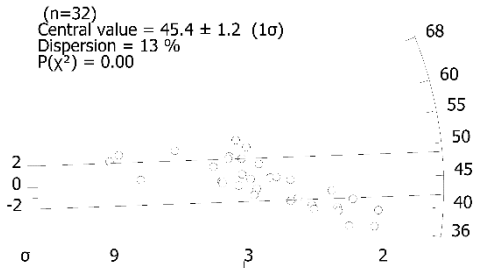

Radial plot

DWL3

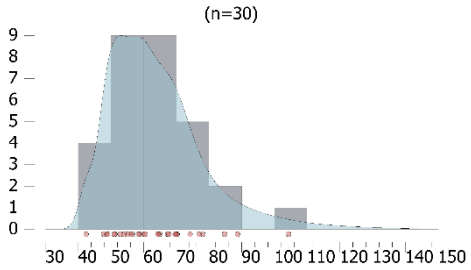

Density plot

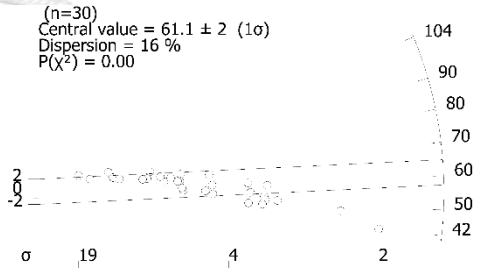

Radial plot

จุฬาลงกรณ์มหาวิทยาลัย

DWL4

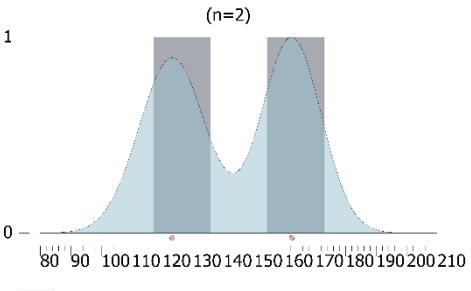

Density plot

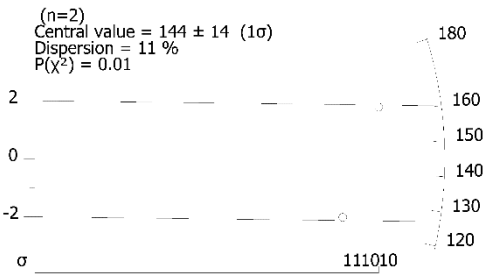

Radial plot

KY1

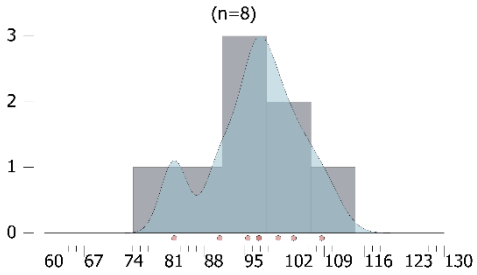

Density plot

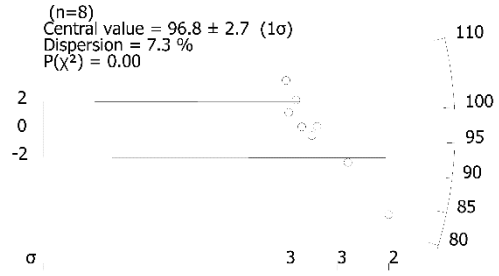

Radial plot

KY2

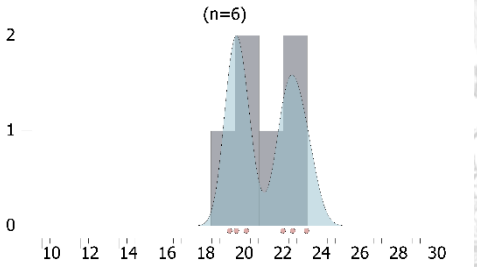

Density plot

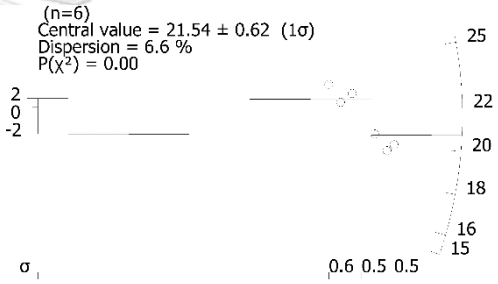

Radial plot

จุฬาลงกรณ์มหาวิทยาลัย

KY3

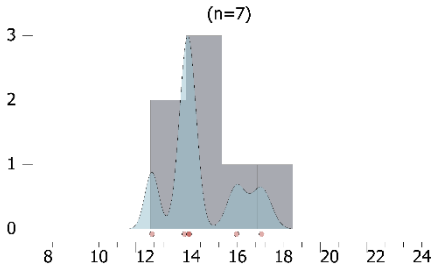

Density plot

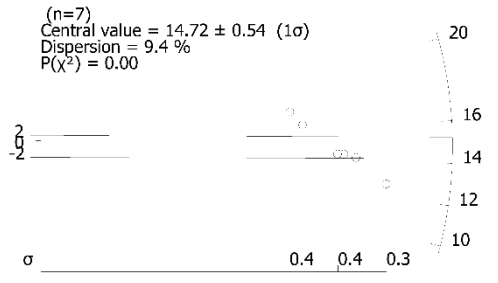

Radial plot

KY4

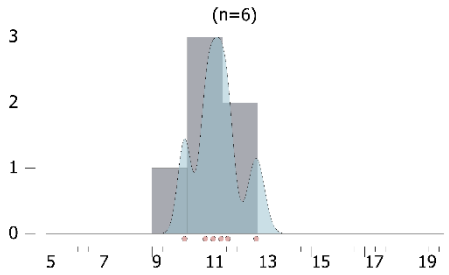

Density plot

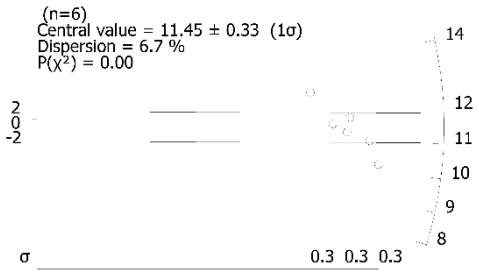

Radial plot

KY5

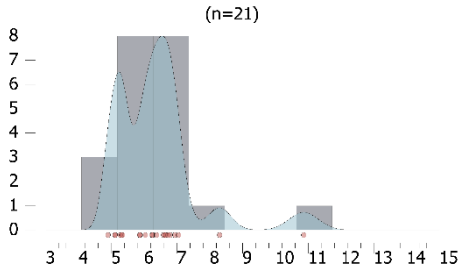

Density plot

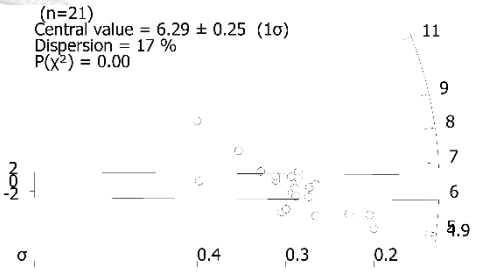

Radial plot

KY7

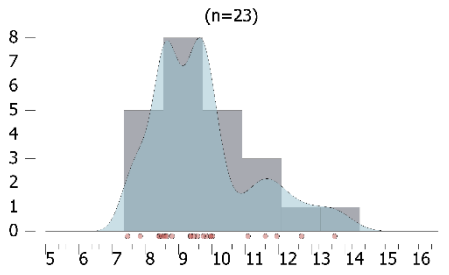

Density plot

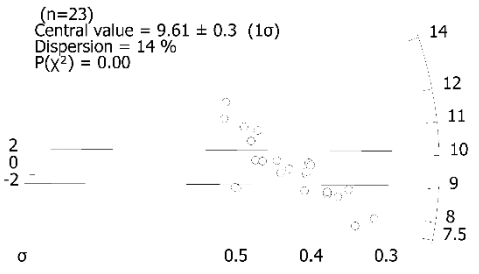

Radial plot

จุฬาลงกรณ์มหาวิทยาลัย

KY8

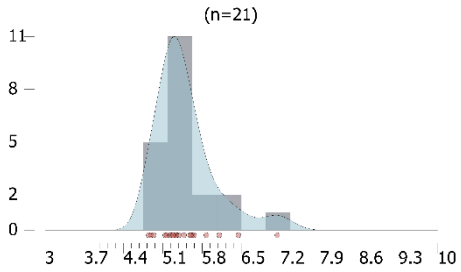

Density plot

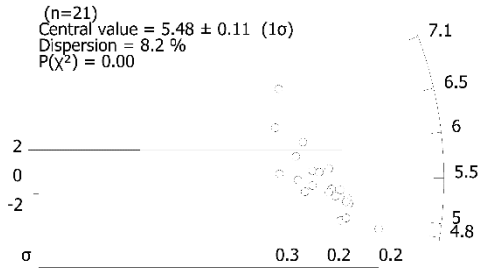

Radial plot

MTL1

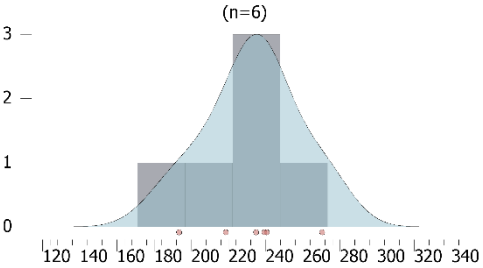

Density plot

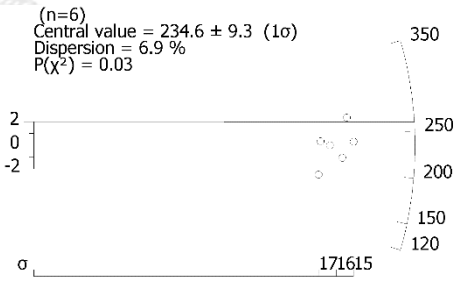

Radial plot

จุฬาลงกรณ์มหาวิทยาลัย
Chulalongkorn University

MTL2

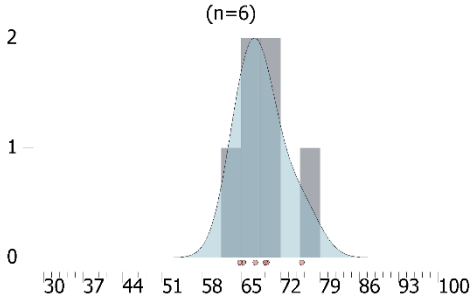

Density plot

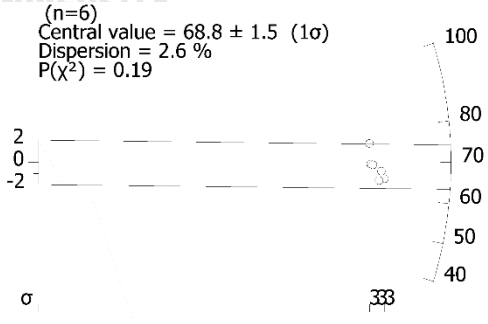

Radial plot

MTL3

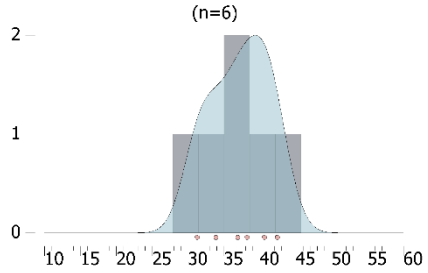

Density plot

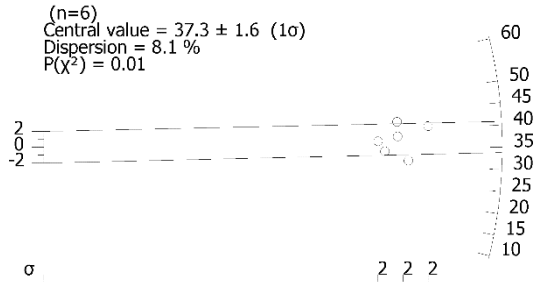

Radial plot

MTL4

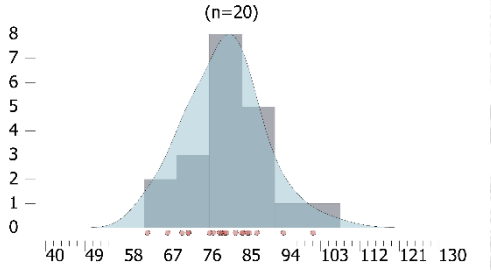

Density plot

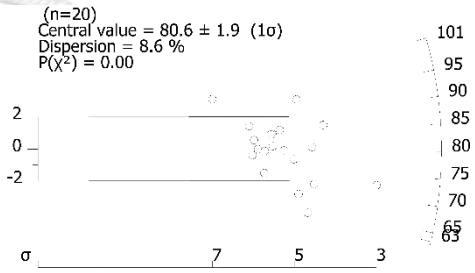

Radial plot

จุฬาลงกรณ์มหาวิทยาลัย
Chulalongkorn University

MTL5

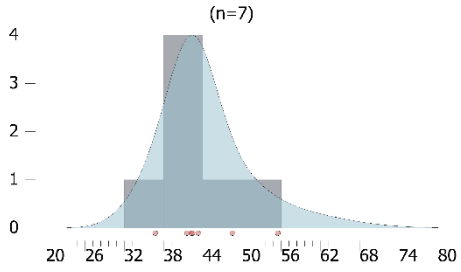

Density plot

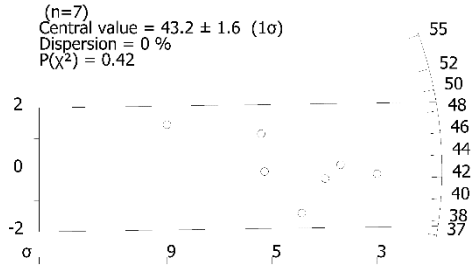

Radial plot

MTL6

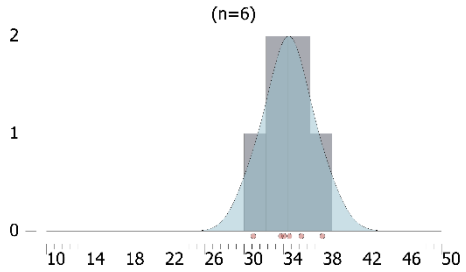

Density plot

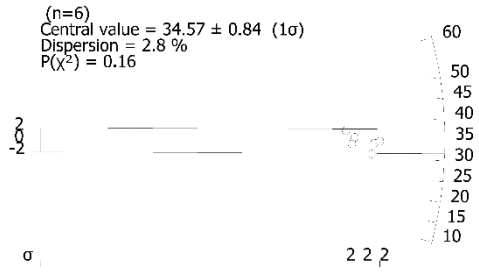

Radial plot

จุฬาลงกรณ์มหาวิทยาลัย
Chulalongkorn University

VITA

NAME	Chanista Chansom
DATE OF BIRTH	8 November 1994
PLACE OF BIRTH	Lamphun, Thailand
INSTITUTIONS ATTENDED	She graduated at high school level from Chakkham Khanathorn School, Lamphun in 2014. In 2017, she received a B.Sc. degree in Geology from the Department of Geology, Faculty of Science, Chaing Mai University, Thailand. In 2017, she enrolled as a graduate student for the M.Sc. program of Geology programe at Graduate School, Chulalongkorn University, Bangkok, Thailand.
PUBLICATION	She published a paper on “Neotectonic evidences along Mae Hong Son Fault, Northern Thailand” in Journal of Remote Sensing and GIS Association of Thailand in 2017 and published another one on “Paleoseismic evidences of the Doi Wiang La fault segment, Mae Hong Son Fault, northern of Thailand” which appeared on Proceeding of International Symposium on The 45th Congress on Science and Technology of Thailand (STT45), Chiang Rai, Thailand.

จุฬาลงกรณ์มหาวิทยาลัย
Chulalongkorn University